GROWTH FACTOR RELEASE FROM GELATIN-BASED HYDROGEL MATRICES FOR TISSUE REGENERATION

MASAYA YAMAMOTO

1998

GROWTH FACTOR RELEASE FROM GELATIN-BASED HYDROGEL MATRICES FOR TISSUE REGENERATION

MASAYA YAMAMOTO

1998

Dedicated to
my parents

Yasuko Yamamoto
Teruo Yamamoto

CONTENTS

Chapter 3. Bone regeneration induced by biodegradable hydrogel matrices incorporating TGF-β1

ABBREVIATIONS

Growth factors

bFGF	Basic fibroblast growth factor
BMP-2	Bone morphogenetic protein-2
TGF-β1	Transforming growth factor-β1
VEGF	Vascular endothelial growth factor

Monomers

AAc	Acrylic acid
MOEP	Methacyloyloxyethylene phosphate

Polymers

PVA	Poly(vinyl alcohol)
PGA	Poly(glycolide)
PET	Poly(ethylene terephthalate)
PAAc	Poly(acrylic acid)
PMOEP	Poly(methacryloyloxyethylene phosphate)

Miscellaneous

ECM	Extracellular matrix
IEP	Isoelectric point
H-E	Hematoxylin-eosin
SEM	Scanning electron microscopy
TEM	Transmission electron microscopy
EDX	Energy dispersive x-ray
SAD	Selected area diffraction
DEXA	Dual-energy x-ray absorptometry
BMD	Bone mineral density
HAp	Hydroxyapatite
DDW	Double distilled water
PBS	Phosphate-buffered saline solution
MEM	Minimum essential medium
RBM	Rat bone marrow

GENERAL INTRODUCTION

Replacement of a defective or lost tissue with the natural tissue is the ultimate goal of reconstructive medicine. However, current clinical treatments can replace only physically the defective or lost tissue with either man-made biomaterials or autogenic and allogenic tissues in case the tissue collection is possible. Although several attempts have been made to improve biomaterials for their clinical use over the past two decades, they still have several disadvantages[1]. One of them is not able to replace the biological function of tissues. For autogenic and allogenic tissues, there are also several problems for their clinical treatments, such as viral transfection and limited source of the tissue donor. Stimulated by these current issues, a new technology has emerged as the next generation for the reconstructive medicine; that is tissue engineering whose objective is to regenerate natural tissues for treatments of defective and lost tissues[2-8].

If a tissue defect is tiny, the tissue regeneration will be spontaneously achieved through the well-organized biological system which involves cells, growth factors, and extracellular matrices (ECMs)[6,9-14]. However, if the tissue defect is seriously large, one cannot expect the natural regeneration in spite of the excellent healing ability of human body. In such a case, it will be at least essential to provide a favorable environment for tissue regeneration using devices. Figure 1 illustrates the biomaterials and technologies required for tissue regeneration engineering. What are very important among them are scaffolds (artificial ECMs), carriers of growth factors, and cells.

Tissue regeneration may be achieved both in vitro and in vivo, if these biomaterials and techniques are appropriately provided. If tissues can be regenerated in vitro on a large scale promptly in response to the request from hospitals, it would be an ideal way. However,

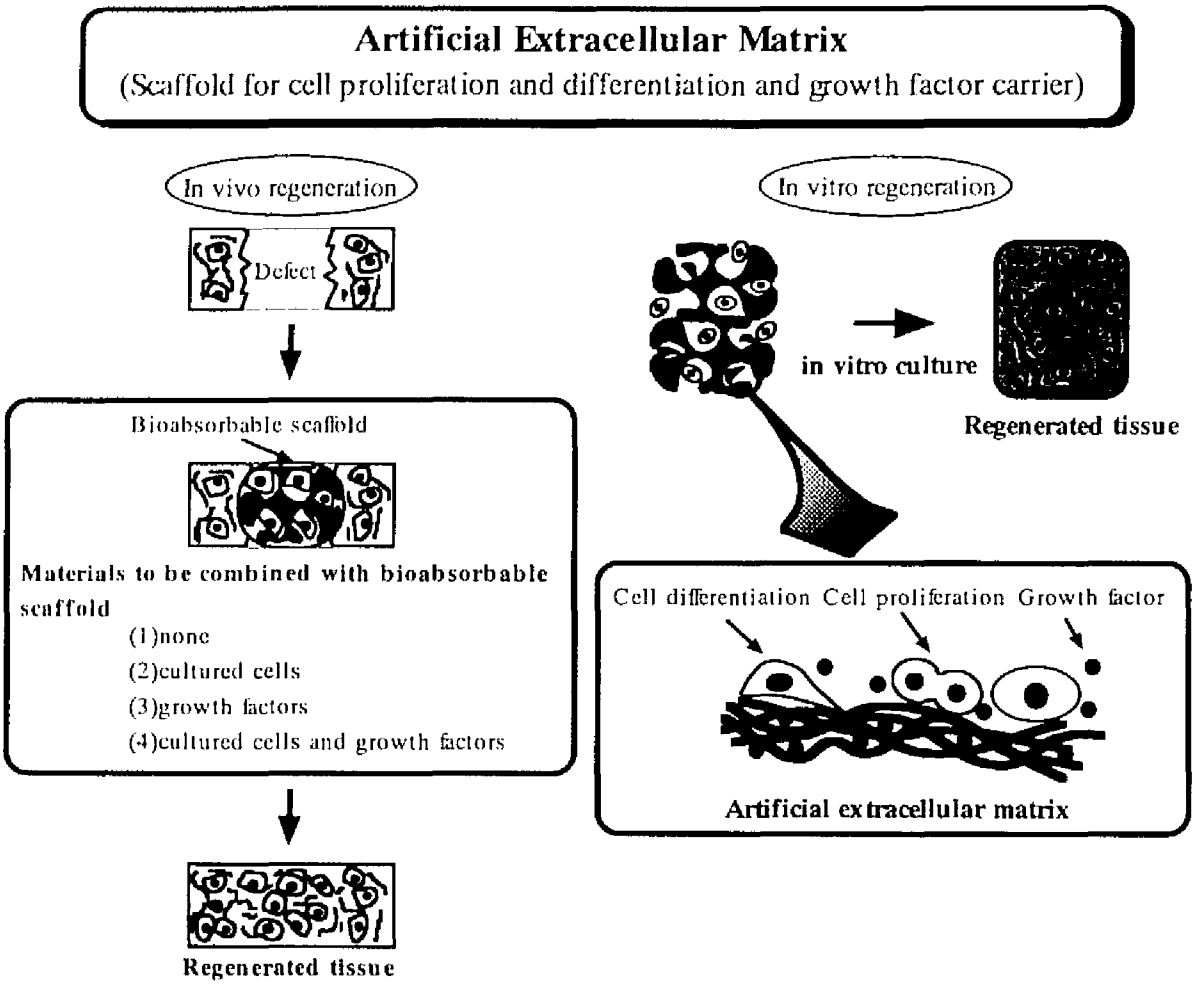

Figure 1. Tissue regeneration through combination of a bioabsorbable material with cultured cells and growth factors

at present, this is practically impossible because knowledge necessary for in vitro tissue regeneration is too scanty. Thus, almost all the attempts on tissue regeneration are being made in vivo at present.

In vivo tissue regeneration needs artificial ECMs (scaffolds), cells, and growth factors. The type of cells and growth factors used in combination with scaffolds depends on the type of tissue to be regenerated and the body site, where the tissue regeneration is performed. A large-sized defect will be naturally filled with fibrous tissues in vivo unless any proper medical treatment is applied. This is because the growth rate of fibrous tissues is generally much higher than that of the tissue regeneration. If this fibrous tissue ingrowth takes place, the lost tissue will never be substituted with the regenerated tissue. One possible way to prevent this fibrous tissue ingrowth is to place a bioabsorbable material into the defect. The material should be bioabsorbed in harmonization with tissue regeneration at the defect. In addition, the material should function as an artificial ECM, that is, a scaffold for ingrowth of blast cells from the surrounding host tissue. Such a scaffold has been prepared from naturally occurring biodegradable polymers (e.g., collagen, gelatin, and fibrin), synthetic biodegradable polymers (e.g., poly(lactic acid), poly(glycolic acid), and their copolymers), and inorganic substances (e.g., hydroxyapatite, calcium triphosphate, and calcium carbonate)[4-6,15-26]. It will be preferable for the scaffold formulation to introduce porous structure into the scaffold in order to facilitate the cell ingrowth as much as possible. This concept of tissue engineering is in marked contrast with that of conventional artificial tissues and organs, since the conventional reconstructive medicine with artificial tissues and organs generally relies on man-made materials alone. In addition, tissue engineering is entirely different from organ transplantation because of no use of immunosuppressant.

The recent advance of biomedical research has revealed how important growth

factors are in cell proliferation and differentiation both in vitro and in vivo[6,13,26-31]. In addition, genetic engineering has made it possible to produce various recombinant growth factors on a large scale, so that they can promote clinical applications of tissue engineering. However, growth factors generally have very short half-life in the body[32,33], and are rapidly excreted from the injected site or deactivated by the attack of enzymes and antibodies, if injected in the solution form. Therefore, drug delivery systems (DDS) have attracted much attention as a very important technology also in tissue engineering, especially when growth factors should be continuously released from carrier for a certain period of time. It is well recognized that growth factors are stored in our body by their covalent or ionic binding to ECM components such as growth factor binding proteins and acidic polysaccharides[29,34]. Moreover, such ECM binding enables the growth factors to maintain the biological activity in vivo. Indeed, it is reported that basic fibroblast growth factor (bFGF) with an isoelectric point (IEP) of 9.6 forms a polyion complex with acidic heparin and heparan sulfate in vitro and in vivo, resulting in stabilization of bFGF biological activities[29,35-37]. Transforming growth factor-β1 (TGF-β1) is also stabilized in ECM by covalent binding to both the TGF-β1 latency associated protein and latent TGF-β1 binding protein[29,38,39]. However, so far as TGF-β1 is in the state of binding to these proteins, it does not exhibit any biological activities that appear only when bioactive TGF-β1 molecules are released as a result of protease cleavage of the bond. Therefore, it will be a promising way to mimic such biological release systems for sustained release of growth factors.

In analogy to the polyion complexation which is very effective in the biological bFGF-polysaccharide system, a bioabsorbable hydrogel is prepared from the gelatin for the sustained release of growth factors in this thesis. Gelatin is a denatured collagen and commercially available as a bioabsorbable polymer. Two types of gelatin with IEPs of 5.0 and

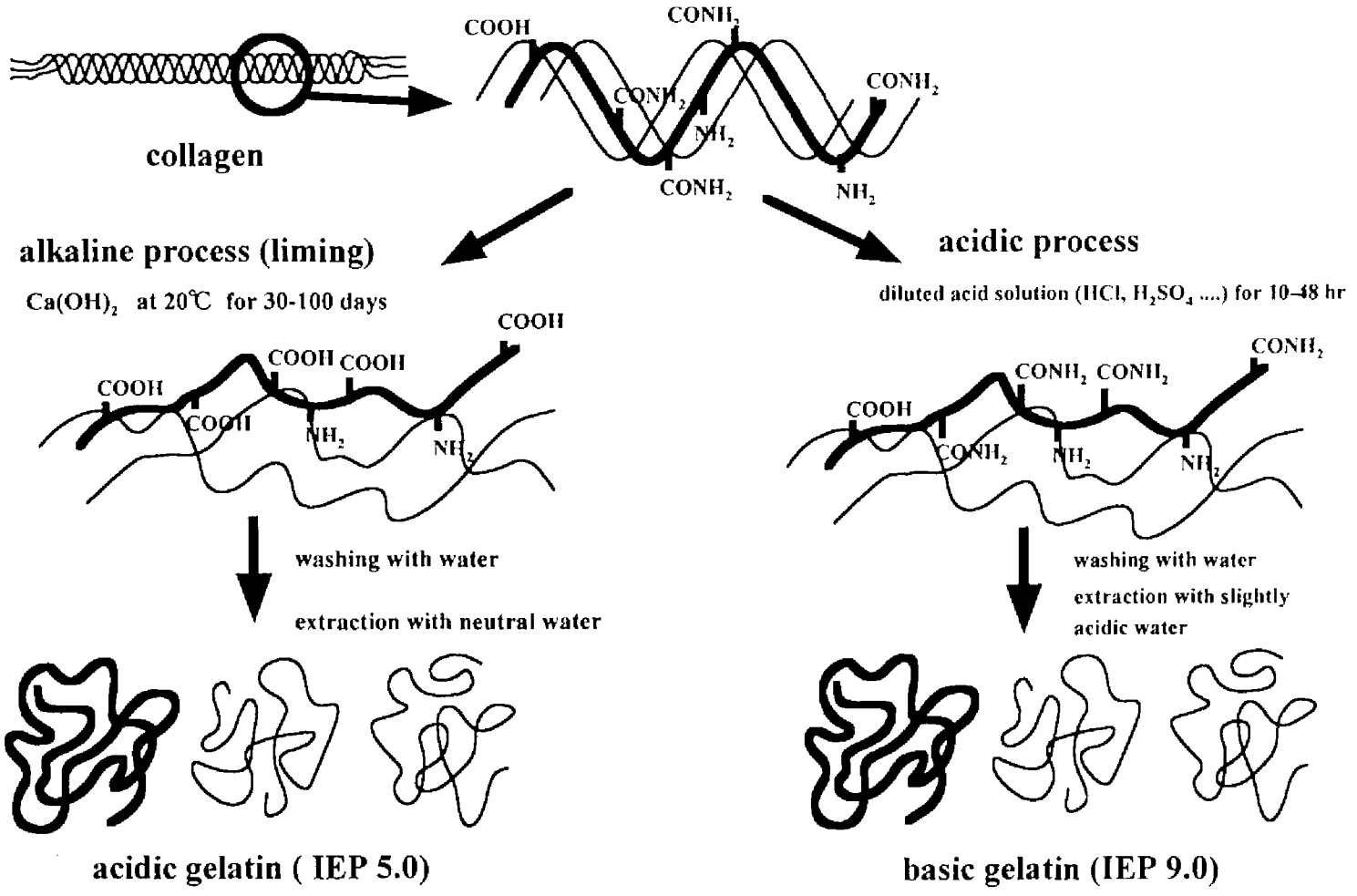

Figure 2. Extraction of gelatin from collagen.

9.0 have been prepared by two different processes from collagen as shown in Figure 2. The alkali- and acid-processed gelatins are designated here acidic and basic gelatin based on their ionic property, respectively. Table 1 gives the characteristics of growth factors used in this study. Since these growth factors have IEPs higher than 7.0, they will form a polyion complex with the acidic gelatin of IEP 5.0. The bioabsorbable hydrogel prepared from this acidic gelatin will be able to immobilize the basic growth factor through the ionic interaction between the two substances. If the hydrogel undergoes enzymatic biodegradation, the immobilized growth factor will be released from the gel. The release kinetics of growth factor from the hydrogel system will be regulated by controlling hydrogel biodegradation kinetics. This proposed hydrogel formulation mimics the manner in which the growth factor is stored in the biological ECM. Biosafety of gelatin has been already proven through its long usage in pharmaceutical, medical, and food applications[40].

The objective of this thesis is to study the tissue regeneration through sustained release of growth factors from the acidic gelatin hydrogel. In Part I, the activity of the gelatin hydrogel incorporating growth factors to induce tissue regeneration is evaluated focusing on the growth factor release, while Part II is concerned with the structure of the regenerated tissues studied by both light and electron microscopies. Chapter 1 describes the sustained release of bFGF, bone morphogenetic protein-2 (BMP-2), TGF-β1, and vascular endothelial growth factor (VEGF) from the bioabsorbable gelatin hydrogel matrix incorporating these growth factors. Their release profile from the hydrogel matrix is evaluated in vitro as well as in vivo, and compared with the profile of matrix degradation to examine the effect of matrix degradation on the in vivo release profile of these growth factors.

It is of prime importance to assess the biological activity of the growth factor released from gelatin hydrogel matrices, even if in vivo retention of the growth factor is

Table 1. Characteristics of the growth factors used in this study

Growth factor	Isoelectric point (IEP)	Molecular structure	Biological substances for growth factor binding	Functions of growth factor
Basic fibroblast growth factor (bFGF)	9.6	Single polypeptide of 16kDa	Heparin or heparan sulfate	Stimulating the cells involved in the healing process (bone, cartilage, nerve, etc). Neovascularization
Transforming growth factor-β1 (TGF-β1)	9.5	Homodimer of disulfide-linked 12-15kDa subunits	Heparin or heparan sulfate Collagen type IV Latency associated protein Latent TGF-β1 binding protein	Enhancing the wound healing. Stimulating the osteoblast proliferation to enhance bone formation
Bone morphogenetic protein-2 (BMP-2)	8.5	Homodimer of disulfide-linked 16kDa subunits	Collagen type IV	Stimulating the mesenchymal stem cells to osteoblast lineage and inducing the bone formation both at bone and ectopic sites.
Vascular endothelial growth factor (VEGF)	8.5	Homodimer of disulfide-linked 19kDa subunits, consisting of 165 amino acids	Heparin or heparan sulfate	Stimulating the endothelial cell growth, angiogenesis, and capillary permeability.

expectedly prolonged by incorporation into the matrices. Chapters 2 through 4 investigate the induction of biological activity by the acidic gelatin hydrogel incorporating growth factors on the basis of the release profile of growth factors. Chapter 2 deals with BMP-2 which is most widely used as a growth factor having a strong bone induction capability both at ectopic and bone sites[26-28,30,41]. Since it is often difficult to distinguish the newly formed bone from the intact one, ectopic bone formation at the back subcutis of mice is examined to evaluate the bone inductive activity of the hydrogel incorporating BMP-2 by comparing with that of free BMP-2.

Chapter 3 focuses on the controlled release of TGF-β1 which can induce bone formation only at bone sites although this growth factor belongs to the same family as BMP-2. The bone induction effect of TGF-β1 is known to be weaker than that of BMP-2, but it is expected that incorporation of TGF-β1 into the acidic gelatin hydrogel promotes bone regeneration at the bone defect, in contrast to TGF-β1 administered in the solution form. In vivo release profile of TGF-β1 from hydrogels with different biodegradation kinetics is compared with bone regeneration effects of the TGF-β1-incorporating hydrogels at the bone defect. This result will clarify the function of the hydrogel matrix in tissue regeneration of the defect both as a carrier of TGF-β1 release and as a barrier for making space to prevent the ingrowth of fibrous tissues into the defect.

One of the crucial factors that should be taken into consideration in connection with the blast cell and scaffold for tissue regeneration is to sufficiently supply nutrients and oxygen for cell survival in the scaffold[6,15-18,22-25,31]. It is very likely that simple diffusional supply of oxygen and nutrients to cells in the scaffold is not sufficient enough for cell survival. One way to provide cells with abundant nutrients is to induce formation of new blood vessels (neovascularization) in the scaffold. The study summarized in Chapter 4 is undertaken to

evaluate the effect of pore size of a scaffold on the ingrowth extent of new blood vessels into the scaffold. The neovascularization is induced by gelatin hydrogel microspheres incorporating an angiogenetic factor, bFGF. Poly (vinyl alcohol) (PVA) sponge with different pore sizes is used as a model porous scaffold, because the porous sponge is easy to keep hydrogel microspheres inside the scaffold and promote the ingrowth blood capillaries into the sponge.

Part II of this thesis is directed to evaluation of structural integration of the bone tissues regenerated by use of polymer matrices together with or without growth factor. The study given in Chapter 5 is carried out in an attempt to accumulate basic information about the ultrastructure of a construct generated by bone forming cells, osteoblastic cells, cultured on a polymer with different surfaces. They are modified with major bone ECM components, type I collagen and hydroxyapatite (HAp), based on a technique of surface graft polymerization. The HAp-predeposited surface is expected to promote in vitro mineral deposition in the ECM produced by osteoblastic cells and to differentiate the cells into cuboid, osteocyte-like cells. If this occurs, the HAp-deposition may be concluded to enable osteoblastic cells to work even in vitro in a manner similar to the natural bone tissue.

Chapter 6 compares the structure of the natural bone tissue with that of the bone-like tissue ectopically regenerated with a non-woven poly(glycolic acid) (PGA) fabric and an acidic gelatin hydrogel matrix incorporating BMP-2. Bone formation is attempted in the rat muscle to evaluate light-microscopically the effect of the shape of matrices on BMP-2-induced bone regeneration and subsequent integration of regenerated bone. This finding will suggest that the structure of the tissue regenerated depends on the texture of growth factor carriers.

In Chapter 7, transmission electron microscope (TEM) observation is performed to

investigate the ultrastructure of the bone ectopically formed with the gelatin hydrogel incorporating BMP-2. A crystallographic analysis with TEM is employed to reveal that the deposition pattern of HAp along collagen fibers in the bone tissue formed is identical with that in the natural bone tissue[42-46].

In summary, this thesis will describe the feasibility of growth factor release from the acidic gelatin hydrogel matrix for tissue regeneration, and the macroscopic and microscopic structures of the tissue regenerated. It will be concluded that this gelatin hydrogel is promising as a release system of growth factors for tissue engineering.

References

1. *Biomaterials science-An introduction to materials in medicine*, B. D. Ratner, A. S. Hoffman, F. J. Schoen, and J. E. Lemons eds., Academic press, California, USA (1996).
2. *Tissue engineering*, R. Skalak and C. F. Fox, Alan R. Liss, New York, USA (1988).
3. R. Langer and J. P. Vacanti, Tissue engineering, *Science*, **260**, 920-926 (1993).
4. *Special issue on tissue engineering*, A. G. Mikos ed., *Biomaterials*, **17**, 81-393 (1996).
5. *Synthetic biodegradable polymer scaffolds*, A. Atala, D. J. Mooney, J. P. Vacanti, and R. Langer eds., Birkhäuser, Boston USA (1997).
6. *Frontiers in tissue engineering*, C. W. Patrick Jr., A. G. Mikos, and L. V. McIntire eds., Pergamon, UK (1998).
7. G. Naughton, Tissue engineering-New challenges, *ASAIO J.*, **44**, 115-116 (1998).
8. *Special issue on polymers for tissue engineering*, M. Shoichet and J. A. Hubbell eds., *J. Biomater. Sci. Polymer Edn.*, **9**, 205-312, 405-518, 627-778 (1998).
9. D. L. Stocum, New tissues from old, *Science*, **276**, 15 (1997).
10. G. K. Michalopoulos and M. C. DeFrances, Liver Regeneration, *Science*, **276**, 60-66 (1997).
11. R. McKay, Stem cell in the central nervous system, *Science*, **276**, 66-71 (1997).
12. D. J. Prockop, Marrow stromal cells as stem cells for nonhematopoietic tissues, *Science*, **276**, 71-74 (1997).
13. P. Martin, Wound healing-Aiming for perfect skin regeneration, *Science*, **276**, 75-81 (1997).

14. J. P. Brockes, Amphibian limb regeneration: Rebuilding a complex structure, *Science*, **276**, 81-87 (1997).

15. L. E. Freed, J. C. Marquis, A. Nohria, J. Emmanual, A. G. Mikos, and R. Langer, Neocartilage formation in vitro and in vivo using cells cultured on synthetic biodegradable polymers, *J. Biomed. Mater. Res.* **27**, 11-23 (1993).

16. A. G. Mikos, G. Sarakinos, S. M. Leite, J. P. Vacanti and R. Langer, Laminated three-dimensional biodegradable forms for use in tissue engineering, *Biomaterials* **14**, 323-330 (1993).

17. A. G. Mikos, G. Sarakinos, M. D. Lyman, D. E. Ingber, J. P. Vacanti, and R. Langer, Prevascularization of porous biodegradable polymers, *Biotech. Bioeng.*, **42**, 716-723 (1993).

18. M. C. Wake, C. W. Patrick, Jr., and A. G. Mikos, Pore morphology effects on the fibrovascular tissue growth in porous polymer substrates, *Cell Transplant.*, **3**, 339-343 (1994).

19. R. C. Thomson, M. J. Yaszemski, J. M. Powers, and A. G. Mikos, Fabrication of biodegradable polymer scaffolds to engineer trabecular bone, *J. Biomater. Sci. Polymer Edn.*, 7, 23-38 (1995).

20. I. V. Yannas, E. Lee, D. P. Orgill, E. M. Skrabut, and G. F. Murphy, Synthesis and characterization of a model extracellular matrix that induces partial regeneration of adult mammalian skin, *Proc. Natl. Acad. Sci. USA*, **86**, 933-937 (1989).

21. B. P. Robinson, J. O. Hollinger, E. H. Szachowicz, and J. Brekke, Calvarial bone repair with porous D, L-polylactide, *Otolaryngol. Head Neck Surg.*, **112**, 707-713 (1995).

22. D. J. Mooney, P. M. Kaufmann, K. Sano, K. M. McNamara, J. P. Vacanti, and R.

Langer, Transplantation of hepatocyres using porous, biodegradable sponges, *Transplant. Proc.*, **26**, 3425-3426 (1994).

23. S. L. Ishaug-Riley, G. M. Crane, A. Gurlek, M. J. Miller, A. W. Yasko, M. J. Yaszemski, and A. G. Mikos, Ectopic bone formation by marrow stromal osteoblast transplantation using poly(DL-lactic-co-glycolic acid) foams implanted into the rat mesentery, *J. Biomed. Mater. Res.*, **36**, 1-8 (1997).

24. S. L. Ishaug, G. M. Crane, A. Gurlek, M. J. Miller, A. W. Yasko, M. J. Yaszemski, and A. G. Mikos, Bone formation by three-dimensional stromal osteoblast culture in biodegradable polymer scaffolds, *J. Biomed. Mater. Res.*, **36**, 17-28 (1997).

25. D. J. Mooney, K. Sano, P. M. Kaufmann, K. Majahod, B. Schloo, J. P. Vacanti and R. Langer, Long-term engraftment of hepatocytes transplanted on biodegradable polymer sponges, *J. Biomed. Mater. Res.*, **37**, 413-420 (1997).

26. R. A. Kenley, K. Yim, J. Abrams, E. Ron, T. Turek, L. J. Marden, and J. O. Hollinger, Biotechnology and bone graft substitute, *Pharm. Res.*, **10**, 1393-1401 (1993).

27. T. A. Linkhart, S. Mohan, and D. J. Baylink, Growth factors for bone growth and repair: IGF, TGF-β and BMP, *Bone*, **Suppl.19**, S1-S2 (1996).

28. M. Lind, Growth factors: Possible new clinical tools, *Acta Orthop. Scand.*, **67**, 407-417 (1997).

29. J. Taipale and J. Keski-Oja, Growth factors in the extracellular matrix, *FASEB J.* **11**, 51-59 (1997).

30. M. E. Nimni, Polypeptide growth factors: targeted delivery systems, *Biomaterials*, **18**, 1201-1225 (1997).

31. G. Ahrendt, D. E. Chickering, and J. P. Ranieri, Angiogenic growth factors: A review for tissue engineering, *Tissue Engineering*, **4**, 117-130 (1998).

32. M. C. Manning, K. Patel, and T. Borchardt, Stability of protein pharmaceuticals, *Pharm. Res.*, **6**, 902-918 (1989).

33. Y. J. Wang and A. Hanson, Parenteral formulations of proteins and peptides: stability and stabilizers, *J. Parenter. Sci. Technol.*, **Suppl. 42**, S2-S26 (1988).

34. Y. Tabata and Y. Ikada, Protein release from gelatin matrices, *Adv. Drug Delivery Review*, **31**, 287-301 (1998).

35. D. Gospodarowizc, N. Ferrara, L. Schweigerer, and G. Neufeld, Structural characterization and biological functions of fibroblast growth factor, *Endocr. Rev.*, **8**, 95-114 (1987).

36. D. B. Rifkin and D. Moscatelli, Recent development in the cell biology of basic fibroblast growth factor, *J. Cell Biol.*, **109**, 1-6 (1989).

37. D. Gospodarowizc, Biological activities of fibroblast growth factor, *Ann. NY Acad. Sci.*, **638**, 1-8 (1991).

38. J. Taipale, K. Miyazono, C. Heldin, and J. Keski-Oja, Latent transforming growth factor-β1 associates to fibroblast extracellular matrix via latent TGF-β1 binding protein, *J. Cell Biol.*, **124**, 171-181 (1994).

39. J. Saharinen, J. Taipale, and J. Keski-Oja, Association of the small latent transforming growth factor-β with an eight cysteine repeat of its binding protein LTBP-1, *EMBO J.*, **15**, 245-253 (1996).

40. D. Zekorn, Modified gelatin as plasma substitutes, *Bibl. Haematol.*, **33**, 30-60 (1969).

41. *Bone morphogenetic proteins: biology, biochemistry, and reconstructive surgery*, T. S. Lindholm ed., R. G. Landes Company and Academic Press Inc., Texas, USA (1996).

42. P. Fratzl, N. Fratzl-Zelman, K. Klaushofer, G. Vogl, and K. Koller, Nucleation and

growth of mineral crystals in bone studied by small-angle X-ray scattering, *Calcif. Tissue Int.*, **48**, 407-413 (1991).

43. W. J. Landis, The strength of a calcified tissue depends in part on the molecular structure and organization of its constituent mineral crystals in their organic matrix, *Bone*, **16**, 533-544 (1995).

44. W. J. Landis, K. J. Hodgens, M. J. Song, J. Arena, S. Kiyonaga, M. Marko, C. Owen, and B. F. McEwen, Mineralization of collagen may occur on fibril surfaces: evidence from conventional and high-voltage electron microscopy and three-dimensional imaging, *J. Struct. Biol.*, **117**, 24-35 (1996).

45. H. B. Wen, F. Z. Cui, Q. L. Feng, and H. D. Li, Microstructural investigation of the early external callus after diaphyseal fractures of human long bone, *J. Struct. Biol.*, **114**, 115-122 (1995).

46. F. Z. Cui, H. B. Wen, X. W. Su, and X. D. Zhu, Microstructures of external periosteal callus of repaired femoral fracture in children, *J. Struct. Biol.*, **117**, 204-208 (1996).

PART I

TISSUE REGENERATION THROUGH SUSTAINED RELEASE OF GROWTH FACTORS

Chapter 1

Comparison in the release profile of various growth factors from biodegradable hydrogel matrices

INTRODUCTION

Various growth factors have been recognized to act on different types of cells in the body to regulate their proliferation and differentiation by which tissue regeneration is promoted[1]. However, if a growth factor with a short half-life period is administered to the body in the solution form, the biological efficacy in tissue regeneration will not be always expected. Therefore, it is necessary to develop a matrix system which can achieve the sustained release of biologically active growth factors over an extended time period.

Gelatin is biodegradable and has been extensively utilized for pharmaceutical and medical purposes. Its biosafety has been proven through long clinical applications[2]. Another advantage of gelatin is the commercial availability of materials with different charges. For example, gelatin prepared with an alkaline process of collagen has an isoelectric point (IEP) of 5.0 and is negatively charged at the physiological pH, while an acidic process gives positively charged gelatin of an IEP of 9.0. Since growth factors are generally basic proteins, the negatively charged "acidic" gelatin will ionically interact with them.

This chapter deals with the sustained release of growth factors on the basis of polyion complexation with biodegradable hydrogels prepared through chemical crosslinking of the

acidic gelatin. In vitro release profile was investigated for several growth factors from the acidic gelatin hydrogel, while the in vivo release of growth factors was evaluated in terms of hydrogel degradation.

EXPERIMENTAL

Materials

Human recombinant bFGF with an IEP of 9.6 and human recombinant BMP-2 with an IEP of 8.5 were kindly supplied from Kaken Pharmaceutical Co. and Yamanouchi Pharmaceutical Co., Tokyo, Japan, respectively. Gelatin samples with IEPs of 5.0 and 9.0 (Nitta Gelatin Co., Osaka, Japan), isolated from the bovine bone with an alkaline process and from the porcine skin with an acidic process, are called here acidic and basic gelatin, respectively, based on their electrical feature. $Na^{125}I$ (740 MBq/ml in 0.1 N NaOH aqueous solution), Bolton-Hunter [^{125}I]-labeled TGF-β1 (IEP=9.5, 185 kBq/ml in 0.05 M sodium acetate buffer), and ^{125}I-labeled VEGF (IEP=8.5, 370 kBq/mL in 0.05 M phosphate buffer), were purchased from NEN Research Products, DuPont, Wilmington, DE. An anion-exchange resin, Dowex 1-8X, was obtained from Dow Chemicals Co., Ltd., Midland, MI. Other chemicals of analytical grade were used without further purification.

Preparation of gelatin hydrogels incorporating growth factors

Glutaraldehyde was added to 30 mL of 5 wt% aqueous solution of acidic or basic gelatin to give the final concentration of 0.05 or 0.9 wt%, respectively. The mixed solution

was cast into a polypropylene mold (138 x 138 mm^2), followed by leaving at 4 °C for 12 hr to allow crosslinking reaction of gelatin to proceed. The resulting hydrogel sheets were punched out to obtain gelatin hydrogel discs (5 mm diameter and 2 mm thickness). They were placed in 100 mM glycine aqueous solution at 37 °C for 1 hr to block residual aldehyde groups of glutaraldehyde, and then washed 3 times with double distilled water (DDW) at 37 °C. Finally, they were freeze-dried and sterilized by ethylene oxide gas. The weight percentage of water in the hydrogel was determined from the hydrogel weight before and after drying at 70 °C under vacuum for 6 hr. The water content of the acidic and basic gelatin hydrogels used in this chapter was approximately 95 wt%[3].

BMP-2 and bFGF were radioiodinated according to the method of Greenwood et al[4]. To impregnate growth factors into acidic and basic gelatin hydrogels, 20 μl of aqueous solution containing one of ^{125}I-labeled growth factors was dropped onto a freeze-dried hydrogel, followed by leaving at 4 °C overnight to obtain a gelatin hydrogel incorporating the ^{125}I-labeled growth factor. Since the volume of growth factor aqueous solution was much less than that theoretically impregnated into each of the hydrogels, 100 % of the added growth factor could be entirely incorporated into the hydrogel. The size of the hydrogel disc did not change during freeze-drying and sterilization processes and the dry weight was 7 mg.

Evaluation of growth factor sorption to hydrogel matrices

Sorption of growth factors into acidic and basic gelatin hydrogels was performed in aqueous solution containing ^{125}I-labeled growth factors at pH 7.4. The solution ionic strength was adjusted to 0, 0.2, 0.4, 0.8, and 1.5 by NaCl addition. Briefly, a freeze-dried hydrogel was pre-swollen at 37 °C for 12 hr in the solution at the same ionic strength as the growth factor

solution used for the sorption study. Then, the swollen hydrogel was placed in 1 mL of growth factor solution at 4 °C. At different time intervals, supernatants were taken out to measure their radioactivity on a gamma counter (ARC-301B, Aloka Co., Tokyo, Japan), while the radioactivity of the gelatin hydrogel and the tube used was measured to estimate the mass balance of growth factors.

Evaluation of in vitro release of growth factors

An acidic gelatin hydrogel incorporating an ^{125}I-labeled growth factor was placed in 1 ml of phosphate-buffered saline solution (PBS, pH 7.4) followed by shaking at 37 °C. The supernatant PBS was periodically taken out to measure the radioactivity on the gamma counter. Fresh PBS of the same volume was added to continue the release test. Similarly, release tests were performed in PBS at ionic strengths ranging from 0 to 1.5 to evaluate the effect of solution ionic strength on the growth factor release. The amount of released growth factors was assessed 3 hr after the release test started.

Evaluation of in vivo release of growth factors

The acidic gelatin hydrogel incorporating an ^{125}I-labeled growth factor was implanted into the back subcutis of 6-week-old female ddY mice (Shimizu Laboratory Animal Supply Co., Ltd., Kyoto, Japan). As a control, 100 μl of aqueous solution of ^{125}I-labeled growth factors at the same dose was subcutaneously injected into the mouse back at the central position 15 mm away from the tail root. Each experimental group was composed of 4-8 mice. At different time intervals, mice were sacrificed, and the back skin (3 x 5 cm^2) around the hydrogel implanted or injected site of growth factors was cut out and the corresponding facia

was thoroughly wiped off with filter paper to absorb the ^{125}I-labeled growth factor. The radioactivity of remaining gelatin hydrogels, the skin piece, and the filter paper was measured on the gamma counter. The percentage of the remaining radioactivity was expressed as the radioactivity ratio of the test samples to the original hydrogel or aqueous solution containing the ^{125}I-labeled growth factors.

Evaluation of in vivo degradation of hydrogel matrices

^{125}I-labeled gelatin hydrogels were implanted in the back subcutis of mice. At different time intervals, the radioactivity of explanted hydrogels and the surrounding tissues was measured to evaluate the time profile of in vivo hydrogel degradation. The percentage of the remaining radioactivity was expressed as the radioactivity ratio of the remaining hydrogels to the original ^{125}I-labeled gelatin hydrogel.

RESULTS

Growth factor sorption to hydrogel matrices

Figure 1 shows the time course for sorption of growth factors to the hydrogels prepared from gelatin with IEPs of 5.0 and 9.0 in DDW at 4 °C. The amount of bFGF and TGF-β1 sorbed to the acidic gelatin hydrogel increased with time, whereas no and less sorption to the basic gelatin was observed for bFGF and TGF-β1, respectively. Both BMP-2 and VEGF were hardly sorbed to both the acidic and basic gelatin hydrogels.

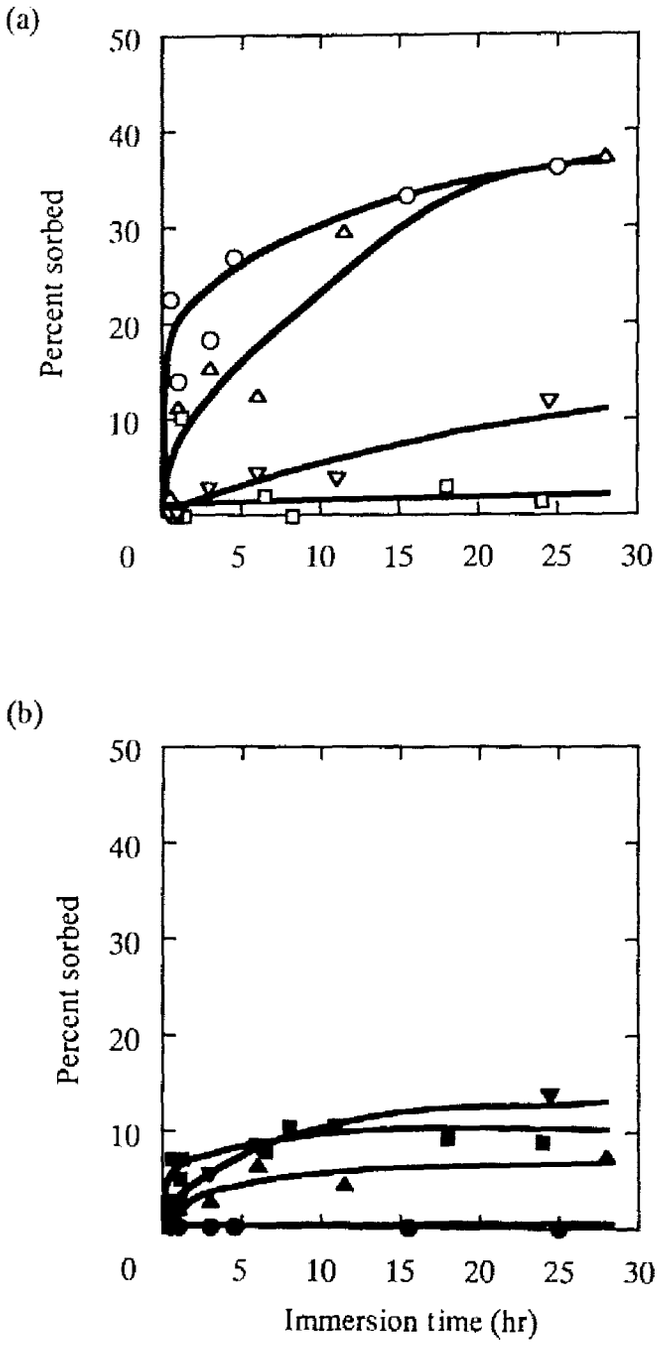

Figure 1. The time course of in vitro sorption of bFGF (○,●), TGF-β1 (△,▲), BMP-2 (□,■), and VEGF (▽,▼) to hydrogels of gelatin with IEPs of 5.0 (a) and 9.0 (b) in DDW at 4°C.

Figure 2 shows the effect of ionic strength on the sorption of growth factors to the acidic gelatin hydrogel in aqueous solution at 4 °C. Apparently, bFGF and TGF-β1 sorption depended on the ionic strength of solution and their sorption reduced with an increase in ionic strength. On the contrary, such a noticeable influence of growth factor sorption on the solution ionic strength was not observed for BMP-2 and VEGF.

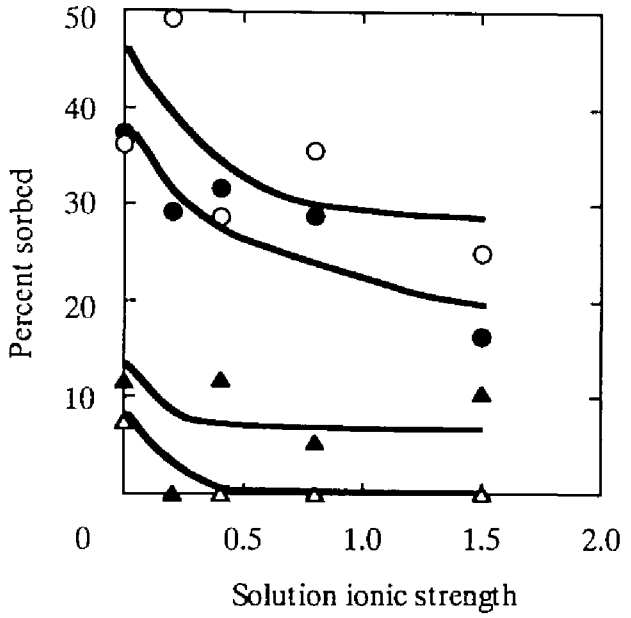

Figure 2. Sorption of bFGF(○), TGF-β1(●), BMP-2 (△), and VEGF (▲) to acidic gelatin hydrogels at 4°C in aqueous solutions of different ionic strengths.

In vitro release of growth factors

Figure 3 shows the in vitro release profile of bFGF, TGF-β1, BMP-2, and VEGF from the acidic gelatin hydrogel incorporating one of the growth factors. Approximately 20 % of the incorporated bFGF and TGF-β1 was released into PBS within the initial 1 hr of release test, but, thereafter, no further release was observed. The amount of released bFGF initially seemed to be lower than that of TGF-β1. On the other hand, more than 80 % of the incorporated BMP-2 was rapidly released from the gelatin hydrogel for scores of minutes.

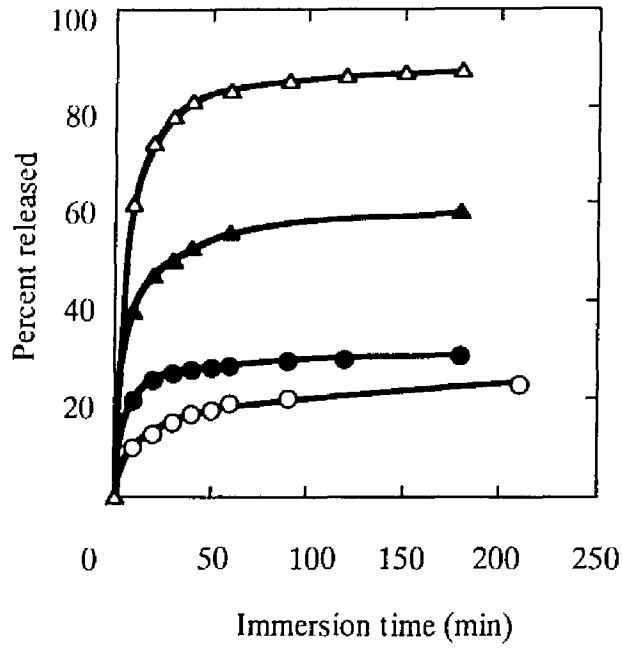

Figure 3. In vitro release profile of growth factors from the acidic gelatin hydrogel incorporating the growth factors at 37 °C in PBS: bFGF (○), TGF-β1 (●), BMP-2 (△), and VEGF (▲).

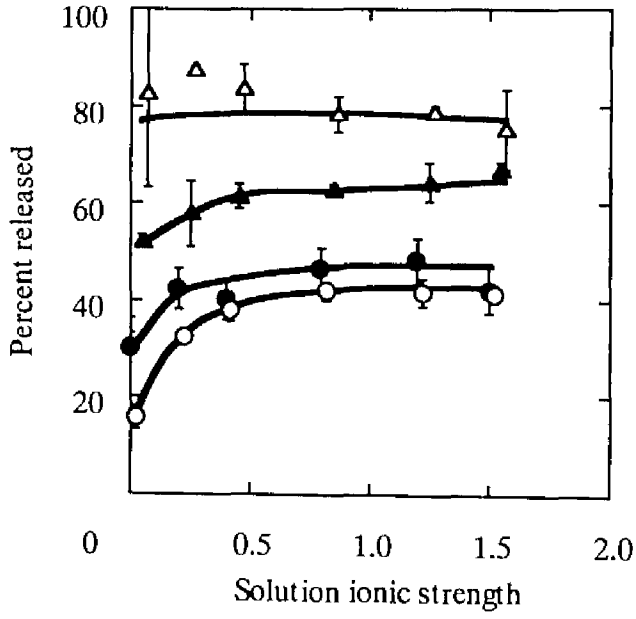

Figure 4. Growth factor release from the acidic gelatin hydrogel incorporating the growth factors at 37°C in PBS of different ionic strengths: bFGF (○), TGF-β1 (●), BMP-2 (△), and VEGF (▲).

The initial release amount of VEGF was between those of the two groups.

Figure 4 shows the effect of solution ionic strength on the in vitro growth factor release at 37 °C. The amount of bFGF, TGF-β1, and VEGF released for the initial 3 hr tended to increase with an increase in the solution ionic strength, in contrast to BMP-2.

In vivo release of growth factors

Figure 5 shows the in vivo decrement pattern of radioactivity for different growth factors after subcutaneous implantation of the gelatin hydrogels incorporating ^{125}I-labeled growth factors into the mouse back. Irrespective of the type of growth factors, more than 80 % of the growth factor injected in the solution form was cleared from the injected site within one day. The radioactivity decrease for bFGF and TGF-β1 incorporated in the acidic gelatin hydrogel was much slower than that injected in their solution form. Incorporation into the gelatin hydrogel prolonged the in vivo retention of bFGF for a longer time period than TGF-β1. However, such prolonged retention by hydrogel incorporation was not observed for BMP-2. Although the radioactivity of VEGF incorporated in the acidic gelatin hydrogel decreased much faster than that of bFGF and TGF-β1, its retention was slightly prolonged compared with that injected in the solution form.

Relationship between the in vivo growth factor release and the gelatin hydrogel degradation

Figure 6 shows the time course of the gelatin radioactivity remaining after subcutaneous implantation of ^{125}I-labeled gelatin hydrogels into the mouse back. The radioactivity of the gelatin hydrogels decreased with implantation time. To evaluate the

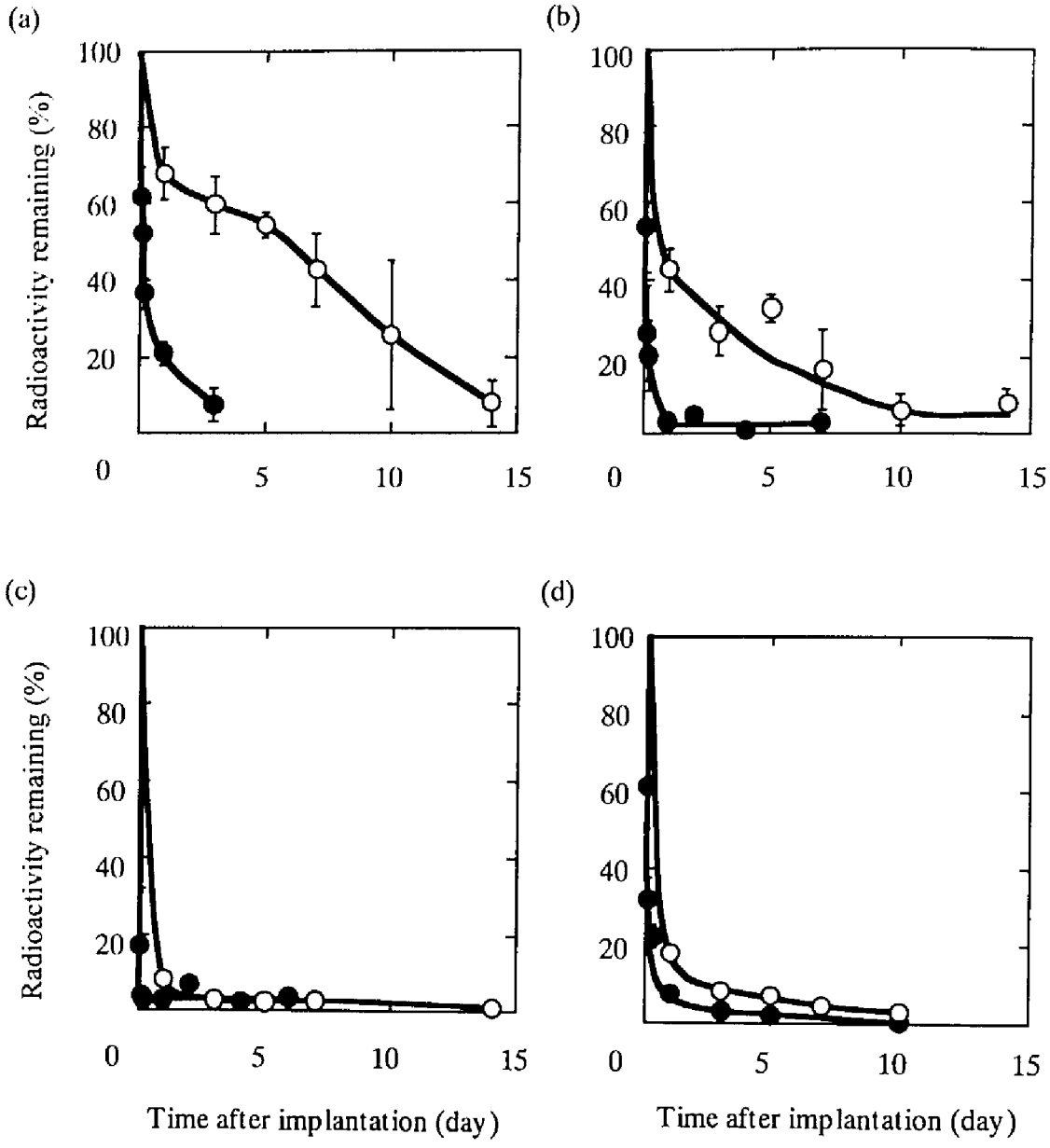

Figure 5. In vivo time profile of the radioactivity remaining in the back subcutis of mice following the subcutaneous implantation of the acidic gelatin hydrogel incorporating ^{125}I-labeled growth factors (○) or the subcutaneous injection of ^{125}I-labeled growth factors in aqueous solution (●): bFGF (a), TGF-β1 (b), BMP-2 (c), and VEGF (d).

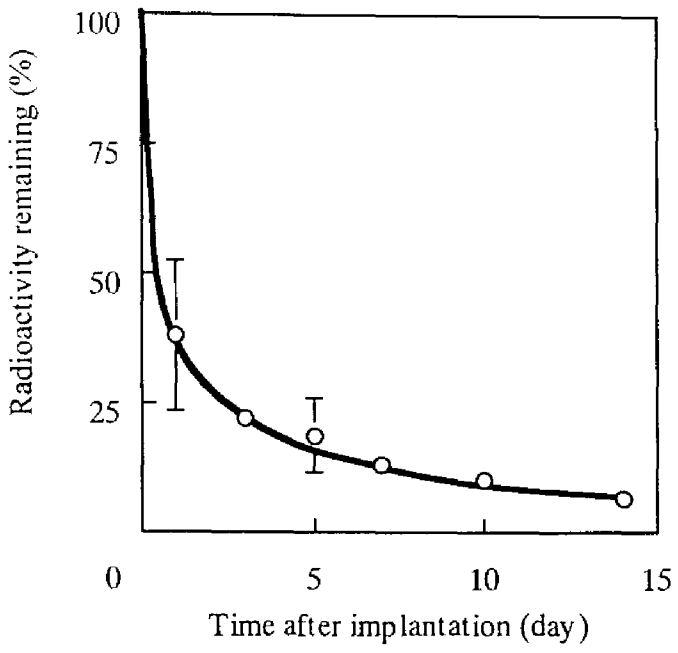

Figure 6. In vivo time profile of the radioactivity remaining in the back subcutis of mice following the subcutaneous implantation of the ^{125}I-labeled acidic gelatin hydrogel.

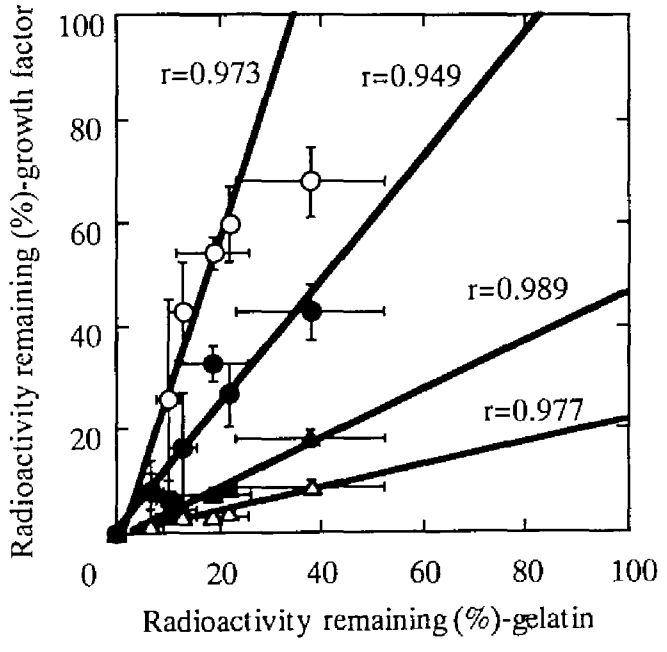

Figure 7. The radioactivity of the remaining ^{125}I-labeled acidic gelatin hydrogel plotted against the radioactivity of the remaining ^{125}I-labeled growth factor: bFGF (○), TGF-β1 (●), BMP-2 (△), and VEGF (▲).

relationship between the growth factor release and the hydrogel degradation, the remaining in vivo radioactivity of acidic gelatin hydrogels incorporating ^{125}I-labeled bFGF, TGF-β1, BMP-2, and VEGF was plotted against that of ^{125}I-labeled gelatin hydrogels at the corresponding time. The result is shown in Figure 7. There was a distinct correlation between the two remaining radioactivities for each growth factor.

DISCUSSION

It is apparent from Figure 1 that basic bFGF and TGF-β1 molecules could be sorbed with time to the acidic gelatin hydrogel, in marked contrast to the basic gelatin hydrogel. This can be explained in terms of the electrostatic interaction between the basic growth factors and the acidic gelatin. It is possible that the basic growth factors electrostatically interact with the acidic gelatin constituting the hydrogel. The electrostatic repulsion between the basic growth factors and the basic gelatin will result in no sorption. The reduced sorption of these two growth factors by an increase in solution ionic strength (Figure 2) also indicates that the electrostatic force contributes to the sorption behavior. However, BMP-2 and VEGF were sorbed to the acidic gelatin hydrogel to a much smaller extent than bFGF and TGF-β1, though BMP-2 and VEGF have IEPs higher than 7.0. It has been reported that the zeta potential of BMP-2 is reduced by binding of oligomannose groups to their surface[5]. It is conceivable that surface covering of the BMP-2 molecule with the sugar residues weakened its electrostatic interaction with gelatin. Taken together, these results indicate that sorption of growth factors

to hydrogels is governed not only by the apparent charge of molecules but also by their three-dimensional structure.

Gelatin does not undergo hydrolytic degradation in media without enzymes, but by proteolysis. Therefore, gelatin hydrogels are not degraded under in vitro conditions unless proteases are present. Basic bFGF was found to be ionically complexed with the acidic gelatin[6]. It is likely that bFGF molecules, once complexed with the acidic gelatin hydrogel, cannot be released from the hydrogel unless hydrogel undergoes degradation. However, the impregnation condition of bFGF into the acidic gelatin hydrogel, e.g., at 4 °C overnight, is not sufficient enough to achieve 100 % complexation[7]. This causes a small bFGF release at the initial period of release test (Figure 3). A large initial burst noticed in BMP-2 release from the acidic gelatin hydrogel may be due to too low capability of BMP-2 to interact with the acidic gelatin. This burst pattern observed for TGF-β1 and VEGF release can be explained from the view point of polyion complexation with the acidic gelatin. The sorption profile of growth factors suggests the order of complexation susceptibility to be bFGF > TGF-β1 >> VEGF > BMP-2. It is possible that the lower the complexation susceptibility of growth factors, the harder the polyion complexation with the acidic gelatin, resulting in larger burst effect of the uncomplexed molecules in the initial release. Figure 4 shows the influence of solution ionic strength on the growth factor release decrease to be in the order of bFGF, TGF-β1, and VEGF, and finally no influence for BMP-2. This also suggests that the initial burst of growth factors is influenced by their ionic interaction.

Since bFGF incorporation had no influence on the in vivo degradation of gelatin hydrogels[3], we can assume that the growth factor-incorporating gelatin hydrogel was degraded in a profile similar to the growth factor-free hydrogel. When experimental data were

approximated by a straight line for each growth factor, the slope of bFGF and TGF-β1 lines was larger than 1.0, whereas that of BMP-2 and VEGF was smaller than 1.0. The order of the line slope magnitude was equivalent to that of the complexation susceptibility with the acidic gelatin. This indicates that the difference in the slope is due to the different growth factor-gelatin interactions. Since BMP-2 does not have sufficient capability to interact with the acidic gelatin, the uninteracted molecules will be released from the hydrogel by simple diffusion (Figure 3). Thus, it is possible that this BMP-2 property causes its rapid release from the hydrogel even in vivo, leading to the smallest slope. The slope of the VEGF line was larger than that of BMP-2, but smaller than that of bFGF and TGF-β1 slope. This may be due to its complexation susceptibility to the acidic gelatin, which is stronger than that of BMP-2, but weaker than that of bFGF and TGF-β1. Since the complexed growth factor does not readily dissociate from the acidic gelatin molecules constituting hydrogels, it will be released only when the gelatin hydrogel is degraded and gelatin molecules become water-soluble. As a result, the radioactivity of remaining bFGF and TGF-β1 would always be high compared with that of the gelatin hydrogel. It is no doubt that the larger slope of the bFGF line than TGF-β1 is ascribed to the stronger interaction of bFGF with the acidic gelatin.

Growth factors are stored in the body under complexation with various components in the extracellular matrix[8]. It is well known that the extracellular matrix protects growth factors from their enzymatic degradation and denaturation. The release system described in this chapter is based on this polyion complexation which is ubiquitously seen in the body. Once a basic growth factor is ionically immobilized in the acidic gelatin hydrogel, it will be released only when the hydrogel is biodegraded. In other words, the growth factor release can be

controlled by biodegradation of the hydrogel itself. This release concept seems to be applicable to other bioactive proteins.

References

1. D.L.Stocum, Frontiers in medicine: regeneration, *Science*, **276**, 59-87 (1997).
2. D. Zekorn, Modified gelatin as plasma substitutes, *Bibl. Haematol.*, **33**, 30-60 (1969).
3. Y. Tabata, S. Hijikata, and Y. Ikada, Enhanced vascularization and tissue granulation by basic fibroblast growth factor impregnated in gelatin hydrogel, *J. Controll. Release*, **31**, 189-199 (1994).
4. F. C. Greenwood, W. M. Hunter, and T. C. Gglover, The preparation of ^{131}I-labeled human growth hormone of high specific radioactivity, *Biochem. J.* **89**, 114-123 (1963).
5. K. Yim, J. Abrams, and A. Hsu, Capillary zone electrophoretic resolution of recombinant human bone morphogenetic protein 2 glycoforms. An investigation into the separation mechanisms for an exquisite separation, *J. Chromatogr. A*, **716**, 401-412 (1995).
6. Md. Muniruzzaman, Y. Tabata, and Y. Ikada, Complexation of basic fibroblast growth factor with gelatin, *J. Biomater. Sci. Polym. Ed.*, **9**, 459-473 (1998).
7. Y. Tabata and Y. Ikada, Protein release from gelatin matrices, *Adv. Drug Delivery Reviews*, **31**, 287-301 (1998).
8. J. Taipale and J. Keski-Oja, Growth factors in the extracellular matrix, *FASEB J.*, **11**, 51-59 (1997).

Chapter 2

Ectopic bone formation induced by biodegradable hydrogel matrices incorporating BMP-2

INTRODUCTION

Bone regeneration has attracted much attention in the field of tissue engineering because of its high clinical requirement. A promising way to induce regeneration of autogeneous osseous tissues in bone defect is to make use of bone-related growth factors, such as BMP[1-24, 38, 39], TGF-β1[25-29], and bFGF[30-32]. Combination of these growth factors with various carriers has been found to be effective in bone regeneration, similar to auto- and allo-bone grafts.

BMP was originally characterized by Urist et al. as a bone inductive material at an ectopic site [7]. Currently, at least seven distinct human BMPs are isolated, identified, and cloned[8, 9]. In addition, some of them are found to stimulate mesenchymal cells and myoblasts to differentiate into cells of osteoblast lineage[3, 5, 9]. However, one cannot always expect expression of its biological function if BMP is injected into the body without any release matrices, since the BMP diffuses quickly from the implantation site. Therefore, various materials, including fibrin glues[10, 11], glycolide-lactide copolymers[12-20], and calcium phosphates[21-24] have been employed as carrier matrices of BMP for its sustained release. All these studies demonstrated high efficacy of the carrier matrices for bone induction. Although a significant relationship

between the release profile of BMP and bone induction has been discussed in some reports, few papers have studied this relationship in detail.

Bone formation is normally evaluated by use of an animal model with a bone defect, but it is often difficult to distinguish the newly formed bone from the intact one, thereby making it difficult to analyze the osteogenic effect of the growth factor-carrier composite. On the contrary, the in vivo efficacy of bone-related growth factors will be readily apparent if bone is ectopically formed in nonosseous tissues. It is well recognized that BMP is the only growth factor that can induce bone formation in the muscle and subcutaneous tissues[7, 8, 10, 11, 13, 17, 19, 21, 38, 39].

Gelatin is biodegradable and used extensively for pharmaceutical and medical purpose. Biosafety of gelatin has been proven through its long clinical application[33]. Other advantages of gelatin are its high chemical reactivity and commercial availability of various charged gelatin samples. Tabata et al. have prepared biodegradable hydrogels from acidic gelatin with an IEP of 5.0 and succeeded in sustained release of biologically active bFGF with significant angiogenetic[34] and osteogenetic effects[32], which were not observed when free bFGF was administered.

The objective of this chapter is to incorporate recombinant human BMP-2 in hydrogels of gelatin with the IEPs of 5.0 and 9.0 and compare the ectopic bone formation induced by this BMP-2-incorporating gelatin hydrogel with that induced by simple BMP-2 aqueous solution. In vitro and in vivo BMP-2 release from the BMP-2-incorporating gelatin hydrogel were examined to assess the efficacy of this hydrogel as the release matrix of BMP-2. Following the subcutaneous implantation of BMP-2-incorporating gelatin hydrogel in the back of mice, the effect of BMP-2 release on ectopic bone formation is described in this chapter.

EXPERIMENTAL

Materials

BMP-2 with an IEP of 8.5 was supplied from Yamanouchi Pharmaceutical Co., Tokyo, Japan. Gelatin samples with IEPs of 5.0 and 9.0 were isolated from the bovine bone with the alkaline process and from the porcine skin with the acid process (Nitta Gelatin Co., Osaka, Japan) and are here called acidic and basic gelatin, respectively, because of their electrical feature. It is known that the alkaline process through hydrolysis of amide groups of collagen yields gelatin having a higher amount of carboxyl groups, resulting in a reduced IEP of gelatin, whereas the acid process dose not affect the collagen IEP[35]. Other chemicals were obtained from Wako Pure Chemical Industries, Osaka, Japan and used without further purification. $Na^{125}I$, 740 MBq/mL in 0.1 N NaOH aqueous solution, and an anion-exchange resin, Dowex 1-8X, were purchased from NEN Research Products, Du Pont, Wilmington, DE and Dow Chemicals Co., Ltd., Midland, MI, respectively.

Radioiodination of BMP-2

BMP-2 was radioiodinated according to the method of Greenwood et al.[36]. Briefly, 4 μL of $Na^{125}I$ and 100 μL of 0.5 M potassium phosphate-buffered solution (KPB, pH 7.5) were added to the mixture of 40 μl of 0.5 mg/mL BMP-2 solution in 5 mM glutamic acid, 2.5 wt% glycine, 0.5 wt% sucrose, and 0.01 wt% Tween 80 (pH 4.5). Then, 100 μL of chloramine-T in 0.05 M KPB solution (pH 7.2) at 0.2 mg/mL was added to the solution mixture. After agitation at room temperature for 2 min, 100 μL of DDW containing 0.4 mg of sodium metabisulfate was added to the mixed solution to stop the radioiodination. The reaction mixture was passed

through a column of an anionic-exchange Dowex to remove the uncoupled, free ^{125}I molecules from the ^{125}I-labeled BMP-2.

Preparation of hydrogel matrices incorporating BMP-2

Hydrogels were prepared through crosslinking of aqueous gelatin solutions with glutaraldehyde according to the method described elsewhere[32]. Briefly, 5 wt% aqueous solution of acidic or basic gelatin containing 0.05 or 0.9 wt% glutaraldehyde, respectively, was cast into a teflon mold of 2 mm depth. Following the crosslinking reaction at 4 °C for 12 hr, crosslinked hydrogels were punched out to produce discs of 5 mm diameter. The hydrogels were immersed in 100 mM aqueous glycine solution at 37 °C for 1 hr to block residual aldehyde groups of glutaraldehyde, followed by washing with DDW. Following immersion in 70 vol% ethanol to sterilize, they were thoroughly rinsed with autoclaved DDW and aseptically freeze-dried. The weight percentage of water in the hydrogel was determined from the hydrogel weight before and after drying at 70 °C under vacuum for 6 hr. The water content of acidic and basic gelatin hydrogels used in this chapter was both approximately 95 wt%[34].

To impregnate BMP-2 into the hydrogels, 20 μL of aqueous solution containing 0.01, 0.05, 0.1, 0.5, 1.0, and 5.0 μg of BMP-2 or 0.5 μg of ^{125}I-labeled BMP-2 was dropped onto the freeze-dried hydrogel, followed by leaving them in the culture dish of 60 mm diameter with sealing with parafilm at 4°C overnight. BMP-2-incorporating gelatin hydrogel was used without washing. Since the volume of BMP-2 aqueous solution is much less than that theoretically impregnated into each hydrogel, the BMP-2 dose incorporated into the hydrogel is equal to the amount impregnated initially. Thus, in this chapter, the dose was indicated as the initial

impregnation amount. The size of hydrogel disc was 5 mm in diameter and 2 mm in thickness and its dry weight was 7 mg.

Evaluation of in vitro BMP-2 release

Gelatin hydrogels incorporating 0.5 μg of ^{125}I-labeled BMP-2 were incubated in 1 mL of PBS at 37 °C under shaking. At different time intervals, the supernatant PBS was taken out to measure the radioactivity on a gamma counter (ARC-301B, Aloka Co., Ltd., Tokyo, Japan), while fresh PBS was added and release test was continued.

Evaluation of in vivo BMP-2 release

^{125}I-labeled BMP-2-incorporating hydrogels were implanted into the back subcutis of 6 week-old female ddY mice. As a control, 100 μL of aqueous solution of ^{125}I-labeled BMP-2 was subcutaneously injected into the mouse back at the central position 15 mm away from their tail root. The dose of ^{125}I-labeled BMP-2 was 0.5 μg for both cases. At different time intervals, mice were sacrificed according to the institutional guidelines of Kyoto University on animal experimentation. The skin on the back of mice around the implanted or injected site of BMP-2 was cut into a strip of 3 x 5 cm^2 and the corresponding fascia was thoroughly wiped off with filter paper to absorb ^{125}I-labeled BMP-2. The radioactivity of gelatin hydrogel remaining, excised skin, and filter paper was measured on the gamma counter to assess the time profile of BMP-2 retention. Measurement of the radioactivity in the other parts of body, such as blood, heart, lung, thymus, thyroid, liver, spleen, gastrointestine, kidney, and carcass, was made to reveal no accumulation of BMP-2 in any specific organ. Gelatin hydrogels and 100 μL aqueous solution containing 0.5 μg of ^{125}I-labeled BMP-2 were kept at room temperature as a standard.

Measurement of the radioactivity of the standard was made together with experimental samples at each sampling time. The in vivo release profile was assessed based on the radioactivity ratio of samples to the standard.

Evaluation of ectopic bone formation

Acidic and basic gelatin hydrogels incorporating 0.01, 0.05, 0.1, 0.5, 1.0, and 5.0 μg of BMP-2 were implanted into the back subcutis of ddY mice, while 100 μL of aqueous BMP-2 solution at concentrations of 1×10^{-4}, 5×10^{-4}, 1×10^{-3}, 5×10^{-3}, 1×10^{-2}, and 5×10^{-2} $\mu g/\mu L$ was injected subcutaneously into mice as described above. Experimental group was composed of 4-8 mice. Acidic and basic gelatin hydrogels incorporating PBS and aqueous PBS solution were implanted as a control.

After 1, 2, and 3 weeks, the implanted site of BMP-2-incorporating gelatin hydrogels and the injected site of aqueous BMP-2 solutions were radiographically examined by soft x-rays (Hitex HX-100, Hitachi, Japan) at 54 KVP and 2.5 mA for 20 sec. When the radiopaque area on the x-ray film was larger by 1 mm^2 than that of PBS-treated groups, ectopic bone formation was defined as positive. The skin tissue was taken out together with the hydrogel implant or injected site, fixed with 10 vol% neutral formalin solution, dehydrated with ethanol, and embedded in paraffin. The fixed skin tissues were cross-sectioned to 10 μm thickness with a microtome and stained with Mayer's hematoxylin-eosin (H-E) solution. In addition, von Kossa staining was done to clarify calcium deposition in the specimens. The histological sections were viewed with an optical microscope.

RESULTS

In vitro BMP-2 release

Figure 1 shows the in vitro release profiles of BMP-2 from BMP-2-incorporating hydrogels prepared from acidic and basic gelatins. The initial BMP-2 dose was 0.5 μg/hydrogel. As can been seen, BMP-2 was gradually released with time from both the gelatin hydrogels, after approximately 60 to 75 % of BMP-2, which amount to 300 to 375 ng of BMP-2 when incorporated in the hydrogels, BMP-2 was released within 24 min. No significant difference was observed in BMP-2 release profile between acidic and basic gelatin hydrogels, while a little higher retention of BMP-2 was observed for the basic gelatin hydrogel than for the acidic one. The BMP-2 dose had little influence on the release from acidic and basic gelatin hydrogels.

In vivo BMP-2 release

Figure 2 shows the in vivo decrement patterns of BMP-2 from the implanted site of BMP-2-incorporating hydrogels or the injected site of aqueous BMP-2 solutions. The initial BMP-2 dose was 0.5 μg and almost 100 % of radioactivity initially applied was recovered. It is apparent that incorporation of BMP-2 into gelatin hydrogels prolonged in vivo BMP-2 retention, irrespective of the gelatin type. For example, 44 ng of BMP-2 was still retained in the vicinity of acidic gelatin hydrogels after 1 day of implantation. The amount of BMP-2 remaining for acidic gelatin hydrogel decreased to about 15 and 3 ng after 1 week and 1 month of implantation, respectively. In the case of basic gelatin hydrogels, 67 ng of BMP-2 was retained in the vicinity of hydrogels after 1 day of implantation and the amount of BMP-2

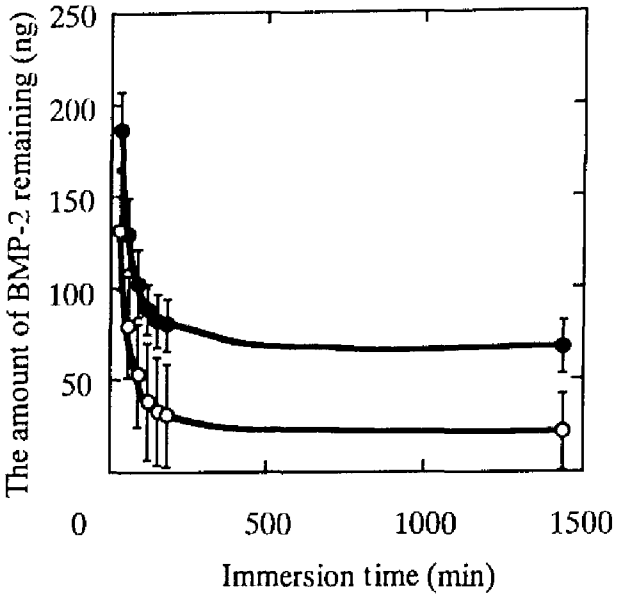

Figure 1. Release profile of BMP-2 in vitro from BMP-2-incorporating hydrogels prepared from acidic (○) and basic gelatin (●). The initial BMP-2 dose is 0.5 μg.

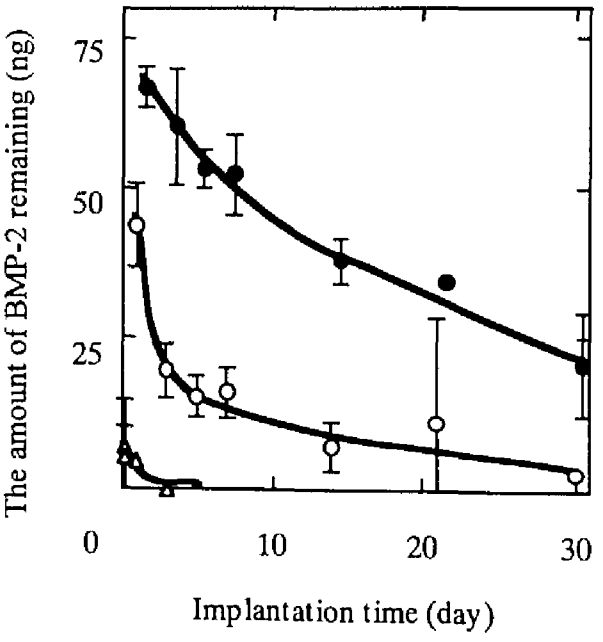

Figure 2. Radioactivity decrement patterns in the back subcutis of mice following subcutaneous implantation of ^{125}I-labeled BMP-2-incorporating hydrogels prepared from acidic (○) and basic gelatin (●) and subcutaneous injection of ^{125}I-labeled BMP-2 in aqueous solution (△). The initial BMP-2 dose is 0.5 μg.

remaining decreased to about 50 and 20 ng after 1 week and 1 month of implantation, respectively. This finding indicates that gelatin hydrogels allow BMP-2 to release over a 1 month period, BMP-2 retention being longer for the basic gelatin hydrogel than the acidic one. During the experiment period, no significant radioactivity accumulation was detected in any organ (data not shown).

On the contrary, approximately 99 % of BMP-2 injected, which amounts to 495 ng of BMP-2, disappeared from the injected site within the first day, and no trace of BMP-2 remained around the injection site 3 days after injection. Approximately 5.0 % and 3.5 % of BMP-2 injected were found in the gastrointestinal tract and other organs after 5 hr of BMP-2 injection. No accumulation of BMP-2 in any specific organ was observed and most of BMP-2 radioactivity was excreted into the urine within first day, suggesting the urinary excretion of BMP-2. A very low radioactivity was detected in the thyroid gland for every experimental group over the time range studied, indicating no release of free radioactive iodine from ^{125}I-labeled BMP-2.

Ectopic bone formation

Figure 3 shows soft x-ray photographs of the mice subcutis after 2 weeks of administration of BMP-2 and PBS in different dosage forms. Apparently, the edge of implants and the subcutaneous tissue became radiopaque strongly on the x-ray film when BMP-2 dose was 5 μg/mouse, irrespective of the dosage form, whereas the weak radiopaque area was found at the gelatin hydrogels and skin when implanted PBS in different dosage forms. It seems that the radiopaque area was larger for BMP-2-incorporating hydrogels than for aqueous BMP-2

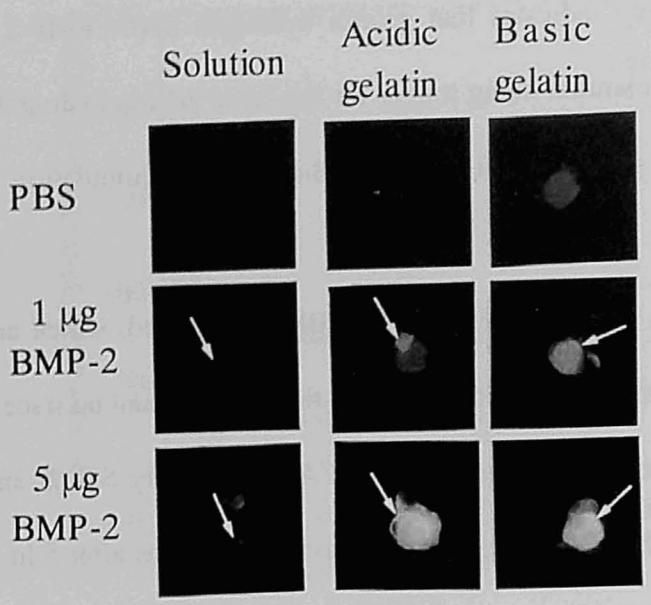

Figure 3. Soft x-ray photographs of ectopically formed bone after 2 weeks of implantation of BMP-2 and PBS in the different dosage forms. Arrows indicate the newly formed bone.

Table 1. Soft X-ray evaluation of ectopic bone formation induced by 5μg of BMP-2 in different dosage forms.

Implantation time (week)	Dosage form		
	Solution	Hydrogel	
		Acidic gelatin	Basic gelatin
1	0/6	1/6	1/6
2	2/8	5/8	3/5
3	4/5	5/5	3/4

Table 2. Soft X-ray evaluation of ectopic bone formation induced by various amounts of BMP-2 in different dosage forms after 2 weeks of implantation.

Amounts of BMP-2 (mg)	Dosage forms	
	Solution	Acidic gelatin hydrogel
0.01	0/4	0/4
0.05	0/4	0/4
0.1	0/4	0/4
0.5	0/4	0/4
1	1/6	1/5
5	2/8	5/8

solutions. The BMP-2 dose effect on the radiopaque area and radiopacity was remarkable when compared with BMP-2 dose of 1.0 μg/mouse. In addition, BMP-2- incorporating hydrogels rendered the implanted site radiopaque, irrespective of the gelatin type, while injection of aqueous BMP-2 solution was not so effective in enhancing the radiopacity.

Table 1 summarizes the implantation schedule and result of soft x-ray evaluation of ectopic bone formation induced by BMP-2-incorporating hydrogels and aqueous BMP-2 solutions. The number of bone induction was estimated by the use of the criterion described above. The rate of bone formation at the implanted site of BMP-2-incorporating gelatin hydrogels was larger than that of at injected site of free BMP-2 solution 1 and 2 weeks after implantation. However, the difference between BMP-2-incorporating gelatin hydrogels and aqueous BMP-2 solutions in the rate of bone formation was not found after 3 weeks of implantation. No significant influence of gelatin IEP was found on the rate of bone formation and no bone induction was detected on the x-ray film after 1 week of BMP-2 solution injection.

The BMP-2 dose effect on the ectopic bone induction by BMP-2-incorporating acidic gelatin hydrogels and BMP-2 solutions is given in Table 2 after 2 weeks of BMP-2 administration. The extent of bone induction was expressed by the number of bone formation at the implanted site of BMP-2-incorporating gelatin hydrogels and aqueous BMP-2 solution injection against the number of treated mice. The number of bone inductions was counted on the x-ray film by the use of the criterion described above. The extent of bone induction increased with the increasing BMP-2 dose in both the dosage forms. BMP-2-incorporating hydrogels exhibited stronger induction than BMP-2 solutions.

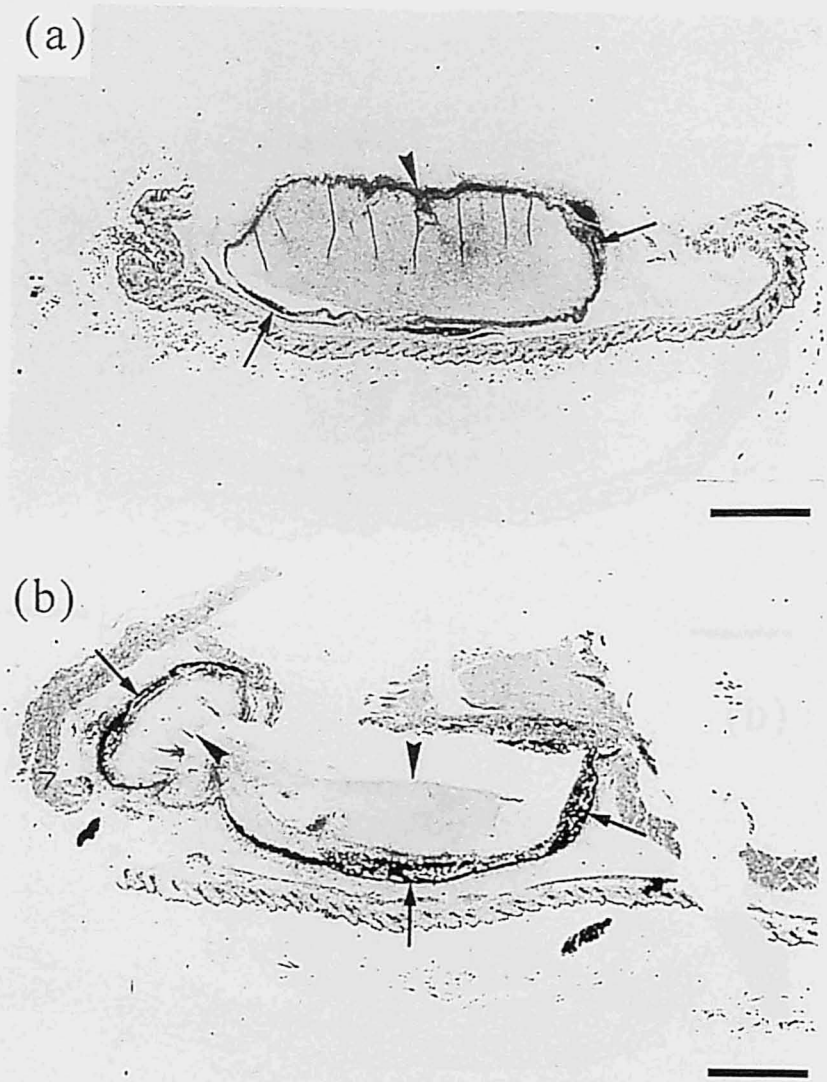

Figure 4. Histological cross-sections of ectopically formed bone after 2 weeks of implantation of BMP-2-incorporating hydrogels prepared from acidic (a, b) and basic (c, d) gelatin and injection of BMP-2 in solutions (e, f): (a, c, e) 1 μg BMP-2/ mouse and (b, d, f) 5 μg BMP-2/ mouse. Each specimen was subjected to von Kossa staining to identify calcium deposition to the extracellular matrix. Arrows and arrowheads indicate the newly formed bone with calcium deposition and the residual gelatin hydrogel, respectively. Bars correspond to 1 mm.

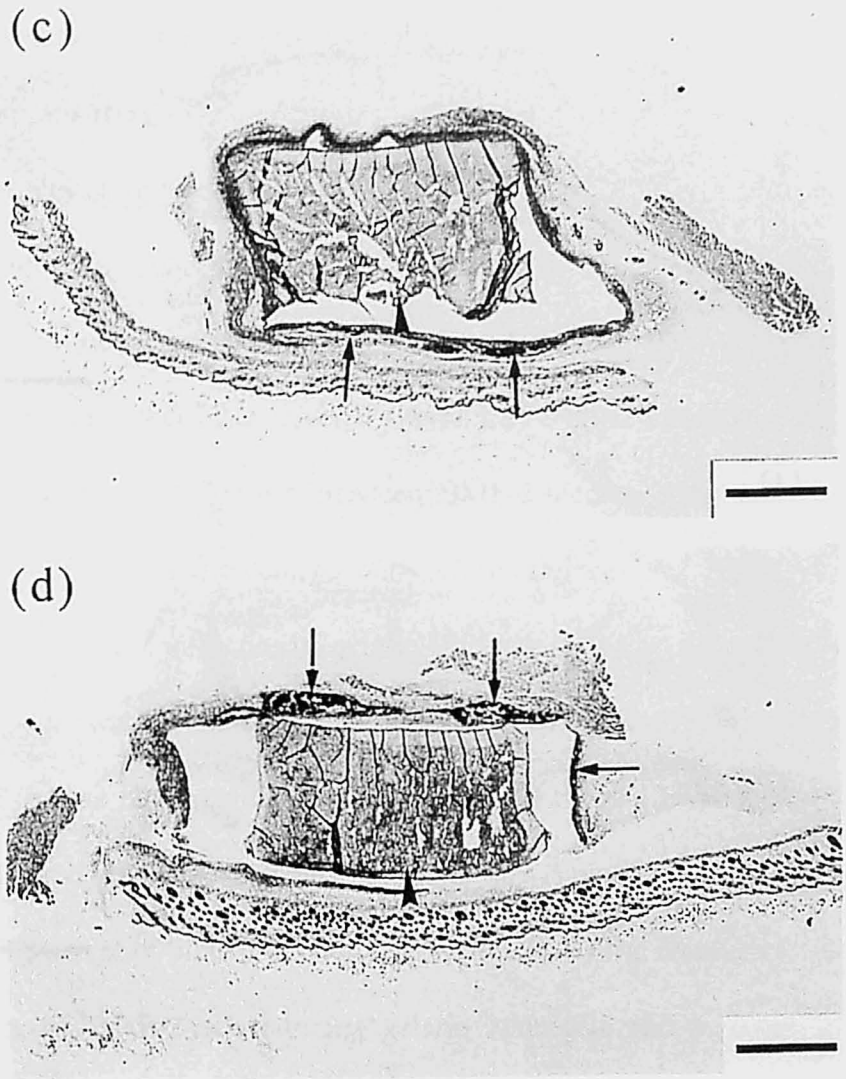

Figure 4. (Continued).

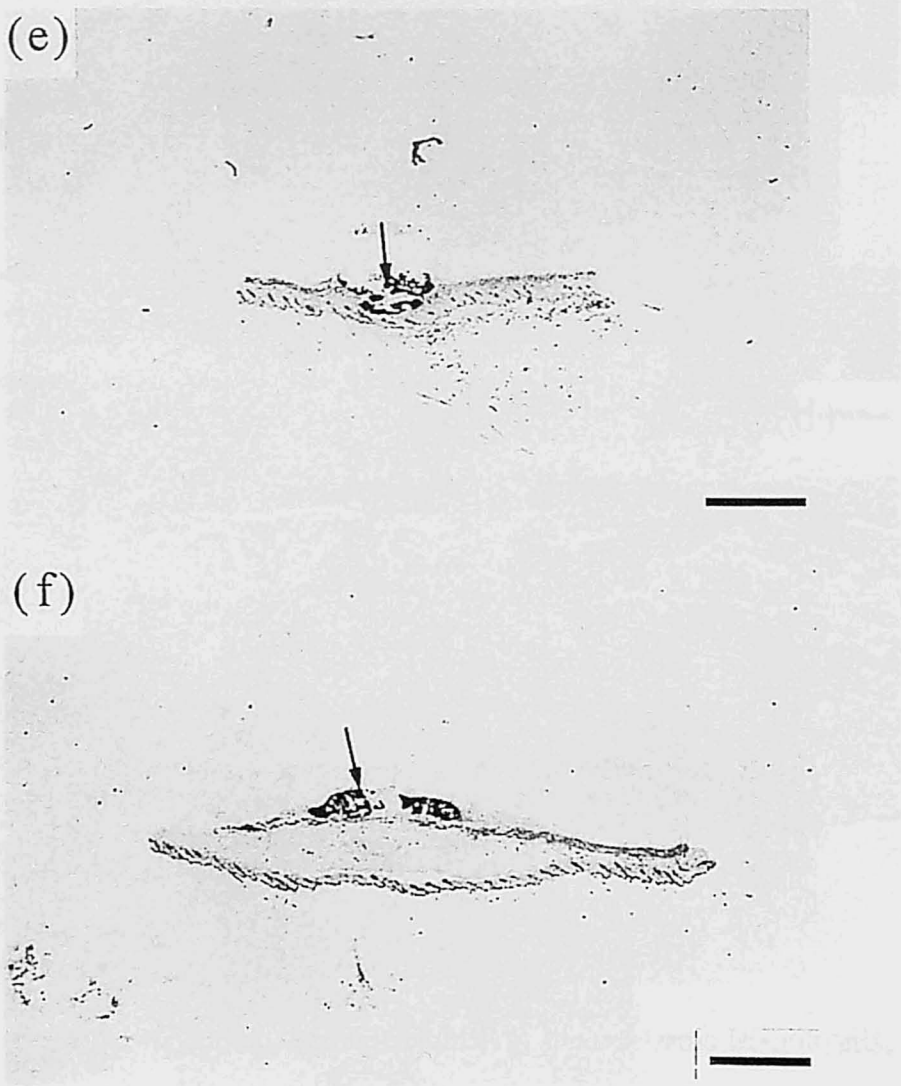

Figure 4. (Continued).

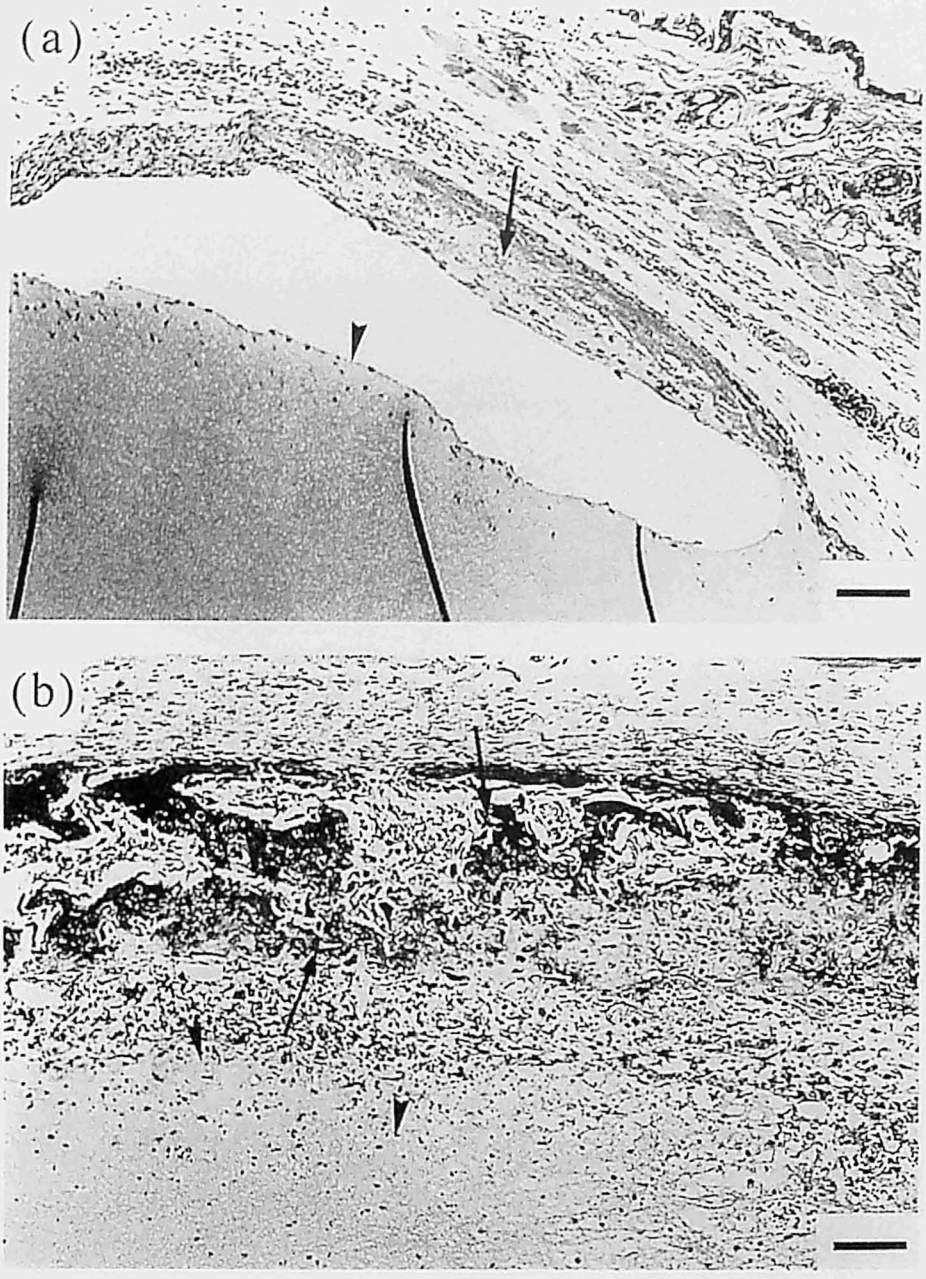

Figure 5. Histological cross-sections of ectopically formed bone after 2 weeks of implantation of BMP-2-incorporating hydrogels prepared from acidic (a, b) and basic (c, d) gelatin and injection of BMP-2 in solutions (e, f): (a, c, e) 1 μg BMP-2/ mouse and (b, d, f) 5 μg BMP-2/ mouse. Each specimen was subjected to H-E staining. Arrows and arrowheads indicate the newly formed bone and the residual gelatin hydrogel, respectively. Bars correspond to 100 μm. At the higher magnification, active cuboidal osteoblasts (Solid arrows) were found at the newly formed bone induced by 5 μg of BMP-2-incorporating hydrogels of acidic and basic gelatin (g, h) and 5 μg of BMP-2 solution (i). Bars correspond to 50 μm.

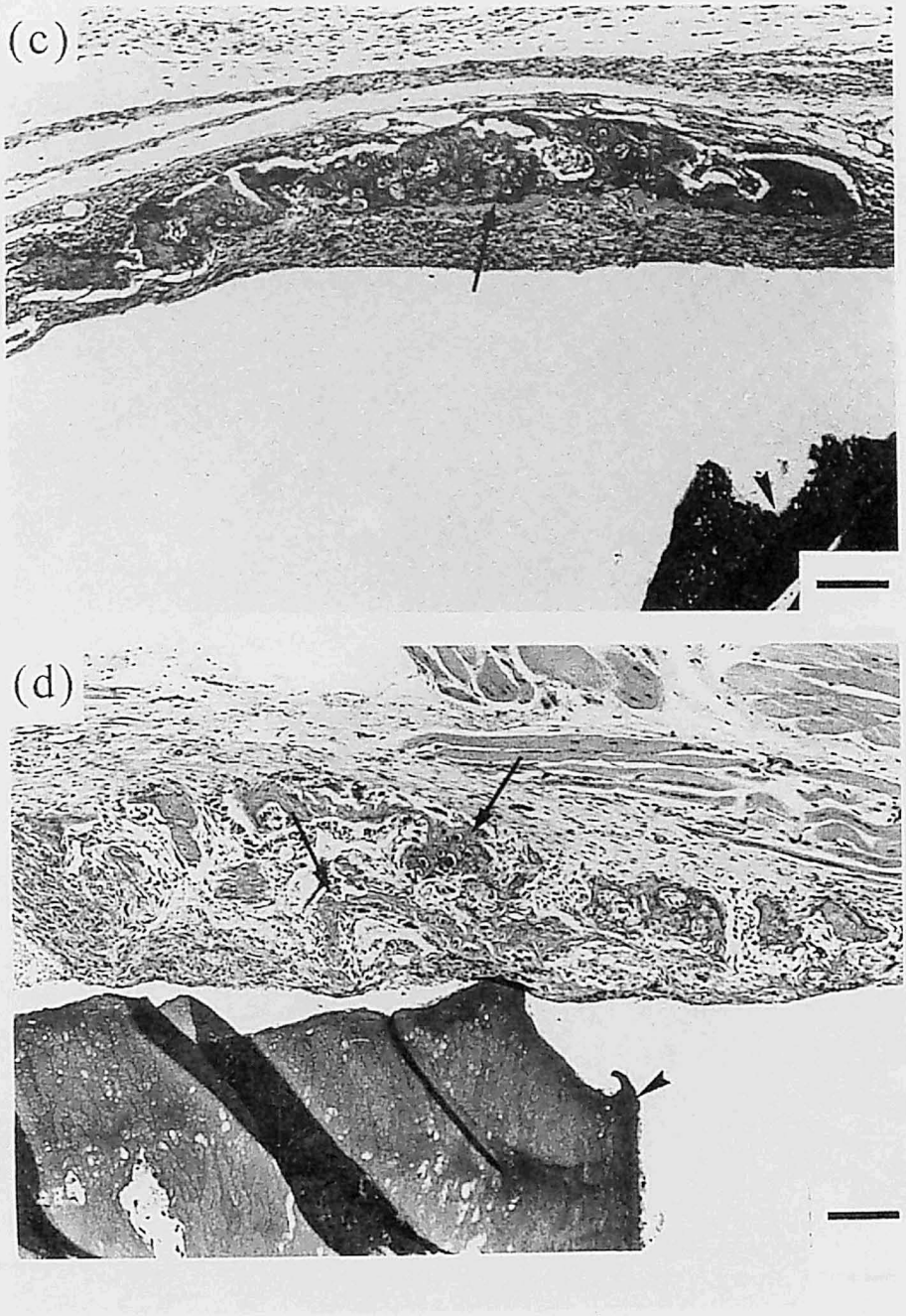

Figure 5. (Continued).

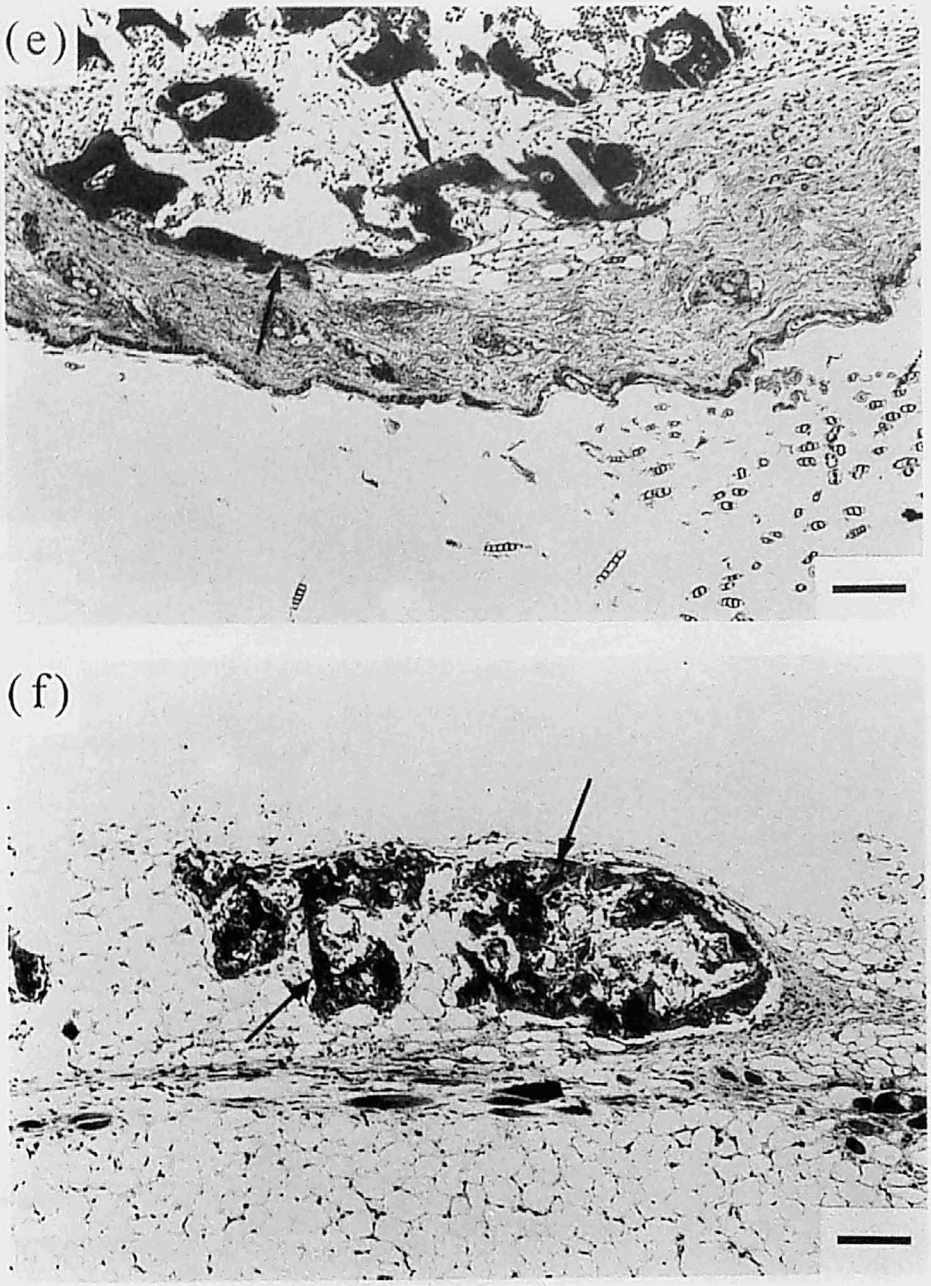

Figure 5. (Continued).

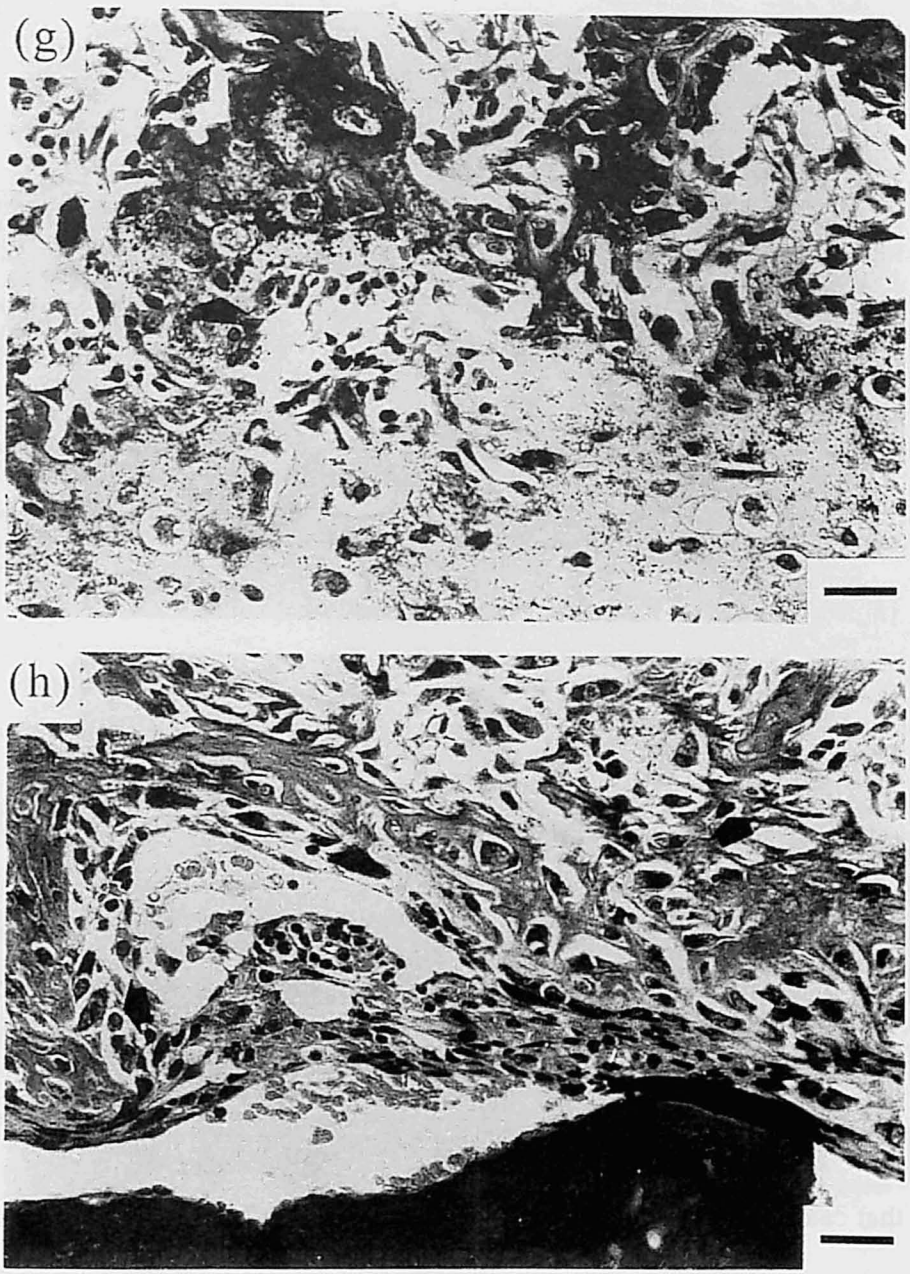

Figure 5. (Continued).

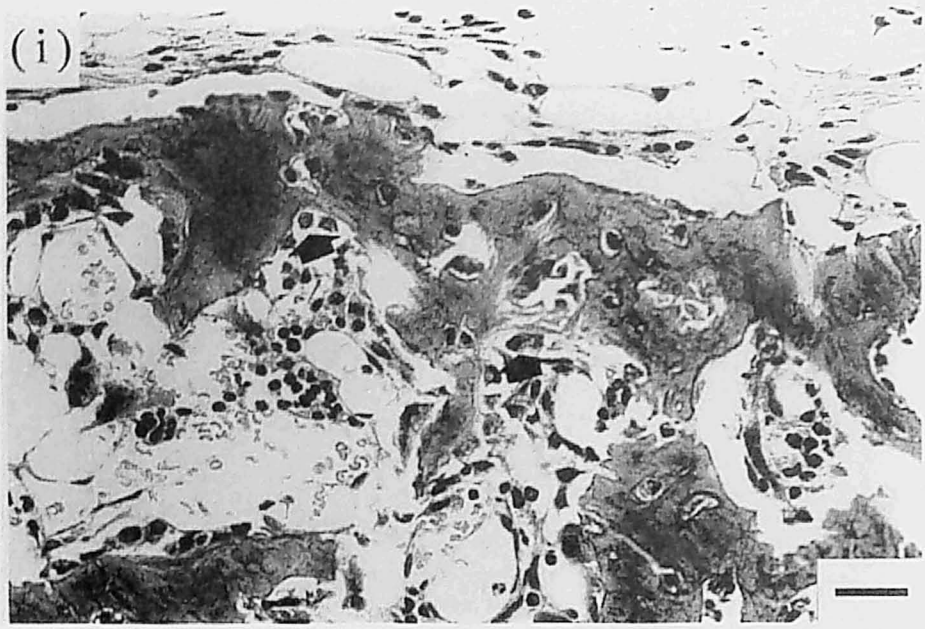

Figure 5. (Continued).

Histological observation on the subcutaneous tissues after 2 weeks of administration is shown in Figures 4, 5, and 6. As is apparent in Figure 4, von Kossa staining demonstrated that both the hydrogels and solutions of BMP-2 induced bone formation in the subcutaneous tissue. Ectopic bone formation was observed only at the injected site of BMP-2 solutions, and bone was formed only along the implanted hydrogel contour, not in the inner portion of the hydrogel. It is seen that calcium deposited area was larger at the BMP-2 concentration of 5 μg/mouse than at 1 μg/mouse, indicating that ectopic bone induction was stronger with an increase in the BMP-2 dose.

Figure 5 shows H-E stained cross-sections of the subcutaneous tissues after 2 weeks of treatments. Newly formed bone was observed at 1 and 5 μg of BMP-2 treated site, irrespective of the dosage form. Partially calcified woven bone was found at the acidic gelatin hydrogel

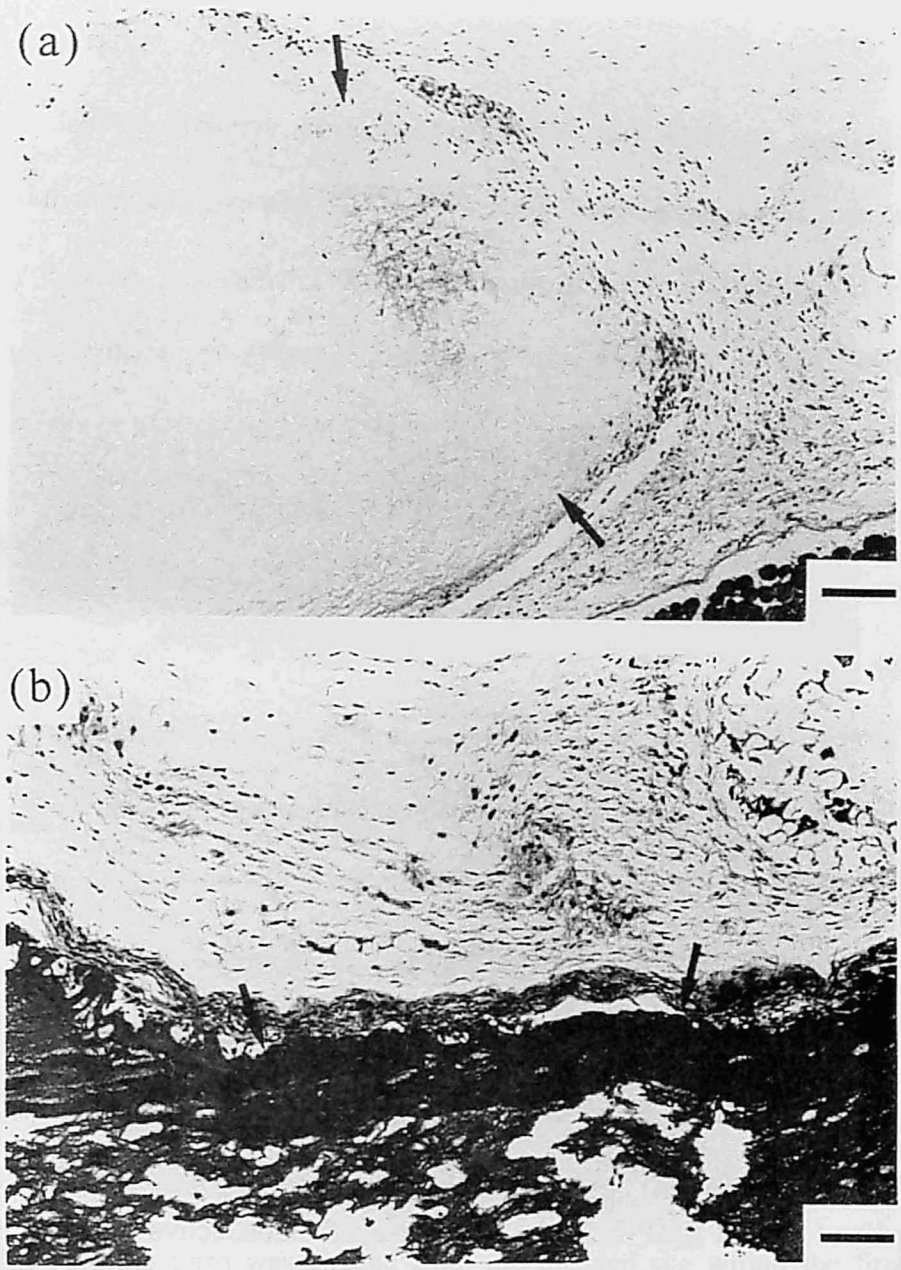

Figure 6. Histological cross-sections of subcutaneous tissues after 2 weeks of implantation of PBS-incorporating hydrogels prepared from acidic (a) and basic (b) gelatin and injection of PBS in solutions (c). Arrows indicate the residual gelatin hydrogels. Bars correspond to 100 μm.

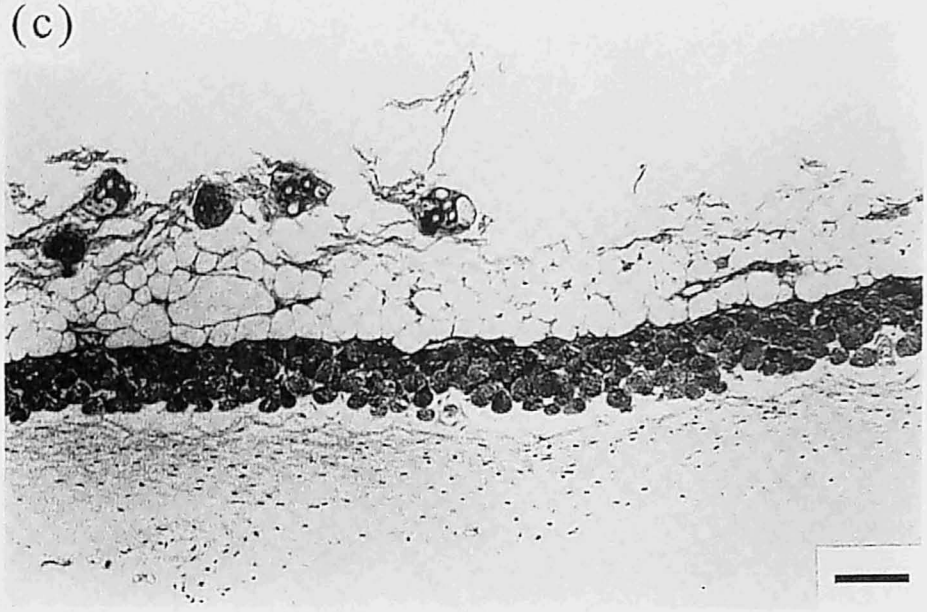

Figure 6. (Continued).

containing 1 and 5 μg of BMP-2. At the higher magnification, active cuboidal osteoblasts were found at the 5 μg of BMP-2 administrated site, irrespective of the dosage form.

On the contrary, no bone formation was observed at the PBS implanted site, irrespective of the dosage form, as shown in Figure 6. The gelatin hydrogels still remained at the implanted site and were encapsulated with fibrous tissues. A little inflammatory cell accumulation and a little cell infiltration into gelatin hydrogels were observed.

DISCUSSION

Various delivery systems have been explored for BMP by combining it with biodegradable polymers and ceramics[1-6, 10-24, 38, 39]. These investigations have evaluated efficacy of the delivery systems in enhancing bone formation in terms of histological examination, calcium deposition, phenotype of bone cells, and gene expression of bone specific proteins. However, the body fate of BMP-2 introduced into the body was not studied at all in these reports although this is very important. Therefore, this chapter focused on the effect of in vivo retention of BMP on its activity of bone induction.

Comparison of the in vivo profile of BMP-2 retention in the mouse subcutis with ectopic bone induction by BMP-2 demonstrated that prolonged retention of BMP-2 in the body in addition to the initial burst release enhanced BMP-2-induced ectopic bone formation. As is apparent from Figure 2, about 10 % of BMP-2 initially incorporated in the acidic gelatin hydrogel, that is, 500 ng, remained in the hydrogel, even if another 90 % was quickly released within 1 day. The amount of BMP-2 remaining in the basic gelatin hydrogel seems to be higher than that in the acidic one. However, the reason for different retention profiles of BMP-2 between the two types of gelatin hydrogels is unclear at present. On the contrary, 99 % of BMP-2 injected in the solution form was cleared from the injected site within the first day. This indicates that incorporation in hydrogels was effective in prolonging the in vivo retention of BMP-2. However, injection of BMP-2 solution also ectopically induced bone formation although the extent was lower than that induced by BMP-2-incorporating hydrogels. This phenomenon may be explained in terms of high potentiality of BMP-2 for bone induction. In other words, it is likely that an extremely low dose of BMP-2 is enough to enhance bone

induction if BMP-2 is appropriately delivered to the site of action. Similar ectopic bone formation was observed for mice treated with BMP-2-incorporating acidic and basic gelatin hydrogels, although the retention profile of BMP-2 was different between the two hydrogels. This finding also suggests that the retention amount of BMP-2 must be high enough compared with that to induce ectopic bone formation. The rate of bone induction by BMP-2 solution injection was similar to that by BMP-2-incorporating hydrogels implantation after 3 weeks of BMP-2 treatment, although the radiopaque area was small at the BMP-2 solution injection site, as is seen in Figures 4 and 5. Such stronger bone induction by BMP-2-incorporating hydrogels than by BMP-2 solution can be ascribed to enhanced retention BMP-2 by gelatin hydrogels. It is possible that retention of BMP-2 in the body continues stimulating differentiation and proliferation of osteoprogenitor cells for a longer time, resulting in enhanced bone formation. It was reported that when BMP-2 was combined with the rat collagenous matrix, the initially given dose required to consistently induce cartilage and bone formation was about 600 ng, but 100 to 200 μg of BMP-2 was required if no matrix was used for rat ectopic bone regeneration[38]. It is safe to say that prolonged retention of BMP-2 in vivo is a promising way to efficiently enhance its osteogenetic actions.

It is interesting to point out that the location of calcium deposition was affected by the dosage form of BMP-2, as demonstrated in Figure 4. When BMP-2 was injected in the solution form, bone formation was induced only at the injected site, while bone was ectopically induced along the periphery of BMP-2-incorporating gelatin hydrogels remaining at the implanted site even at 2 weeks after implantation. When the gelatin hydrogel with a water content of 95 wt% is swollen, the hydrogel pore is occupied with water. It is likely that this water presence did not allow cells to infiltrate into the interior of hydrogel unless it is remarkably degraded (Figures 4,

5, and 6)[39]. As a result, ectopic bone formation must be induced around the periphery of hydrogels, because only the osteoprogenitor cells recruited around hydrogels will be most strongly stimulated to differentiate into osteoblasts by BMP-2 released from the hydrogels.

It has been demonstrated that bFGF molecules with the IEP of 9.6 ionically interacted with hydrogels of the acidic gelatin with an IEP of 5.0, resulting in sustained release of bFGF accompanied with hydrogel biodegradation[34]. Thus, we expected polyion complexation between BMP-2 and the acidic gelatin, similar to the bFGF-acidic gelatin complex, because of high IEP of BMP-2 (8.5). However, the expected polyionic complex between BMP-2 and acidic gelatin was not practically formed and the in vitro release profile of BMP-2 from the acidic gelatin hydrogel was similar to that from the basic gelatin hydrogel (Figure 1). This unexpected result seems to be due to a difference in biochemical nature between BMP-2 and bFGF. Unlike bFGF, BMP-2 is a glycoprotein[37] and requires a surfactant to make it water-soluble at high concentrations. Although lysozyme and avidin are both basic proteins with a similar IEP, the glycoprotein avidin was sorbed to the acidic gelatin hydrogel to a less extent than the non-glycoprotein lysozyme. In addition, a small amount of avidin was sorbed to the basic gelatin hydrogel, whereas no lysozyme sorption to the basic gelatin hydrogel was observed (data not shown). This finding suggests that the positively charged site on the avidin molecule may be covered with sugar moieties, preventing avidin both from forming polyion complex with acidic gelatin and from repelling basic gelatin. It is possible that the presence of sugar moieties and surfactant also prevents BMP from ionically interacting with acidic gelatin, resulting in no difference in the release profile of BMP-2 between acidic and basic gelatin hydrogels. Protein was permeated through gelatin hydrogels, although the permeation rate was influenced by their water content[40]. In addition, a similar in vitro release profile of BMP-2 was observed for gelatin

hydrogels with different water contents, irrespective of their IEP (data not shown). Probably, BMP-2 molecules are small enough to permeate through acidic and basic gelatin hydrogels with the water content around 95 %, although the crosslinking extents are different among the two hydrogels. This indicates that there is no structural difference between acidic and basic gelatin hydrogels affecting the release profile of BMP-2. It is conceivable that difference in the BMP-2 retention in hydrogels may be caused by intermolecular interaction between BMP-2 and gelatin, such as an electrostatic interaction and hydrophobic interactions. These interactions will result in different profiles of BMP-2 retention between the two gelatin hydrogels.

Difference in the time profile of BMP-2 retention between in vitro and in vivo systems may be explained in terms of biological substance presence in the body. This suggests that an initial burst from BMP-2-incorporating gelatin hydrogels in vivo is similar to that in vitro. When gelatin hydrogels are implanted in the subcutis, biological substances originally present in the body, such as proteins, will interact both with gelatin and BMP-2 molecules. It is possible that this interaction reinforced the affinity of BMP-2 for the hydrogels, resulting in prolonged retention of BMP-2 in vivo. Moreover, many cells infiltrating around the hydrogels will modify the in vivo BMP-2 retention. These events will result in a delayed in vivo release of BMP-2 compared with that in vitro.

In conclusion, BMP-2 incorporation into gelatin hydrogels prolonged the in vivo retention of BMP-2 and enhanced ectopic bone formation. Injection of free BMP-2 also formed ectopically bone only at the injected site, although the extent and the induction area were less prominent than that of BMP-2-incorporating hydrogels. Such stronger bone induction of the hydrogels can be ascribed to their property to prolong in vivo BMP-2.

References

1. C. J. Damien and J. R. Parsons, Bone graft and bone graft substitutes: a review of current technology and applications, *J. Appl. Biomater.*, **2**, 187-208 (1991).
2. T. S. Lindholm and T. J. Gao, Functional carriers for bone morphogenetic proteins, *Ann. Chir. Gynaecol.*, **82**, 3-12 (1993).
3. R. A. Kenley, K. Yim, J. Abrams, E. Ron, T. Turek, L. J. Mardden, and J. O. Hollinger, Biotechnology and bone graft substitute, *Pharm. Res.*, **10** , 1393 (1993).
4. J. Yaszemski, R. G. Payne, W. C. Hayes, R. Langer, and A. G. Mikos, Evolution of bone transplantation: molecular, cellular and tissue strategies to engineer human bone, *Biomaterials*, **17**, 175-185 (1996).
5. *Bone Morphogenetic Proteins: Biology, Biochemistry and Reconstructive Surgery*, T. S. Lindholm ed., R. G. Landes Company and Academic Press, Inc., Texas (1996).
6. U. Ripamonti and N. Duneas, Tissue engineering bone by osteoinductive biomaterials, *MRS BULLETIN*, **21**, 36-39 (1996).
7. M. R. Urist, A. Mikulski, and A. Lietze, Solublized and insolublized bone morphogenetic protein, *Proc. Natl. Acad. Sci. USA*, **76**, 1828-1832 (1979b).
8. J. M. Wozney, V. Rosen, A. J. Celeste, L. M. Mitsock, M. J. Whitters, R. W. Kriz, R. M. Hewick, and E. A. Wang, Novel regulators of bone formation: molecular clones and activities, *Science*, **242**, 1528-1534 (1988).
9. J. M. Wozney, The potential role of bone morphogenetic proteins in periodontal reconstruction, *J. Periodontol.*, **66**, 506-510 (1995).

10. M. Kawamura and M. R. Urist, Human fibrin is a physiologic delivery system for bone morphogenetic protein, *Clin. Orthop. Rel. Res.*, **235**, 302-310 (1987).

11. N. Schwarz, H. Redl, L. Zeng, G. Schlag, H. P. Dinges, and J. Eschberger, Early osteoinduction in rats is not altered by fibrin sealant, *Clin. Orthop. Rel. Res.*, **293**, 353-359 (1993).

12. M. C. Meikle, S. Papaioannou, T. J. Ratledge, P. M. Speight, S. R. Watt-Smith, P. A. Hill, and J. J. Reynolds, Effect of poly DL-lactide-co-glycolide implants and xenogeneic bone matrix-derived growth factors on calvarial bone repair in the rabbit, *Biomaterials.*, **15**, 513-21 (1994).

13. S. Miyamoto, K. Takaoka, T. Okada, H. Yoshikawa, J. Hashimoto, S. Suzuki, and K. Ono, Polylactic acid-polyethylene glycol block copolymer, *Clin. Orthop. Rel. Res.*, **294**, 333-343 (1993).

14. S. C. Lee, M. Shea, M. A. Battle, K. Kozitza, E. Ron, T. Turek, R. G. Schaub, and W. C. Hayes, Healing of large segmental defects in rat femurs is aided by rhBMP-2 in PLGA matrix, *J. Biomed. Mater. Res.*, **28**, 1149-1156 (1994).

15. T. J. Sigurdsson, M. B. Lee, K. Kubota, T. J. Turek, J. M. Wozney, and U. M. E. Wikesjö, Periodontal repair in dogs: recombinant human bone morphogenetic protein-2 significantly enhances periodontal regeneration, *J. Periodontol.*, **66**, 131-138 (1995).

16. J. L. Smith, L. Jin, T. Parsons, T. Turek, E. Ron, C. M. Philbrook, R. A. Kenley, L. Marden, J. Hollinger, M. P. G. Bostrom, E. Tomin, and J. M. Lane, Osseous regeneration in preclinical models using bioabsorbable delivery technology for

recombinant human bone morphogenetic protein 2 (rhBMP-2), *J. Controll. Release*, **36**, 183-195 (1995).

17. Y. Yamazaki, S. Oida, K. Ishihara, and N. Nakabayashi, Ectopic induction of cartilage and bone by bovine bone morphogenetic protein using a biodegradable polymer reservoir, *J. Biomed. Mater. Res.*, **30**, 1-4 (1996).

18. J. O. Hollinger and K. Leong, Poly(α-hydroxy acids): carriers for bone morphogenetic proteins, *Biomaterials*, **17**, 187-194 (1996).

19. M. Isobe, Y. Yamazaki, S. Oida, K. Ishihara, N. Nakabayashi, and T. Amagasa, Bone morphogenetic protein encapsulated with a biodegradable and biocompatible polymer, *J. Biomed. Mater. Res.*, **32**, 433-438 (1996).

20. G. Zellin and A. Linde, Importance of delivery systems for growth factor-stimulatory factors in combination with osteopromotive membranes. An experimental study using rhBMP-2 in rat mandibular defects, *J. Biomed. Mater. Res.*, **35**, 181-190 (1997).

21. M. R. Urist, A. Lietze, and E. Dawson, β-tricalcium phosphate delivery system for bone morphogenetic protein, *Clin. Orthop. Rel. Res.*, **187**, 277-280 (1984).

22. Y. Horisaka, Y. Okamoto, N. Matsumoto, Y. Yoshimura, J. Kawada, K. Yamashita, and T. Takagi, Subperiosteal implantation of bone morphogenetic protein adsorbed to hydroxyapatite, *Clin. Orthop. Rel. Res.*, **268**, 303-312 (1991).

23. T. Sato, M. Kawamura, K. Sato, H. Iwata, and T. Miura, Bone morphogenesis of rabbit bone morphogenetic protein-bound hydroxyapatite-fibrin composite, *Clin. Orthop. Rel. Res.*, **263**, 254-262 (1988).

24. I. Ono, T. Ohura, M. Murata, H. Yamaguchi, Y. Ohnuma, and Y. Kuboki, A study on bone induction in hydroxyapatite combined with bone morphogenetic protein, *Plast. Reconstr. Surg.*, **90**, 870-879 (1991).

25. L. S. Beck, E. P. Amento, Y. Xu, L. Deguzman, W. P. Lee, T. Nguyen, and N. A. Gillett, TGF-β_1 induces bone closure of skull defects: temporal dynamics of bone formation in defects exposed to rhTGF-β1, *J. Bone Mineral Res.*, **8**, 753-761 (1993).

26. T. Tanaka, Y. Taniguchi, K. Gotoh, R. Satoh, M. Inazu, and H. Ozawa, Morphological study of recombinant human transforming growth factor β1-induced intramembranous ossification in neonatal rat parietal bone, *Bone*, **14**, 117-123 (1993).

27. W. R. Gombotz, S. C. Pankey, L. S. Bouchard, D. H. Phan, and P. Puolakkainen, Stimulation of bone healing by transforming growth factor-beta1 released from polymeric or ceramic implants, *J. Appl. Biomater.*, **5**, 141-150 (1994).

28. D. R. Sumner, T. M. Turner, A. F. Purchio, W. R. Gombotz, and J. O. Galante, Enhancement of bone ingrowth by transforming growth factor-β, *J. Bone Joint Surg.*, **77-A**, 1135-1147 (1995).

29. U. Ripamonti, C. Bosch, B. V. D. Heever, N. Duneas, B. Melsen, and R. Ebner, Limited chondro-osteogenesis by recombinant human transforming growth factor-β1 in calvarial defects of adult baboons *(Papio ursinus)*, *J. Bone Miner. Res.*, **11**, 938-944 (1996).

30. T. Nakamura, K. Hanada, M. Tamura, T. Shibanushi, H. Nigi, M. Tagawa, S. Fukumoto, and T. Matsumoto, Stimulation of endosteal bone formation by systemic

injections of recombinant basic fibroblast growth factor in rats, *Endocrinology*, **136**, 1276-1284 (1995).

31. J. S. Wang, Basic fibroblast growth factor for stimulation of bone formation in osteoinductive or conductive implants, *Acta. Orthop. Scand.*, **67 (Suppl.269)**, 1-33 (1996)

32. K. Yamada, Y. Tabata, K. Yamamoto, S. Miyamoto, I. Nagata, H. Kikuchi, and Y. Ikada, Potential efficacy of basic fibroblast growth factor incorporated in biodegradable hydrogels for skull bone regeneration, *J. Neurosurg.*, **86**, 871-875 (1997).

33. D. Zekorn, Modified gelatin as plasma substitutes, *Bibl. Haematol.*, **33**, 30-60 (1969).

34. Y. Tabata, S. Hijikata, and Y. Ikada, Enhanced vascularization and tissue granulation by basic fibroblast growth factor impregnated in gelatin hydrogel, *J. Controll. Release*, **31**, 189-199 (1994).

35. A. Veis, *The Macromolecular Chemistry of Gelatin*. Academic Press Inc., New York (1964).

36. F. C. Greenwood, W. M. Hunter, and T. C. Gglover, The preparation of ^{131}I-labeled human growth hormone of high specific radioactivity, *Biochem. J.* **89**, 114-123 (1963).

37. K. Yim, J. Abrams, and A. Hsu, Capillary zone electrophoretic resolution of recombinant human bone morphogenetic protein 2 glycoforms. An investigation into the separation mechanisms for an exquisite separation, *J. Chromatogr. A*, **716**, 401-412 (1995).

38. E. A. Wang, V. Rosen, J. S. D'Alessandro, M. Bauduy, P. Cordes, T. Harada, D. I. Israel, R. M. Hewick, K. M. Kerns, P. Lapan, D. P. Luxenberg, D. McQuaid, I. K. Moutsatsos, J. Nove, and J. M. Wozney, *Proc. Natl. Acad. Sci. USA*, **87**, 2220-2224 (1990).

39. M. Yamamoto, K. Kato, and Y. Ikada, Effect of the structure of bone morphogenetic protein carriers on ectopic bone regeneration, *Tissue Engineering*, **2**, 315-326 (1998).

40. MD. Muniruzzaman, Y. Tabata, and Y. Ikada, Complexation of basic fibroblast growth factor with gelatin, *J. Biomater. Sci. Polym. Ed.*, **9**, 459-473 (1998).

Chapter 3

Bone regeneration induced by biodegradable hydrogel matrices incorporating TGF-β1

INTRODUCTION

The sustained release of growth factors with short half-life periods is a key technology for successful tissue engineering because they play an important role in cell proliferation and differentiation. Bone regeneration is an attractive research field of tissue engineering since it is of highly clinical requirement. It is well known that the formation and destruction of tissues are regulated by various types of growth factors[1]. Thus, if one can accelerate bone formation using growth factors in a suitable manner, this technology will provide a new clinical way to fill the bone defect, which is currently substituted with autografts, allografts, and biomaterial implants. It has been demonstrated that various growth factors, such as TGF-β1, BMP, and bFGF, regulate the proliferation and differentiation of osteogenic cells and enhance bone regeneration in vivo[1-3].

TGF-β1, a basic protein with high hydrophobicity, regulates proliferation and differentiation of fibroblasts, keratinocytes, and osteoblasts, extracellular matrix metabolism in the bone or the connective tissue, and immunological system. It is widely recognized that TGF-β1 molecules bind to latency-associated peptide, and latent TGF-β1 binding protein

through non-covalent and covalent bonds, respectively. These binding enables in vivo unstable TGF-β1 molecules to be stored in the extracellular matrix and to regulate its cellular functions. TGF-β1 molecules are released in an active form from the extracellular matrix by the bond cleavage. In addition, other extracellular matrix components, such as heparin, heparan sulfate, and type IV collagen, also bind to active TGF-β1 to modulate its biological activity[4-7]. Thus, for the in vivo use of TGF-β1, this protein should be incorporated into a carrier that can protect from its enzymatic digestion and denaturation. As carrier matrices of TGF-β1, collagen[8], hydroxyapatite[9], demineralized bone matrix (DBM)[10-12], DBM coated with poly(lactide-co-glycolide)[13,14], calcium sulfate[14], and methylcellulose gel[15], have been studied to demonstrate that they are feasible as the matrix carrier to induce bone regeneration. However, few studies have been reported on bone regeneration by the controlled release of TGF-β1.

Biodegradable gelatin has been extensively used for pharmaceutical, medical, and food purposes because of its biosafety, which has been proven through its long clinical application[16]. Other advantages of gelatin are its high chemical reactivity and commercial availability of gelatin samples with different charges. A biodegradable hydrogel has been prepared from acidic gelatin with an IEP of 5.0. This gelatin is negatively charged at the physiological pH of 7.0. It was found that a positively charged bFGF was electrostatically complexed with the negatively charged, acidic gelatin. The bFGF molecules complexed with the acidic gelatin hydrogel were released in vivo as a result of hydrogel biodegradation[17,18]. Tabata et al. have succeeded in sustained release of biologically active bFGF from this biodegradable hydrogel based on polyion complexation and achieved remarkable enhanced angiogenetic[19] and osteogenetic effects[20] in marked contrast to bFGF in the solution form.

This chapter describes the sustained release system of this biodegradable gelatin hydrogel to TGF-β1 and evaluates in vitro sorption of TGF-β1 to the acidic and basic gelatin hydrogels and their release profiles. Following subcutaneous implantation of ^{125}I-labeled TGF-β1 into the back subcutis of mice, the time profile of TGF-β1 release is compared with that of the hydrogel biodegradation. In addition, effects of TGF-β1-incorporating acidic gelatin hydrogels on bone regeneration are evaluated by use of a rabbit model having a skull bone defect.

EXPERIMENTAL

Materials

TGF-β1 with IEP of 9.5 was purchased from Sigma, Missouri, USA. Gelatin samples with IEPs of 5.0 and 9.0 (Nitta Gelatin Co., Osaka, Japan), isolated from the bovine bone with the alkaline process and from the porcine skin with the acidic process, are here named as acidic and basic gelatin, respectively, based on their electrical feature. N-succinimidyl-3-(4-hydroxy-3,5-di [^{125}I] iodophenyl) propionate (^{125}I-Bolton-Hunter Reagent, 147 MBq/ml in anhydrous benzene) and aqueous solution of Bolton-Hunter [^{125}I]-labeled TGF-β1 in 0.05 M sodium acetate buffer containing 5 % sucrose and 0.25 % bovine serum albumin (185 kBq/mL, pH4.0, the specific activity of 6310 kBq/μg) were purchased from NEN Research Products, Du Pont, Wilmington, USA. Other chemicals were obtained from Wako Pure Chemical Industries, Osaka, Japan or Nacalai Tesque, Kyoto, Japan and used without further purification.

Preparation of hydrogel matrices

Hydrogels were prepared by crosslinking of aqueous gelatin solutions with glutaraldehyde according to the method described elsewhere[18]. Aqueous solution of either acidic or basic gelatin was cast into a polypropylene dish of 138 x 138 cm^2 and 2 mm depth at various concentrations of glutaraldehyde, as summarized in Table 1.

Table 1. Preparation conditions of gelatin hydrogels with different water contents.

Gelatin type	Concentration of gelatin solution (wt%)	Concentration of glutaraldehyde (wt%)	Water content (wt%)
Acidic	15	0.40	85
Acidic	10	0.25	90
Acidic	5	0.063	95
Acidic	3	0.050	98
Basic	5	0.89	95

Following crosslinking reaction at 4 °C for 12 hr, the crosslinked hydrogel sheet was punched out to obtain discs of 6 mm in diameter. They were placed in 100 mM aqueous glycine solution at 37 °C for 1 hr to block residual aldehyde groups of glutaraldehyde, followed by washing with DDW. They were freeze-dried and then sterilized with ethylene oxide gas. Their weight was measured before and after drying at 70 °C under vacuum to calculate their water content, which was defined by the weight percentage of water in the wet hydrogel[18]. The size of hydrogel discs used in this chapter was 6 mm in diameter and 2 mm in thickness and their wet weight was 0.16 g.

Radiolabeling of hydrogel matrices

Gelatin hydrogels with a water content of 95 wt% were radioiodinated by use of ^{125}I-Bolton-Hunter reagent[21]. Briefly, 100 μL of ^{125}I-Bolton-Hunter reagent solution in anhydrous benzene was bubbled with dry nitrogen gas until benzene evaporation was completed. Then, 125 μL of DDW was added to the dried reagent, followed by agitating to prepare aqueous ^{125}I-Bolton-Hunter solution. The aqueous solution was dropped on freeze-dried discs of gelatin hydrogels (30 μL per hydrogel disc), and then the resulting swollen hydrogel discs were left at 4 °C for 3 hr for radioiodination of gelatin. The resulting gelatin hydrogel discs were rinsed with DDW at 4 °C for 4 days to exclude non-coupled, free ^{125}I-labeled reagent from ^{125}I-labeled gelatin hydrogels and then freeze-dried. When measured periodically, the DDW radioactivity decreased to the background level after 4-day rinsing. No shape change of swollen hydrogel discs was observed during radiolabeling and the subsequent rinsing process.

Evaluation of TGF-β1 sorption to hydrogel matrices

TGF-β1 sorption to gelatin hydrogels was performed in DDW at 4 °C in a polypropylene test tube. The aqueous solution containing 50 pg of ^{125}I-labeled TGF-β1 (900 μL) was added to acidic and basic gelatin hydrogel discs with the water content of 95 wt%. These discs were preswollen with 100 μL of DDW at 37 °C for 12 hr. The gelatin hydrogels were soaked in the ^{125}I-labeled TGF-β1 solution at 4 °C. At different time periods after incubation at 4 °C, the supernatant was taken out to measure the radioactivity on a gamma counter (ARC-301B, Aloka Co., Tokyo, Japan), while the radioactivity of gelatin hydrogels and test tubes was measured to estimate the mass balance of TGF-β1.

Preparation of hydrogel matrices incorporating TGF-β1

For TGF-β1 incorporation into acidic gelatin hydrogels, 20 μL of aqueous solution containing 0.1 μg of TGF-β1 and 50 pg of ^{125}I-labeled TGF-β1 was dropped onto freeze-dried hydrogel discs, followed by leaving them in culture dishes of 60 mm diameter under sealing with parafilm at 4°C overnight. The prepared TGF-β1-incorporating acidic gelatin hydrogel discs were used without washing for the following experiments. Since the volume of TGF-β1 aqueous solution was much less than that theoretically impregnated into each hydrogel, the dose of TGF-β1 incorporated was defined as the amount initially added for TGF-β1 incorporation.

Evaluation of in vivo TGF-β1 release

Acidic gelatin hydrogel discs incorporating ^{125}I-labeled TGF-β1 with water contents of 85, 90, 95, and 98 wt% were implanted into the back subcutis of 6 week-old female ddY mice[22]. As a control, 100 μL of aqueous solution containing ^{125}I-labeled TGF-β1 was subcutaneously injected into the mouse back at the central position 15 mm away from their tail root. The dose of ^{125}I-labeled TGF-β1 was 50 pg for both the forms. At different time intervals, mice were sacrificed according to the institutional guidelines of Kyoto University on animal experimentation. The skin on the back of mice around the implanted or injected site of TGF-β1 was cut into a strip of 3 x 5 cm^2 and the corresponding facia was thoroughly wiped off with filter paper to absorb ^{125}I-labeled TGF-β1. The radioactivity of remaining hydrogels, excised skin, and filter paper was measured on the gamma counter to assess the time profile of in vivo TGF-β1 retention. Radioactivity measurements for other organs and tissues

revealed that no accumulation of TGF-β1 was found in any specific organ. The radioactivity of gelatin hydrogels and aqueous solution containing ^{125}I-labeled TGF-β1 as a standard was measured at each sampling time and the radioactivity ratio of the samples to the standard was calculated to assess the profile of in vivo TGF-β1 retention.

Evaluation of in vivo degradation of hydrogel matrices

In vivo hydrogel degradation was evaluated in terms of radioactivity loss of the ^{125}I-labeled gelatin hydrogels incorporating TGF-β1[18]. After subcutaneous implantation of ^{125}I-labeled acidic gelatin hydrogel discs incorporating TGF-β1 in the back of mice, the radioactivity of hydrogels and the surrounding tissue was measured at different time intervals according to the same method as described above.

Assessment of bone regeneration

The bone regeneration effect was evaluated by use of a rabbit model with a skull bone defect [20]. Under anesthetization, the head skin of Japanese White rabbits weighing between 2 and 2.5 kg was cut to expose the skull bone and, after pericranium incision, bilateral skull defects of 6 mm in diameter were carefully prepared by a microdrill with the aid of an operating microscope not so as to injure the underlying dura mater. The acidic gelatin hydrogel incorporating 0.1 μg of TGF-β1 was applied to the rabbit skull defect. As controls, the TGF-β1-free empty gelatin hydrogel and 100 μL of PBS with or without 0.1 μg of TGF-β1 were employed. After treatment, the pericranium and skin were carefully sutured with No. 4-0 nylon monofilament. Each experimental group was composed of 4 rabbits and 4 different defects were treated with either the right or left defect being selected randomly. After 8 weeks

postoperatively, the skull bone was removed together with the defect and fixed with 10 vol% aqueous neutral formalin solution.

Bone regeneration at the skull defect was assessed by Dual-Energy X-ray Absorptometry (DEXA) and histological examination of formalin-fixed specimen. The bone mineral density (BMD) of each defect was measured by DEXA using a bone mineral analyzer (model DCS600, Aloka Co., Tokyo, Japan) in the region of interest of 5 x 5 mm^2. Bone specimens were demineralized in 10 wt% ethylenediamine tetraacetic acid solution at 4 °C for 3 days, embedded in paraffin, and sectioned to 2 μm thickness. The section preparation was done by cutting the specimen at the center of the skull defect or at the site as near as possible, and stained with H-E. The histological sections were viewed using a light microscope to evaluate the bone regeneration.

RESULTS

TGF-β1 sorption to hydrogel matrices

Figure 1 shows the in vitro sorption profile of TGF-β1 to the hydrogels of acidic and basic gelatin at 4 °C. As can be seen, TGF-β1 was clearly sorbed with time to the acidic gelatin hydrogel and approximately 40 % of TGF-β1 applied initially was found to be stored in the hydrogel 27 hr after immersion. On the other hand, the amount of TGF-β1 sorbed was only 5 % of the total TGF-β1 for the basic gelatin hydrogel.

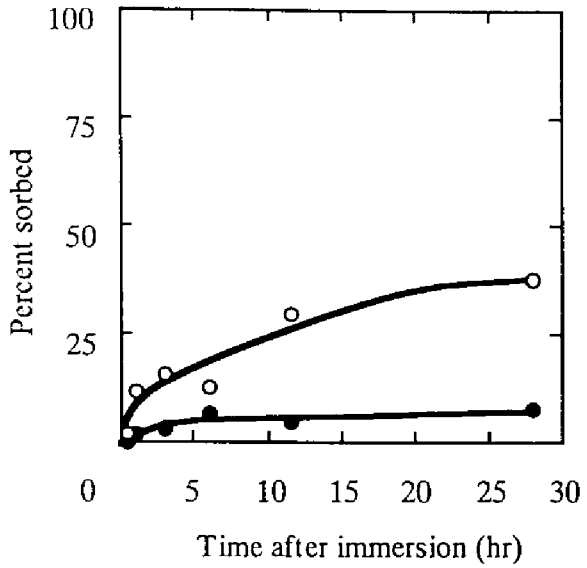

Figure 1. The time course of in vitro TGF-β1 sorption to hydrogels of gelatin with IEPs of 5.0 (○) and 9.0 (●).

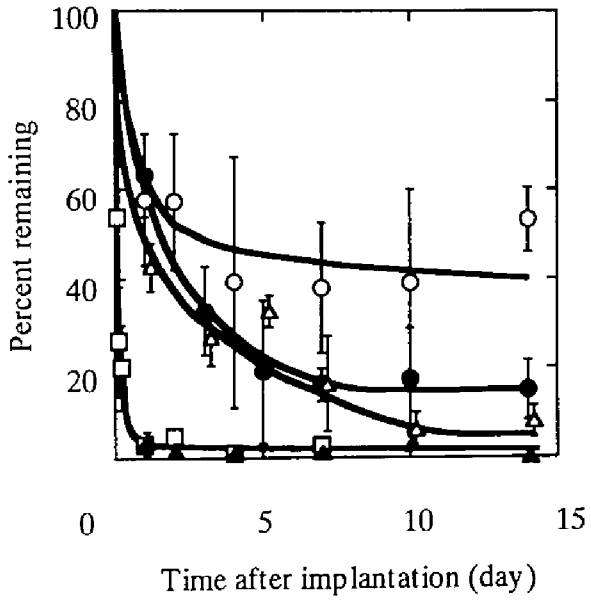

Figure 2. The in vivo decrement patterns of the radioactivity remaining in the back of mice after subcutaneous implantation of ^{125}I-labeled TGF-β1-incorporated into acidic gelatin hydrogels with water contents of 85 (○), 90 (●), 95 (△), and 98 wt% (▲) or subcutaneous injection of ^{125}I-labeled TGF-β1 aqueous solution (□).

In vivo TGF-β1 release

Figure 2 shows the in vivo decrement patterns of radioactivity from the implanted site of ^{125}I-labeled TGF-β1-incorporating acidic gelatin hydrogels with water contents of 85, 90, 95, and 98 wt% or the injected site of aqueous ^{125}I-labeled TGF-β1 solution. For TGF-β1-incorporating gelatin hydrogels with water contents lower than 98 wt%, TGF-β1 was retained in the mouse subcutis for longer time periods than free TGF-β1 injection. More than 50 % of TGF-β1 initially applied was retained in the vicinity of the hydrogels one day after implantation of acidic gelatin hydrogels with water contents of 85, 90, and 95 wt%, whereas almost 100 % of free TGF-β1 disappeared from the injected site within one day. Incorporation into the gelatin hydrogel with the water content of 98 wt% did not prolong the in vivo retention of TGF-β1 and the time profile was similar to that of injected free TGF-β1. The prolonged period of TGF-β1 retention depended on the water content of hydrogels. The lower the water content of the hydrogels, the higher the amount of TGF-β1 remaining. No significant radioactivity accumulation was detected in any organ during the experiment period, irrespective of the dosage form (data not shown). Neglectively low radioactivity was detected in the thyroid gland for each experimental group, indicating no release of free radioactive iodine from ^{125}I-labeled TGF-β1 (data not shown).

In vivo degradation of hydrogel matrices

Figure 3 shows the time course of remaining radioactivity after subcutaneous implantation of ^{125}I-labeled acidic gelatin hydrogels incorporating TGF-β1. The remaining radioactivity decreased with time and the radioactivity was retained for more than 2 weeks. No significant radioactivity accumulation was found in any specific organ although a low

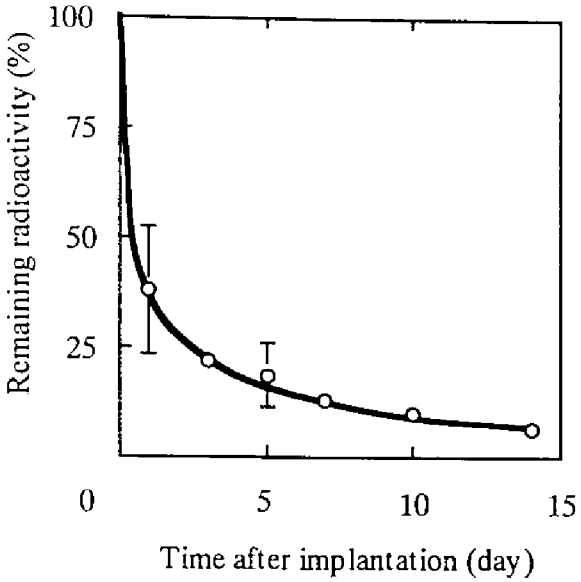

Figure 3. The in vivo time profile of the radioactivity remaining in the back of mice after subcutaneous implantation of TGF-β1-incorporated into ^{125}I-labeled-acidic gelatin hydrogel with a water content of 95 wt%.

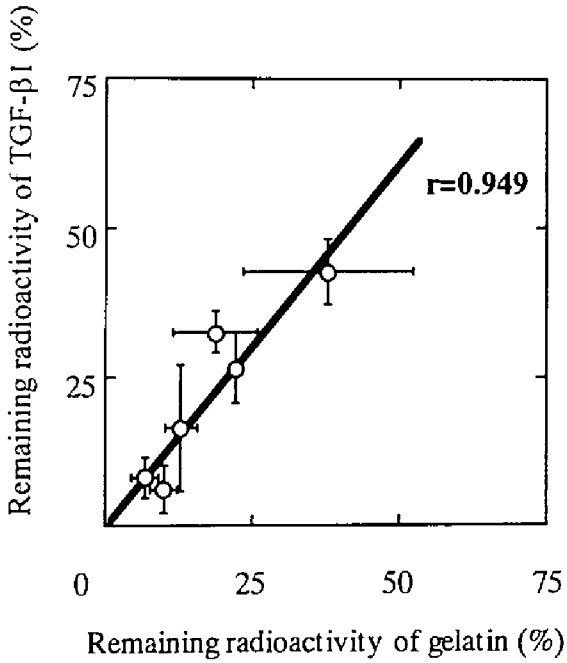

Figure 4. The in vivo remaining radioactivity of ^{125}I-labeled TGF-β1-incorporated into acidic gelatin hydrogels plotted against that of ^{125}I-labeled acidic gelatin hydrogels incorporating TGF-β1. The water content of hydrogels is 95 wt%.

percentage of radioactivity was observed for the tissue around the hydrogels during the early period after implantation (data not shown).

Relationship between the TGF-β1 release and the hydrogel matrices degradation in vivo

Figure 4 shows the remaining radioactivity of TGF-β1 plotted as a function of that of acidic gelatin hydrogels. It is apparent that there was a good correlation between the two remaining radioactivities. The remaining radioactivity of TGF-β1 increased in a proportional manner to that of the gelatin hydrogel at a correlation coefficient of 0.949.

Bone regeneration

Table 2 summarizes the bone mineral density at the skull defect of rabbits 8 weeks after treatment with TGF-β1-incorporating acidic gelatin hydrogels or other agents. The BMD at the skull defect was measured by DEXA and the TGF-β1 dose was 0.1 μg for a skull defect. It is clear that both the TGF-β1-incorporating acidic gelatin hydrogels with water contents of 90 and 95 wt% enhanced the BMD of the skull defect to a significantly higher extent than free TGF-β1. The BMD value was similar to that of the intact bone. No significant enhancement of the BMD at the skull defect was detected for TGF-β1-incorporating acidic gelatin hydrogels with water contents of 85 and 98 wt%. Free TGF-β1 did not enhance the BMD value at the bone defect, although it tended to be somewhat higher than that of PBS-treated control rabbits. Irrespective of the hydrogel water content, TGF-β1-free empty gelatin hydrogels did not contribute to any increase in BMD of the skull defect of rabbits.

Table 2. Bone mineral density (BMD) at the skull defect of rabbits 8 weeks after different treatments.

Treatment with	Water content (wt%)	BMD (mg/cm^2) [a]
TGF-β1-incorporated into gelatin hydrogels (0.1μg TGF-β1/rabbit)	85	60.5 ± 8.0
	90	84.3 ± 5.2 **,§§,¶¶,††,‡‡
	95	84.3 ± 12.0 **,§,¶,†,###
	98	65.0 ± 6.1
Free TGF-β1 (0.1μg TGF-β1/rabbit)	—	64.9 ± 7.0
Empty gelatin hydrogels	85	62.1 ± 8.3
	90	60.8 ± 2.1
	95	58.0 ± 5.0
	98	60.7 ± 8.6
PBS	—	60.2 ± 11.6

a) **p<0.01 versus the PBS-treated group; §p<0.05, §§p<0.01 versus the free TGF-β1-treated group; ¶ p<0.05, ¶¶ p<0.01 versus group treated with TGF-β1-incorporated into gelatin hydrogel (85 wt%); † p<0.05, †† p<0.01 versus group treated with TGF-β1-incorporated into gelatin hydrogel (98 wt%); ‡‡ p<0.01 versus the group treated with empty gelatin hydrogel (90 wt%), ### p<0.001 versus the group treated with empty gelatin hydrogel (95 wt%).

Figure 5 shows histological sections of the skull defect 8 weeks after different treatments. The dose of TGF-β1 was 0.1 μg per skull defect. When the skull defect of rabbits was treated with PBS and empty gelatin hydrogels with water contents of 85, 90, 95, and 98 wt%, insignificant bone regeneration was observed and soft connective tissues were infiltrated to the defect. On the contrary, bone regeneration was found in the skull defects of rabbits treated with TGF-β1-incorporating acidic gelatin hydrogels with water contents of 90 and 95 wt% and the defect was completely occupied by the newly formed bone. TGF-β1-incorporating gelatin hydrogels with water contents of 85 and 98 wt% did not exhibit bone regeneration as strong as those with other water contents. All of the acidic gelatin hydrogels except for that with the water content of 85 wt% were completely degraded in the defect within 8 weeks and little inflammatory response was found to the hydrogels.

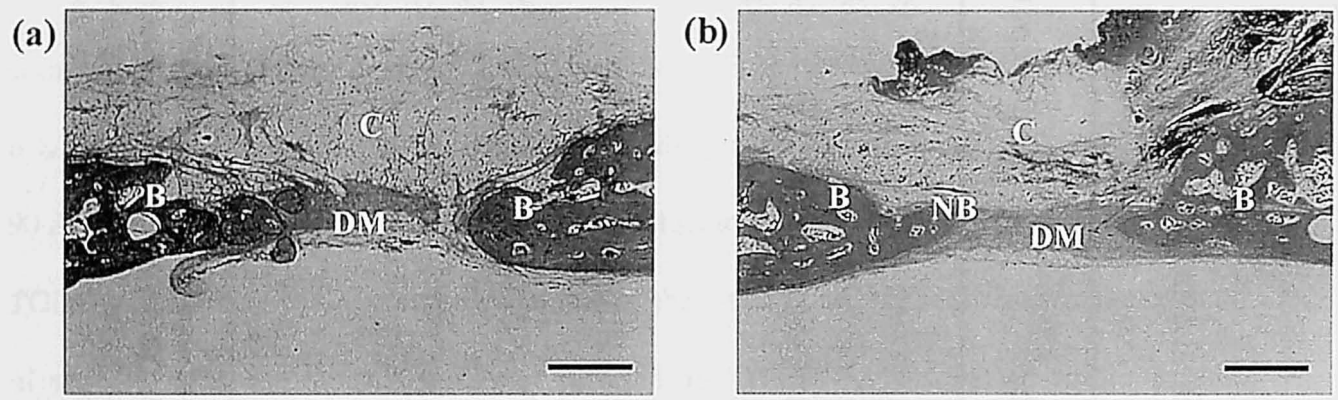

Figure 5. Histological cross-sections at the skull defect of rabbits 8 weeks after treatment with PBS (a), 0.1 μg of free TGF-β1 (b), TGF-β1-free, empty acidic gelatin hydrogels (c, e, g, and i), and TGF-β1 (0.1 μg)-incorporating acidic gelatin hydrogels (d, f, h, and j). The water contents of hydrogels are 85 (c and d), 90 (e and f), 95 (g and h), and 98 wt% (i and j). B; Bone, DM; Dura mater, C; Connective tissue, and NB; New bone. Asterisks indicate acidic gelatin hydrogels with or without TGF-β1 remaining in the defect (H-E staining). Every bar corresponds to 1 mm length.

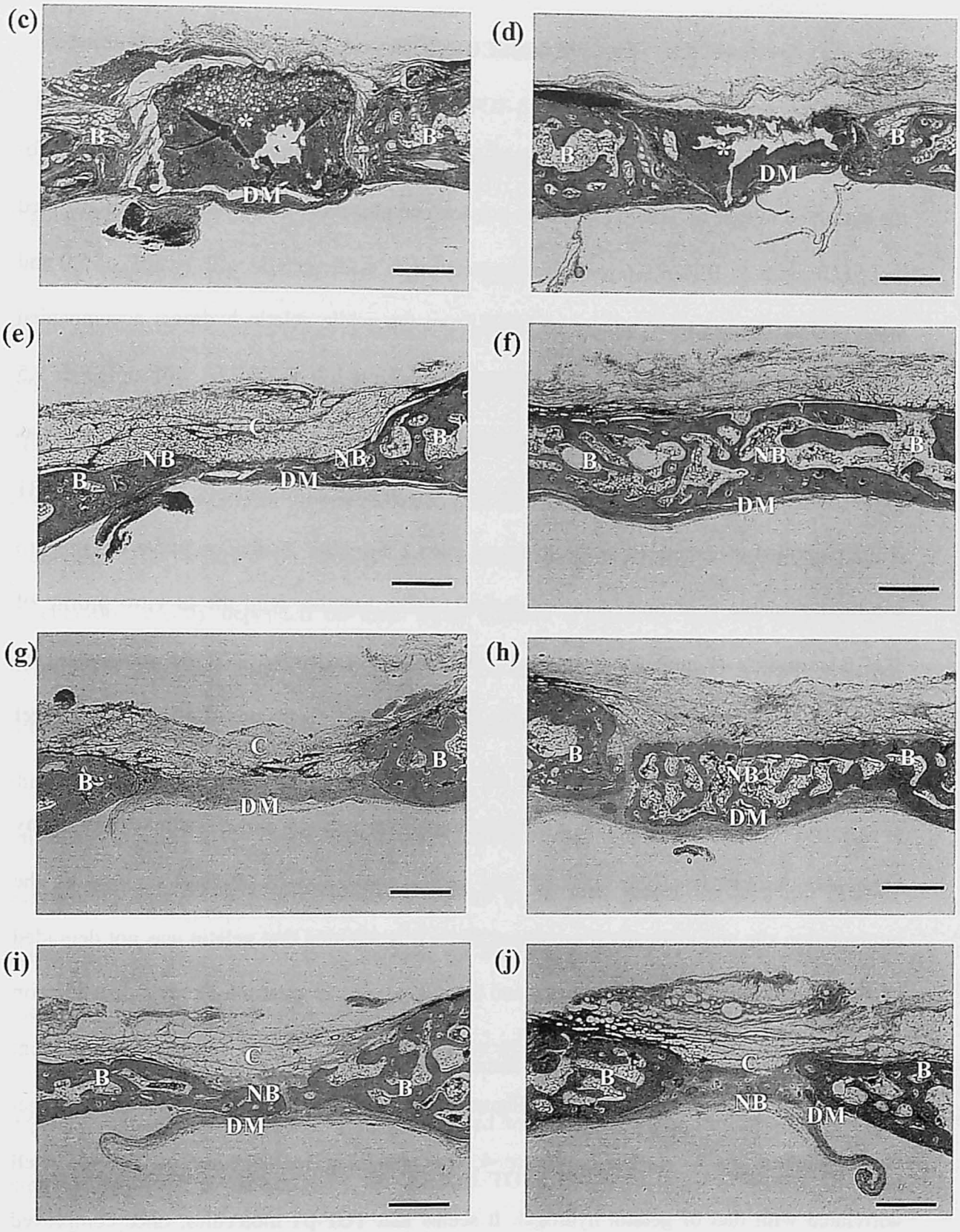

Figure 5. (Continued).

DISCUSSION

This chapter attempted to develop hydrogel carrier system composed of gelatin for the sustained release of TGF-β1 based on polyion complexation. A recent study demonstrated that bFGF with an IEP of 9.6 ionically interacted with acidic gelatin with an IEP of 5.0 and succeeded in the sustained release of bFGF from the acidic gelatin hydrogel accompanied with hydrogel biodegradation[17-19]. It is likely that, similar to bFGF, TGF-β1 with an IEP of 9.5 is immobilized into the acidic gelatin hydrogel based on polyion complex. When TGF-β1 was sorbed into the acidic gelatin hydrogel at 4 °C overnight, approximately 80 % of TGF-β1 initially applied was retained in the hydrogel even 1 day after incubation under the in vitro non-biodegradable condition (data not shown). Taken together with the in vitro profile of TGF-β1 sorption (Figure 1), it is likely that positively charged TGF-β1 molecules are electrostatically complexed with negatively charged gelatin chains constituting the hydrogel carrier.

Radioactivity localization around the implanted hydrogel and no radioactivity in any organ demonstrate that both TGF-β1 and gelatin were slowly released in vivo at the implantation site and gradually disappeared there. It is reported that gelatin was not degraded by simple hydrolysis but by proteolysis and the degradation of gelatin hydrogels depended on their water content[18, 23]. The prolonged in vivo retention of TGF-β1 and the water content dependence of the retention period (Figure 2) may be explained in terms of hydrogel biodegradation. As is shown in Figure 4, the remaining radioactivity of TGF-β1 well correlated with that of gelatin hydrogel. It seems that TGF-β1 molecules, once complexed with the acidic gelatin, cannot be released from the acidic gelatin hydrogels unless hydrogel

degradation occurs. TGF-β1-incorporating acidic gelatin hydrogels with lower water contents will be degraded more slowly, leading to the TGF-β1 release for longer time periods than those with higher water contents. In this system, the TGF-β1 release from the hydrogel can be regulated by hydrogel biodegradation.

The bioactivity of TGF-β1 released from TGF-β1-incorporating acidic gelatin hydrogels was evaluated in terms of bone regeneration by use of a rabbit model with a skull defect. Free TGF-β1 treatment did not significantly enhance the BMD at the skull defect (Table 2). A similar BMD at the defect of rabbits treated with TGF-β1-free, empty gelatin hydrogels to that of control rabbits indicated that the hydrogel itself had no ability for bone induction. The activity of TGF-β1-incorporating gelatin hydrogels to induce bone regeneration greatly depended on their water content. It is likely that the fast-degraded hydrogel neither contributed to prolonged retention of TGF-β1 nor to protect the defect from the ingrowth of soft tissues. When the rate of hydrogel degradation is too slow compared with that of bone regeneration at the skull defect, the hydrogel remaining in the defect will physically impair bone regeneration, even though long-termed release of TGF-β1 is achievable. This finding indicates that a balance in the time profile between the TGF-β1 release and the bone formation is essential for the bone regeneration induced by TGF-β1-incorporating gelatin hydrogels.

Based on the suggested release mechanism of TGF-β1 from the gelatin hydrogel, TGF-β1 molecules are released being complexed with degraded gelatin fragments. Further study is required to confirm how the released TGF-β1 acts to target cells and exert its biological function in vivo.

References

1. M. Lind, Growth factors: Possible new clinical tools A review, *Acta. Orthop. Scand.*, **67**, 407-417 (1996).
2. T. A. Linkhart, S. Mohan and D. J. Baylink, Growth factors for bone growth and repair: IGF, TGF-β and BMP, *Bone*, **19 Supplement**, 1S-2S (1996).
3. M. E. Nimni, Polypeptide growth factors: targeted delivery systems, *Biomaterials*, **18**, 1201-1225 (1997).
4. J. Taipale and J. Keski-Oja, Growth factors in the extracellular matrix, *FASEB J.*, **11**, 51-59 (1997).
5. T. A. McCaffrey, D. J. Falcone and B. Du, Transforming growth factor-β1 is a heparin-binding protein: identification of putative heparin-binding regions and isolation of heparins with varying affinity for TGF-β1, *J. Cell. Physiol.*,**152**, 430-440 (1992).
6. M. Lyon, G. Rushton and J. T. Gallagher, The interaction of the transforming growth factor-βs with heparin/heparan sulfate is isoform-specific, *J. Biol. Chem.*, **272**, 18000-18006 (1997).
7. V. M. Paralkar, S. Vukicevic and A. H. Reddi, Transforming growth factor β type 1 binds to collagen IV of basement membrane matrix: implications for development, *Develop. Biol.*, **143**, 303-308 (1991).
8. B. S. Strates and J. F. Connolly, Osteogenesis in cranial defects and diffusion chambers. *Acta Orthop. Scand.*, **60**, 200-203 (1980).
9. D. R. Sumner, T. M. Turner, A. F. Purchio, W. R. Gombotz, R. M. Urban and J. O.

Galante, Enhancement of bone ingrowth by transforming growth factor-β, *J. Bone Joint Surg.*, **77-A**, 1135-1147 (1995).

10. U. Ripamonti, B. B. Van Den Heever, N. Duneas, B. Melsen and R. Ebner, Limited chondro-osteogenesis by recombinant human transforming growth factor-β1 in calvarial defects of adult baboons (*papio ursinus*), *J. Bone Miner. Res.*, **11**, 938-945 (1996).

11. J. P. Moxham, D. J. Kibblewhite, A. G. Bruce, T. Rigley, T. Gillespy III and J. Lane, Transforming growth factor-β1 in a guanidine-extracted demineralized bone matrix carrier rapidly closes a rabbit critical calvarial defect, *J. Otolaryngol.*, **25**, 82-87 (1996).

12. J. P. Moxham, D. J. Kibblewhite, M. Dvorak, B. Perey, A. F. Tencer, A. G. Bruce and D. M. Strong, TGF-β1 forms functionally normal bone in a segmental sheep tibial diaphyseal defect, *J. Otolaryngol.*, **25**, 388-392 (1996).

13. W. R. Gombotz, S. C. Pankey, L. S. Bouchard, J. Ranchalis and P. Puolakkainen, Controlled release of TGF-β1 from a biodegradable matrix for bone regeneration, *J. Biomater. Polymer Edn.*, **5**, 49-63 (1993).

14. W. R. Gombotz, S. C. Pankey, L. S. Bouchard, D. H. Phan and P. Puolakkainen, Stimulation of bone healing by transforming growth factor-beta1 released from polymeric or ceramic implants, *J. Appl. Biomater.*, **5**, 141-150 (1994).

15. L. S. Steven Beck, E. P. Amento, Y. Xu, L. Deguzman, W. P. Lee, T. Nguyen and N. A. Gillett, TGF-β1 induces bone closure of skull defects: temporal dynamics of bone formation in defects exposed to rhTGF-β1, *J. Bone Miner. Res.*, **8**, 753-761 (1993).

16. D. Zekorn, Modified gelatin as plasma substitutes, *Bibl. Haematol.*, **33**, 30-60 (1969).

17. Y. Tabata and Y. Ikada, Protein release from gelatin matrices, *Adv. Drug Delivery Reviews*, **31**, 287-301 (1998).

18. Y. Tabata, A. Nagano and Y. Ikada, In vitro sorption and desorption of basic fibroblast growth factor for biodegradable hydrogels, *Tissue engineering* (1998) in press.

19. Y. Tabata, S. Hijikata and Y. Ikada, Enhanced vascularization and tissue granulation by basic fibroblast growth factor impregnated in gelatin hydrogels, *J. Controlled Release*, **31**, 189-199 (1994).

20. K. Yamada, Y. Tabata, K. Yamamoto, S. Miyamoto, I. Nagata, H. Kikuchi and Y. Ikada, Potential efficacy of basic fibroblast growth factor incorporated in biodegradable hydrogels for skull bone regeneration, *J. Neurosurg.*, **86**, 871-875 (1997).

21. A. E. Bolton and W. M. Hunter, The labeling of proteins to high specific radioactivities by conjugation to a ^{125}I-containing acylating agent, *Biochem. J.*, **133**, 529-539 (1973).

22. M. Yamamoto, Y. Tabata, and Y. Ikada, Ectopic bone formation induced by biodegradable hydrogels incorporating bone morphogenetic protein, *J. Biomater. Sci. Polym. Eds.*, **9**, 439-458 (1998).

23. K. Tomihata, K. Burczak, K. Shiraki and Y. Ikada, Cross-linking and biodegradation of native and denatured collagen, in *"Polymers of biological and biomedical significance"* S. W. Shalaby, Y. Ikada, R. Langer, and J. Williams eds., ACS Symposium Series 540, ACS, Washington, DC, 1994, pp. 275-286.

Chapter 4

Promoted ingrowth of fibrovascular tissue into porous sponges by bFGF

INTRODUCTION

A number of porous biomaterials have been prepared from poly (L-lactide) (PLLA), L-lactide and glycolide copolymers (PLGA), collagen, and hydroxyapatite to demonstrate the efficacy as scaffolds for cell seeding and tissue regeneration in tissue engineering[1-7,11-15]. The scaffolds function as temporary substrates for proliferation and differentiation of cells seeded or infiltrated from the surrounding host tissue, and finally are integrated into or degraded in the regenerated tissue. It has been widely accepted that cell-scaffold interaction is greatly influenced by their porous structure, especially by their pore size. It is known that there is an optimal pore size for cell infiltration and host tissue ingrowth; for instance, 5-15 μm for fibroblasts[8], 20-125 μm for adult mammalian skin tissues[9,10], 100-350 μm for bone tissues[8,11], and 40-100 μm for osteoid tissues[8].

However, seeded cells do not always survive for a long time period in a scaffold, because oxygen and nutrients are not sufficiently supplied to transplanted cells due to their poor diffusion through the scaffold. Vascularization in the interior of scaffold seems to be a very good means to overcome this problem. For example, hepatocytes were seeded into a porous biodegradable scaffold, followed by transplantation at the rat mesentery having abundant blood vessels, since this tissue may provide the cells with oxygen and nutrients

sufficient enough for survival[12,13]. Angiogenic growth factors, including bFGF, platelet-derived growth factor, and vascular endothelial growth factor, have been used to induce capillary formation in porous scaffolds[14-17].

The objective of this chapter is to investigate the effect of bFGF addition and pore size of a scaffold on the ingrowth of fibrovascular tissue. As the scaffold, poly (vinyl alcohol) (PVA) sponges with different pore sizes were employed, while bFGF was selected to induce the fibrovascularization. Two methods were applied for incorporation of bFGF into the sponge: one is by incorporating bFGF into gelatin microspheres and the other is by direct deposition of bFGF from solution into the PVA sponges. The hydrogel microspheres were prepared from "acidic" gelatin with an IEP of 5.0, as this polymer is able to form polyion complex with "basic" bFGF[18]. A recent study demonstrated that the polyion complex could release bFGF in the biologically-active state as a result of gelatin biodegradation[18] and enhanced the angiogenetic effect, in marked contrast to free bFGF[18-20]. The PVA sponges receiving bFGF-containing gelatin microspheres or free bFGF in solution were subcutaneously implanted in the back of mice and ingrowth of fibrous tissues and formation of new capillaries were histologically compared with those without bFGF.

EXPERIMENTAL

Materials

Aqueous solution of bFGF with an IEP of 9.6 was supplied by Kaken Pharmaceutical Co., Ltd., Tokyo, Japan. A gelatin sample with an IEP of 5.0 (Nitta Gelatin Co., Osaka, Japan)

was extracted from bovine bone with an alkaline process. PVA sponge sheets with interconnected pores of various average pore sizes but a similar porosity were kindly supplied by Kanebou Co., Ltd., Osaka, Japan (Table 1). These sponges were synthesized by formalization of PVA in the presence of starch, followed by starch extraction. The extent of formalization was approximately 80 mol%. Glutaraldehyde (GA), glycine, and other chemicals were purchased from Wako Pure Chemical Industries, Osaka, Japan and used without further purification.

Table 1. The pore size and porosity of PVA sponges used in this study.

Average pore size (μm)	Porosity (%)
30	91
60	88
110	88
250	90
350	91
700	90

Preparation of biodegradable hydrogel microspheres incorporating bFGF

Gelatin microspheres were prepared through GA crosslinking of gelatin aqueous solution in w/o dispersion as described elsewhere[20]. Immediately after mixing 25 μL of GA aqueous solution (25 wt%) with 10 mL of 10 wt% gelatin solution preheated at 40 °C, the mixture was dropwise added to 375 mL of olive oil under stirring at 420 rpm and 40 °C. Stirring was continued for 24 hr at room temperature to allow chemical crosslinking of gelatin to proceed. After an addition of 100 mL of acetone to the mixture, the resulting crosslinked

microspheres were collected by centrifugation (4 °C, 3000 rpm, 5 min) and washed 5 times with acetone by centrifugation. The washed microspheres were placed in 100 mL of 100 mM glycine aqueous solution containing Tween 80 (0.1 wt%), followed by agitation at 37 °C for 1 hr to block residual aldehyde groups of unreacted GA. Then, the resulting microspheres were washed twice with DDW by centrifugation, freeze-dried, and sterilized with ethylene oxide gas. The water content of gelatin microspheres was calculated from the microsphere volume before and after swelling in PBS (pH 7.4) for 24 hr at 37 °C. The microsphere used in this chapter had the water content of 95 vol%[19]. The microsphere diameter was measured for at least 100 microspheres by viewing with a light microscope to calculate their volume. The average diameter of microspheres was 100 μm.

bFGF was impregnated into gelatin microspheres by drop-wise addition of 10 mg/mL of bFGF solution (10 μL) onto 2 mg of freeze-dried gelatin microspheres. They were left at room temperature for 1 hr. Empty gelatin microspheres without bFGF were prepared in the same way as above except using DDW as the solution to add. The solutions (10 μL) were completely sorbed into the microspheres during swelling, because the solution volume was less than that theoretically required for the equilibrated swelling of microspheres.

bFGF incorporation into PVA sponges

PVA sponge sheets of 1 mm thick were punched out to obtain sponge discs of 6 mm in diameter. Two pieces of PVA sponge discs were overlapped and peripherally sutured together with a 7-0 polypropylene monofilament under a wet condition to make sponges soft for easy sewing and tight suturing. The two-layered PVA sponges (2 mm in thickness, 6 mm in diameter) were dried and sterilized with ethylene oxide gas.

The gelatin microspheres (2 mg) with or without bFGF were suspended in 0.2 mL of DDW and the microsphere suspension was aseptically added into the central portion of two-layered sponges. During this process, excess DDW was diffused out while the microspheres were trapped in the center of sponges, irrespective of the pore size. In addition, 10 μL of PBS containing 100 μg of bFGF was given to PVA sponges to incorporate free bFGF into the sponges. As a control, 10 μL of PBS alone was added to PVA sponges.

Assessment of fibrous tissue ingrowth and capillary formation in PVA sponges

Sponges with or without bFGF were subcutaneously implanted into the back of female ddY mice, 6 week-old (Shimizu laboratory supply, Kyoto, Japan). Each experimental group was composed of 3 mice and the bFGF dose was fixed to 100 μg / mouse. At 1, 3, and 6 weeks post-implantation, mice were sacrificed and the implanted PVA sponges were removed together with their surrounding fibrovascular tissue. The explanted sponges were fixed with 10 % neutralized formalin solution, embedded in paraffin, and sectioned at the center of PVA sponges or at the site as close as possible to the center (2 μm thickness), followed by staining with H-E.

Photomicrographs of histological sections were taken at a magnification of 40 to evaluate the ingrowth of fibrous tissue and capillary formation in PVA sponges. Six areas were randomly selected from each of microphotographs. The distance from the sponge edge to the front line of the fibrous tissue ingrown into the sponges was measured and the number of capillaries newly formed in the same area was counted and expressed as the mean ± standard error.

RESULTS

Ingrowth of fibrous tissue into PVA sponges

Figure 1 shows the typical histological sections of PVA sponges with and without bFGF 3 weeks after implantation. bFGF was incorporated in gelatin microspheres. The sponge pore size had a great influence on the ingrowth of fibrous tissue accompanied with new capillary formation into the sponges. Remarkable fibrous tissue ingrowth was observed for the sponge having a pore size of 250 μm, whereas pores were not occupied with the fibrous tissue but with a fibrin-like tissue for the sponge with a large pore size, such as 700 μm.

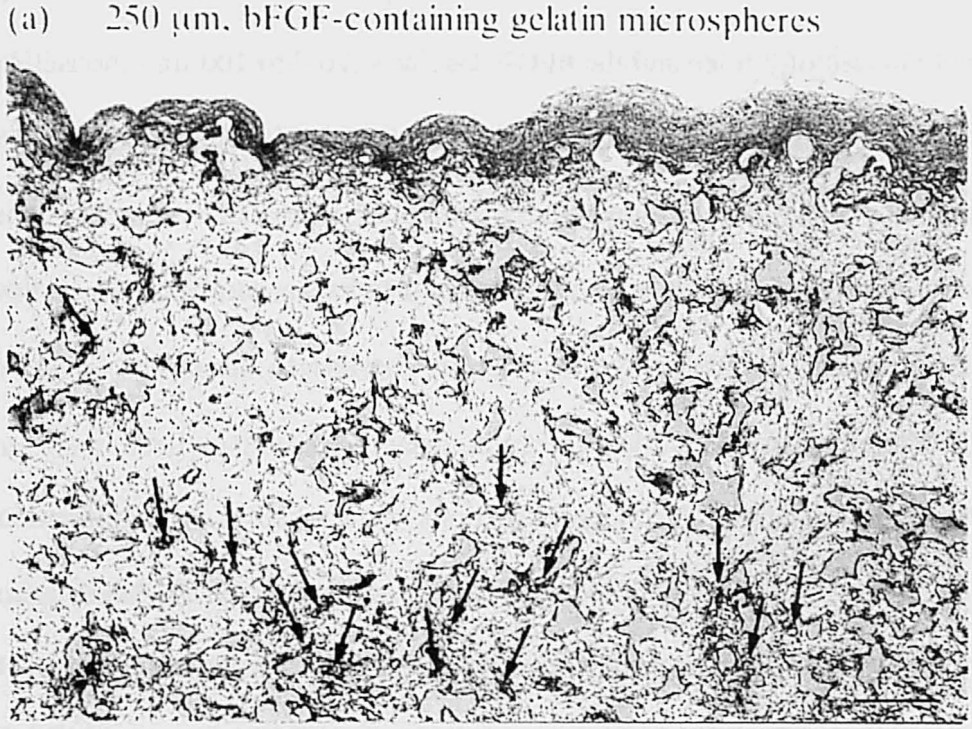

Figure 1. Histological sections of PVA sponges incorporating bFGF-containing gelatin microspheres 3 weeks after implantation in the back subcutis of mice. The pore size of the sponges was 250 (a) and 700 μm (b). Arrows indicate capillaries newly formed in PVA sponges. Histological sections were viewed at the magnification of 40 following H-E staining. Bars correspond to 100 μm.

(b) 700μm, bFGF-containing gelatin microspheres

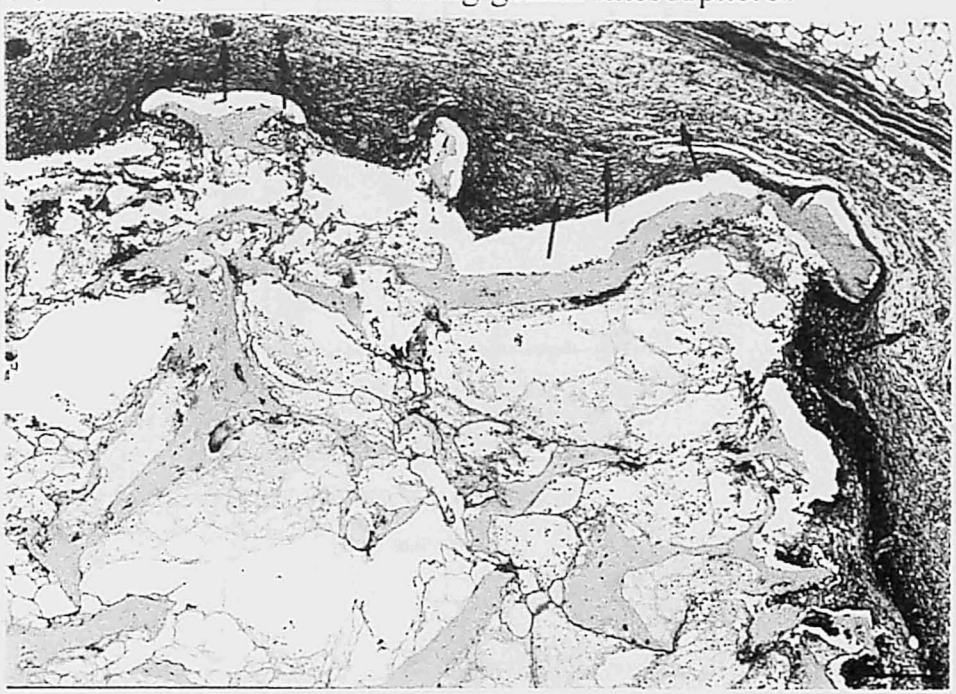

(c) 250μm, PBS

Figure 1 (Continued)

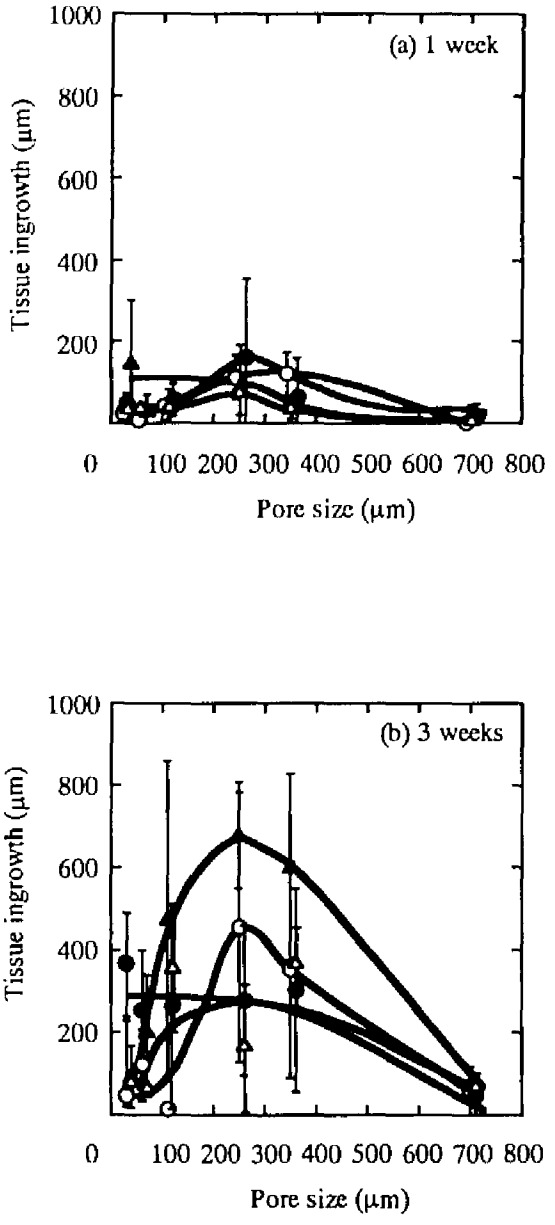

Figure 2. The effect of pore size on the fibrous tissue ingrowth into PVA sponges incorporating PBS (○), free bFGF (●), empty gelatin microspheres (△), and bFGF-containing gelatin microspheres (▲). The sponge sections were viewed 1 (a), 3 (b), and 6 weeks (c) after subcutaneous implantation in the back of mice. The bFGF dose was 100 μg / mouse.

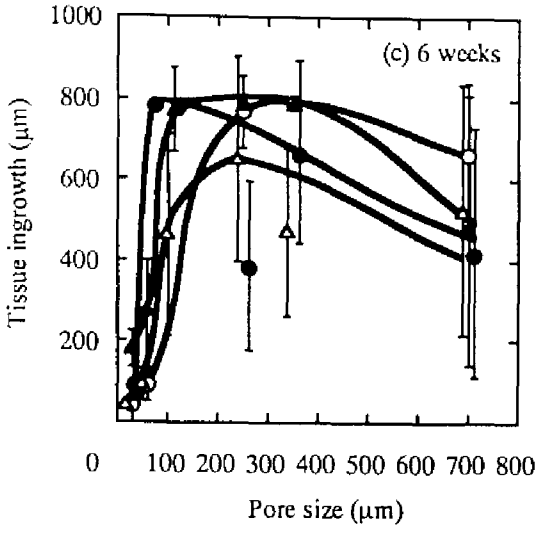

Figure 2. (Continued).

The time course of fibrous tissue ingrowth is shown in Figure 2 after subcutaneous implantation of sponges with different pore sizes. It is apparent that tissue ingrowth depended on both the pore size of PVA sponges and their bFGF incorporation. Tissue ingrowth seems to become the highest around the medium pore size (250 μm) at least 1 and 3 weeks after implantation. The bFGF entrapped in gelatin microspheres appears to have more markedly promoted the ingrowth of fibrous tissue into sponges than the others at 3 weeks post-implantation, irrespective of the pore size. Empty gelatin microspheres did not contribute to any enhancement of tissue ingrowth. On 6 weeks postoperatively, the pores of PVA sponges were almost completely filled with fibrous tissue, regardless of the presence of bFGF. However, tissue ingrowth virtually did not occur for PVA sponges with the pore sizes of 30 and 60 μm, while less ingrowth was observed for the sponge with the largest pore (700 μm). In this case, bFGF-containing gelatin microspheres enhanced tissue ingrowth, even though the pore size was very large.

New capillary formation in PVA sponges

Figure 3 shows the number of capillaries newly formed in the PVA sponges as a function of the distance from their periphery 3 and 6 weeks after subcutaneous implantation in the back of mice. It is apparent that bFGF was effective in promoting neovascularization in the sponges. When bFGF-containing gelatin microspheres had been given to PVA sponges prior to implantation, new capillaries were formed in the sponge at a slightly higher rate and more deeply into the interior region than free bFGF. Enhanced capillary formation was noticed for the PVA sponges with medium pore sizes of 250 and 350 μm than with the smaller or larger sizes. Empty microspheres and PBS did not induce any significant capillary formation in the sponges, irrespective of the pore size. On 6 weeks after implantation, free bFGF promoted capillary formation to a little less extent than the bFGF-containing gelatin microspheres.

DISCUSSION

bFGF was used as an angiogenetic factor in this chapter, because this growth factor is known to have an inherent ability to let both fibroblasts and capillary endothelial cells proliferate in vitro. In addition, bFGF is effective also in vivo, as evidenced by enhanced wound healing through vascularization[21,22]. However, such a high bFGF efficacy is not always achieved when administrated directly in the body without any carrier, probably because of its very short half-life in the body. As one trial to effectively induce the biological activity of bFGF, sustained release systems have been created and it was demonstrated that

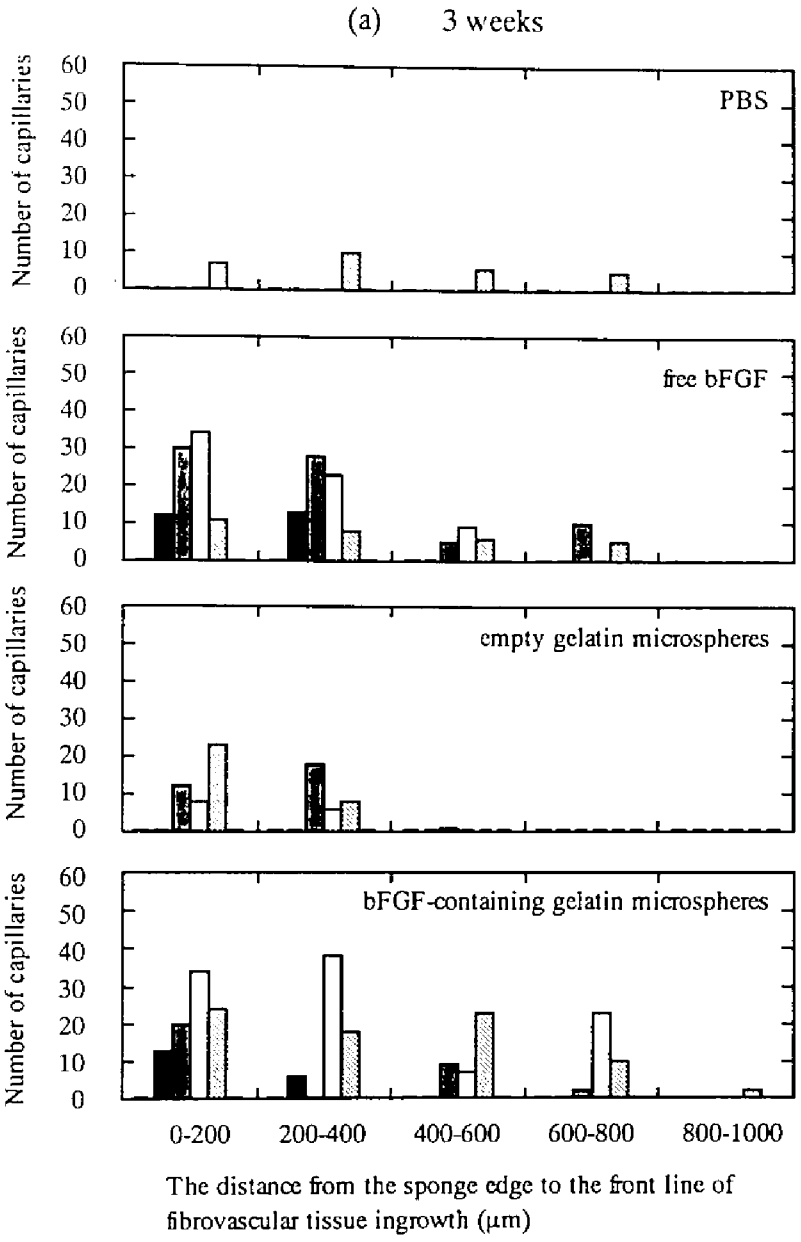

Figure 3. The number of newly formed capillaries as a function of the diameter from the sponge edge to the front line of fibrovascular tissue ingrowth for PVA sponges incorporating PBS, free bFGF, empty gelatin microspheres, and bFGF-containing gelatin microspheres 3 (a) and 6 weeks (b) after subcutaneous implantation in the back of mice. The pore size of PVA sponges was 30 (□), 60 (■), 110 (▣), 250 (□), 350 (▣), and 700 (▣) μm.

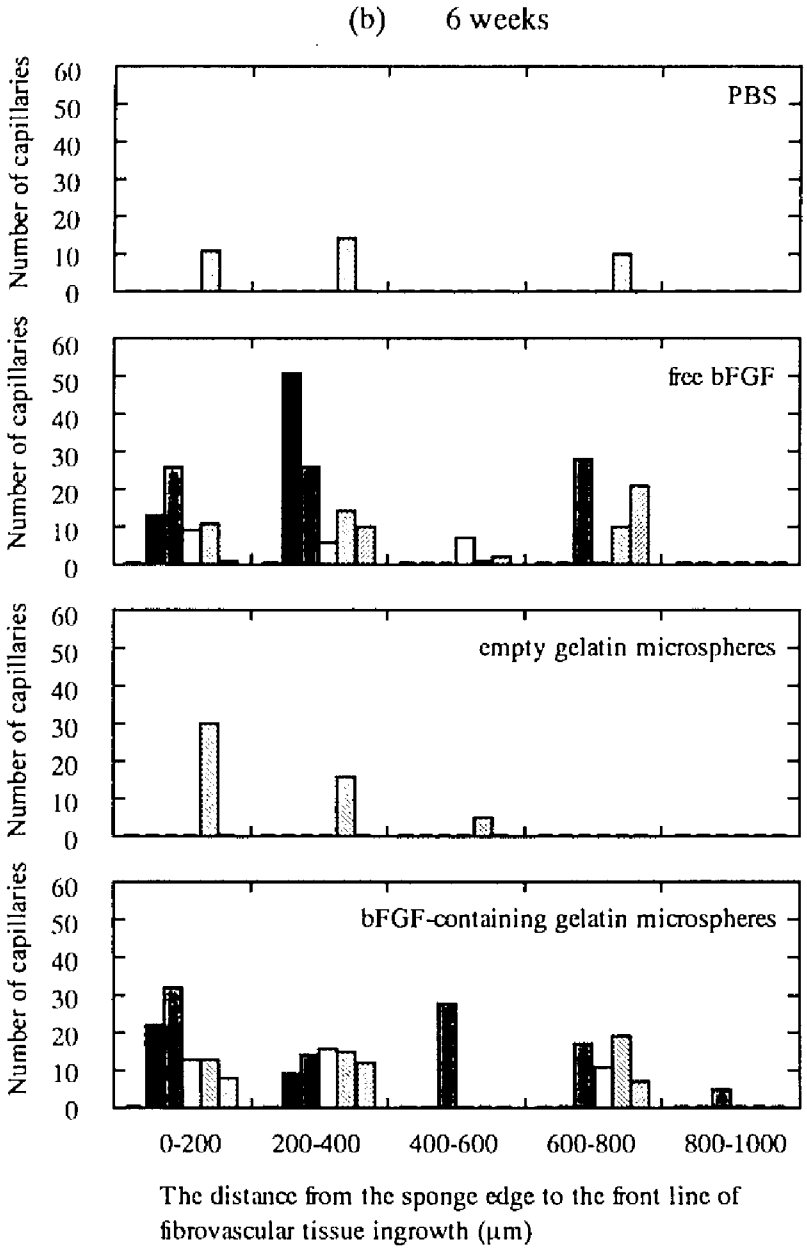

Figure 3. (Continued).

vascularization, granulation, and osteogenesis were markedly promoted by sustained release of bFGF, in marked contrast to direct administration of bFGF[18-20,23]. However, the results shown above revealed that the release system using gelatin microspheres had a neovascularization effect, but only a little superior to free bFGF in solution. This unexpected result seems to be ascribed to the physical adsorption of bFGF molecules onto the PVA sponge wall.

PVA sponges have an interconnected pore structure with a relatively narrow pore size distribution. As PVA is not biodegradable but bio-inert[24], one can evaluate the fibrovascular tissue ingrowth without taking into consideration the scaffold degradation. A most interesting finding of this chapter is that there was an optimum pore size for fibrovascular tissue ingrowth into sponges. Practically no tissue ingrowth was observed in the sponges with small pore sizes of 30 and 60 μm even if they were much larger than the fibroblast size. It seems necessary for sponges of tissue ingrowth to have preconditioning on the pore surface by biological substances, such as protein adsorption and fibrin deposition for cell adhesion. However, implantation of PVA sponge may not require such preconditioning, because the pore wall of this sponge is wettable and is rapidly adsorbed by serum proteins after implantation. Profound protein adsorption might reduce the pore size to a level preventing cell infiltration especially for sponges with small pores, resulting in no ingrowth of fibrous tissue. On the other hand, the decreased tissue ingrowth observed for the PVA sponge with the largest pore size may be ascribed to too large surface area for cell to attach. It is reasonable to assume that there is an optimal surface area required for cell attachment and the subsequent tissue ingrowth in the sponge. The balance in these two factors, preconditioning and surface area, must be a key factor for tissue ingrowth. As the surface area of sponges

decreases with the increasing pore size, the most favorable fibrovascular tissue ingrowth must have occurred into the PVA sponge with the medium pore size ranging from 110 to 350 μm.

This chapter has also demonstrated that bFGF incorporation is essential in inducing new formation of capillaries in sponges. The enhanced vascularization by bFGF entrapped in gelatin microspheres is obviously due to sustained release of bFGF[20]. However, the bFGF injected in solution could also promote vascularization, to a little smaller extent than the bFGF entrapped in microspheres, although free bFGF seems to be rapidly excreted from the injection site. This is likely to be due to strong protein adsorption to the PVA sponge wall. The adsorption seems to have helped the sustained release of bFGF, because of slow desorption of bFGF molecules from the PVA sponge wall. The average number of capillaries in the PVA sponges was larger as the pore size decreased. This suggests that a large space must be required for capillary formation because of canalization, contrary to fibrous tissue ingrowth. This may be also the reason why no vascularization was seen in the PVA sponge with the smallest pore size.

In conclusion, fibrous tissue ingrowth occurred into PVA sponges and the ingrowth rate showed a maximum at pore sizes around 250 μm, probably due to the balance in two factors, preconditioning of the pore surface for cell infiltration and surface area of the sponges for cell attachment. Incorporation of bFGF into the sponges promoted the growth of fibrous tissue especially at 3 weeks post-implantation, and more greatly enhanced formation of new capillaries, regardless of the pore size. There was no significant difference in capillary formation between the bFGF entrapped in gelatin microspheres and free bFGF. It was concluded that incorporation of bFGF-containing gelatin microspheres was a potential way to induce fibrovascular tissue ingrowth in the pore of sponges.

References

1. *Frontiers in tissue engineering*, C. W. Patrick Jr., A. G. Mikos, and L. V. McIntire eds., Pergamon, UK (1998).
2. *Synthetic biodegradable polymer scaffolds*, A. Atala, D. J. Mooney, J. P. Vacanti, and R. Langer eds., Birkhäuser, Boston USA (1997).
3. L. E. Freed, J. C. Marquis, A. Nohria, J. Emmanual, A. G. Mikos, and R. Langer, Neocartilage formation in vitro and in vivo using cells cultured on synthetic biodegradable polymers, *J. Biomed. Mater. Res.* **27**, 11-23 (1993).
4. A. G. Mikos, G. Sarakinos, S. M. Leite, J. P. Vacanti and R. Langer, Laminated three-dimensional biodegradable forms for use in tissue engineering, *Biomaterials* **14**, 323-330 (1993).
5. A. G. Mikos, G. Sarakinos, M. D. Lyman, D. E. Ingber, J. P. Vacanti, and R. Langer, Prevascularization of porous biodegradable polymers, *Biotech. Bioeng.*, **42**, 716-723 (1993).
6. M. C. Wake, C. W. Patrick, Jr., and A. G. Mikos, Pore morphology effects on the fibrovascular tissue growth in porous polymer substrates, *Cell Transplant.*, **3**, 339-343 (1994).
7. R. C. Thomson, M. J. Yaszemski, J. M. Powers, and A. G. Mikos, Fabrication of biodegradable polymer scaffolds to engineer trabecular bone, *J. Biomater. Sci. Polymer Edn.*, **7**, 23-38 (1995).
8. J. J. Klawitter and S. F. Hulbert, Application of porous ceramics for the attachment of load bearing internal orthopedic applications, *J. Biomed. Mater. Res. Sympo.*, **2**,

161-229 (1971).

9. S. Gogolewski and A. J. Pennings, An artificial skin based on biodegradable mixtures of polylactides and polyurethanes for full-thickness skin wound covering, *Macromol. Chem., Rapid Commun.*, **4**, 675-680 (1983).

10. I. V. Yannas, E. Lee, D. P. Orgill, E. M. Skrabut, and G. F. Murphy, Synthesis and characterization of a model extracellular matrix that induces partial regeneration of adult mammalian skin, *Proc. Natl. Acad. Sci. USA,* **86**, 933-937 (1989).

11. B. P. Robinson, J. O. Hollinger, E. H. Szachowicz, and J. Brekke, Calvarial bone repair with porous D, L-polylactide, *Otolaryngol. Head Neck Surg.*, **112**, 707-713 (1995).

12. D. J. Mooney, P. M. Kaufmann, K. Sano, K. M. McNamara, J. P. Vacanti, and R. Langer, Transplantation of hepatocytes using porous, biodegradable sponges, *Transplant. Proc.*, **26**, 3425-3426 (1994).

13. D. J. Mooney, K. Sano, P. M. Kaufmann, K. Majahod, B. Schloo, J. P. Vacanti and R. Langer, Long-term engraftment of hepatocytes transplanted on biodegradable polymer sponges, *J. Biomed. Mater. Res.*, **37**, 413-420 (1997).

14. S. P. Andrade, R. D. P. Machado, A. S. Teixeira, A. V. Belo, A. M. Tarso, and T. Beraldo, Sponge-induced angiogenesis in mice and the pharmacological reactivity of the neovasculature quantitated by a fluorimetric method, *Micovasc. Res.*, **54**, 253-261 (1997).

15. J. W. Wang and P. Aspenberg, Basic fibroblast growth factor promotes bone ingrowth in porous hydroxyapatite, *Clin. Orthop. Rel. Res.*,**333**, 252-260 (1996).

16. G. Ahrendt, D. E. Chickering, and J. P. Ranieri, Angiogenic growth factors: A review

for tissue engineering, *Tissue Engineering*, **4**, 117-130 (1998).

17. M. E. Nimni, Polypeptide growth factors: targeted delivery systems, *Biomaterials*, **18**, 1201-1225 (1997).

18. Y. Tabata and Y. Ikada, Protein release from gelatin matrices, *Adv. Drug Delivery Review*, **31**, 287-301 (1998).

19. Y. Tabata, S. Hijikata, and Y. Ikada, Enhanced vascularization and tissue granulation by basic fibroblast growth factor impregnated in gelatin hydrogel, *J. Controll. Release*, **31**, 189-199 (1994).

20. Y. Tabata, S. Hijikata, MD. Muniruzzaman, and Y. Ikada, Neovascularization effect of biodegradable gelatin microspheres incorporating basic fibroblast growth factor, *J. Biomater. Sci. Polym. Edn.*, (1998) in press.

21. P. Buntrock, K. D. Jentzsch, and G. Hender, Stimulation of wound healing, using brain extract with fibroblast growth factor (FGF) activity. II. Histological and morphometric examination of cells and capillaries, *Exp. Pathol.*, **21**, 62-67 (1982).

22. G. S. McGee, J. M. Cavidson, A. Buckley, A. Sommer, S. C. Woodward, A. M. Aquino, R. Barbour, and A. A. Demetrious, *J. Surg. Res.*, **45**, 145-153 (1988).

23. Y. Tabata, K. Yamada, S. Miyamoto, I. Nagata, H. Kikuchi, I. Aoyama, M. Tamura, and Y. Ikada, Bone regeneration by basic fibroblast growth factor complexed with biodegradable hydrogels, *Biomaterials*, **19**, 807-815 (1998).

24. Y. Tamada and Y. Ikada, Cell attachment to various polymer surfaces, in "*Polymer in Medicine 2*", E. Chiellini, P. Giusti, C. Migliaresi, and L. Nicolais eds., Plenum Publishing Co., .New York (1986), p. 101-115.

PART II

STRUCTURE OF BONE TISSUE REGENERATED WITH POLYMER MATRICES

Chapter 5

Ultrastructure of construct generated by osteoblasts cultured on surface-modified polymer substrates

INTRODUCTION

The ultrastructure of the interface between an implant surface and its adjacent bone tissue is expected to greatly depend on the chemical nature of the implant surface. Since this may play an important role in the establishment of firm fixation of the implant to the bone, many research groups have studied on such material/bone interfaces to elucidate the course of bone apposition which will enhance implant fixation[1-7]. Most of these studies on the ultrastructure of material/bone interface have been made utilizing in vitro bone-forming cell culture. Such a system allows us to avoid the complexity associated with the in vivo environment which involves many factors interfering the interface analysis. For in vitro studies, several types of osteoblast-lineages have been isolated from periosteum and calvarium of several species including chick, mouse, rat, and human[8]. In 1988, Maniatopoulos et al. developed the in vitro bone cell culture system in which osteoblasts derived from rat bone marrow (RBM) cells elaborate an extracellular matrix containing collagen and eventually form calcified nodules, similar to the bone tissue[9]. Using this RBM cell culture technique, several research groups have attempted to investigate bone/implant interfaces[10-13].

This chapter aims at analyzing the ultrastructure of the interface between cultured osteoblasts derived from RBM cells and four kinds of material surfaces by use of transmission electron microscopy (TEM). All of the modified surfaces used in this chapter are created through a surface grafting technique onto a conventional hydrophobic polyester film. The surfaces used for cell culture include the untreated polyester surface and three modified surfaces with grafted phosphate polymer chains, immobilized collagen molecules, and a deposited thin hydroxyapatite (HAp) layer. The use of the same starting substrate with chemically different surfaces allows us to analyze their ultrastructure of interfaces with cells in the same experimental procedure.

EXPERIMENTAL

Surface modification

A poly(ethylene terephthalate) (PET) film of 50 μm thickness donated by Teijin Co. Ltd., Tokyo, Japan, was used as the starting polymer substrate for surface modification. After Soxhlet extraction with methanol for over 24 hr, the film was subjected to photo-induced graft polymerization of acrylic acid (AAc, Wako Pure Chemical Industries Ltd., Osaka, Japan) and methacryloyloxyethyl phosphate (MOEP, Unichemical Co. Ltd., Nara, Japan). The chemical structure and polymerization conditions of the monomers are given in Table 1. The detailed procedure of grafting was reported elsewhere[14].

The PET film with grafted AAc polymer chains was further subjected to covalent immobilization of type I atelocollagen (Cellmatrix type I-P, Nitta Gelatin Co. Ltd., Japan) onto

Table 1. Chemical structure of the monomers used in this study and their graft polymerization

Monomer	Chemical structure	Monomer concentration (wt%)	UV irradiation time (hr)	Graft density ($\mu g/cm^2$)
Acrylic acid (AAc)	$CH_2=CH-\underset{\underset{O}{\|}}{C}-OH$	10	3	4.2 ± 0.3
Methacryloyloxyethyl phosphate (MOEP)	$CH_2=\overset{\overset{CH_3}{\|}}{C}-\underset{\underset{O}{\|}}{C}-O-CH_2CH_2O-\overset{\overset{OH}{\|}}{\underset{\underset{O}{\|}}{P}}-OH$	10 (in CH_3COOH / H_2O, 1:4, v/v)	4	1.1 ± 0.2

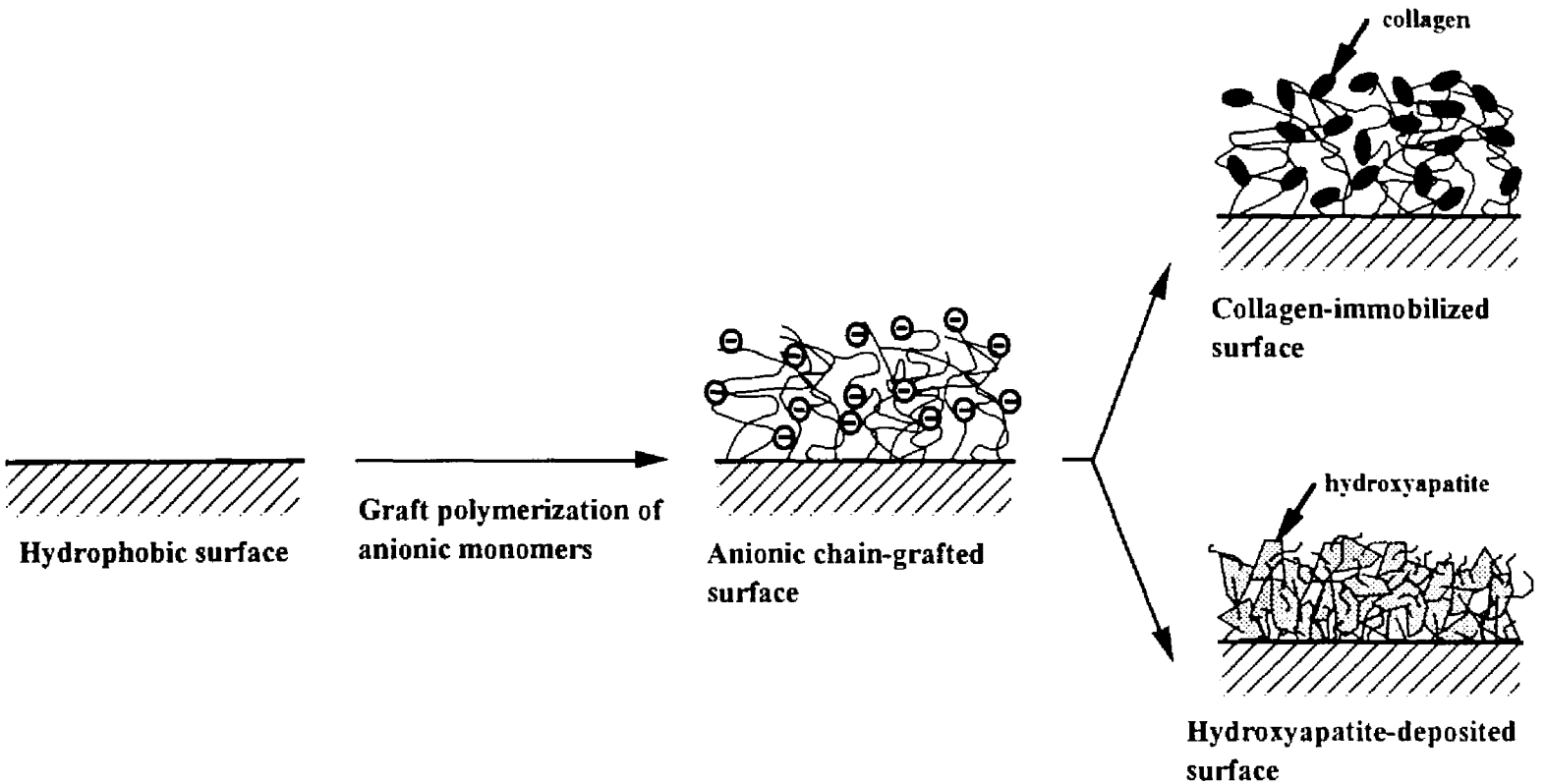

Figure 1. Preparation of polymer surfaces by immobilizing anionic polymer chains, collagen molecules, and hydroxyapatite.

its surface with the use of 1-ethyl-3-(3-dimethylaminopropyl)-carbodiimide[15]. On the other hand, the PET film with grafted MOEP polymer chains was used for cell culture, or a thin HAp microcrystalline layer was deposited onto the polyMOEP (PMOEP)-grafted surface by immersing the film into aqueous solution of calcium and phosphate ions of pH 7.4 according to the method reported elsewhere[16]. The density of immobilized collagen molecules and deposited HAp onto the grafted PET film was 2.7 and 25.9 $\mu g/cm^2$, respectively.

The surface structure of the modified substrates is schematically represented in Figure 1.

Cell isolation and culture

All the modified films were cut into disc with a diameter of 1.5 cm and then sterilized with ethylene oxide gas. RBM cells were obtained from femora of 8-week-old male Wistar rats according to the method reported by Maniatopoulos[9]. After 1 week primary culture of the bone marrow cells on a commercial polystyrene culture dish, the cells were seeded onto the film substrates placed on the bottom of polystyrene cell culture dishes at a cell density of $1.0x10^4$ cells/cm^2 and then maintained in Eagle's minimal essential medium (MEM) supplemented with 15 % fetal bovine serum, 10 nM dexamethasone, 50 μg/mL ascorbic acid, and 10 mM β-glycerophosphate for 1–3 weeks in a humidified atmosphere of 95 % air and 5 % CO_2.

Ultrastructure examination of cell-induced construct

After 1–3 weeks of subculture on each of the substrates, cells were washed in 0.1 M sodium cacodylate buffer (pH 7.2) together with the substrates and fixed for 1 hr at 4 °C in the same buffer solution but containing 0.5 % glutaraldehyde, 2 % paraformaldehyde, 0.1 % tannic acid, 10 μg/mL calcium chloride, and 10 μg/mL magnesium chloride. Postfixation was

performed with 1 % osmium tetroxide in the cacodylate buffer for 1 hr at 4 °C. After washing with 0.1 M sodium acetate, the specimens were subjected to en-block staining with 3 % uranyl acetate in 30 % methanol for 1 hr. All the specimens were then dehydrated through graded ethanol, rinsed with propylene oxide, and embedded in a Spurr resin (TAAB Laboratories Equipment Ltd., Berkshire, UK). The ultrathin cross-sections with a thickness of 80 nm were cut from the specimens with an ultramicrotome and stained with uranyl acetate and lead citrate. Ultrastructural morphology of the material/cell interfaces was observed with TEM (JEM-1200 EX II , JEOL, Tokyo, Japan) operated at 80 kV.

Energy dispersive X-ray (EDX) microanalysis was carried out on the same cross-sections using TEM (H-700X, Hitachi, Japan) operated at 75 kV.

RESULTS

Surface in cell-free medium

Figure 2 shows TEM photographs of the substrates immersed in the culture medium without cells for 1 week. Apparently, no change is observed at the surface of the untreated PET film, while a thin electron-dense layer is formed at the vicinity of the PMOEP-grafted surface, probably due to deposition of calcium phosphate from the medium, as described elsewhere[18]. The two other surfaces having a layer of immobilized collagen (Figure 2c) and deposited HAp (Figure 2d) do not show any remarkable changes upon soaking in the culture medium.

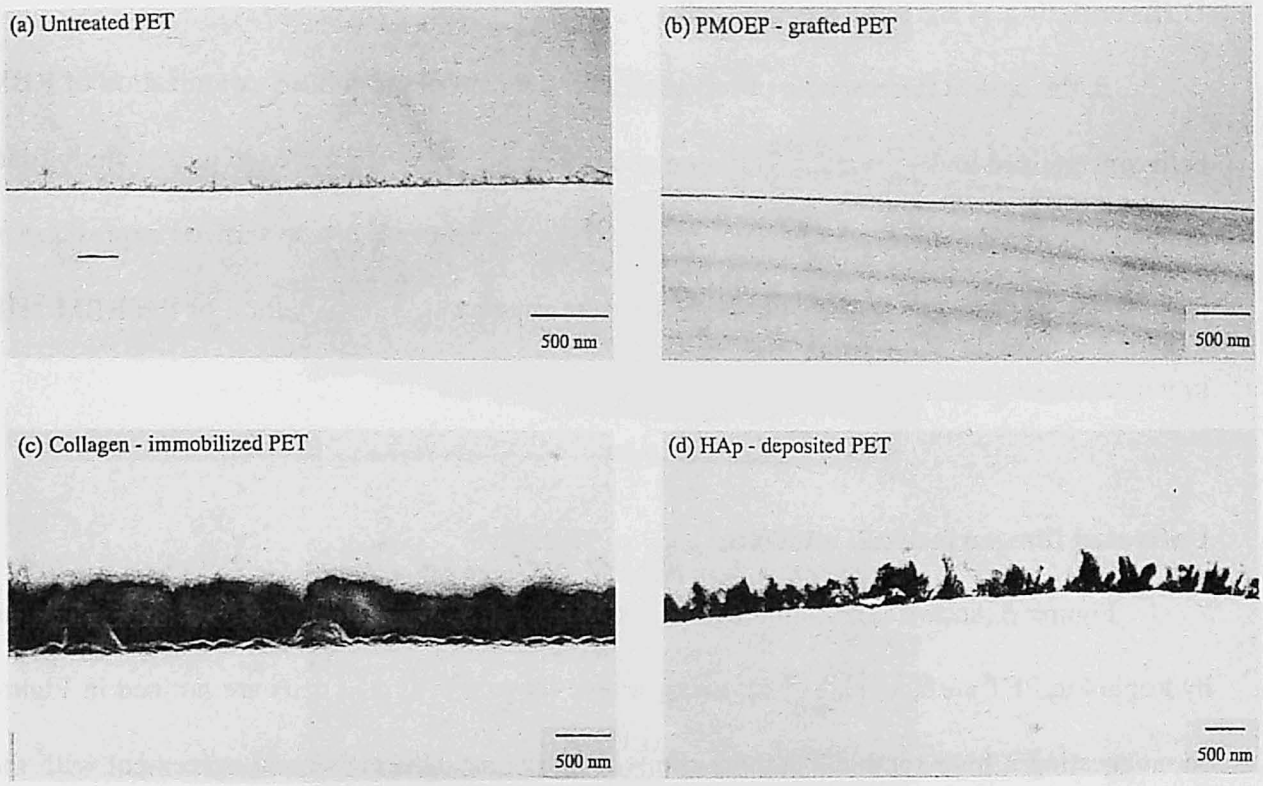

Figure 2. TEM photographs of the cross-section of substrates immersed in the culture medium without any cells for 1 week. (a) untreated PET, (b) PMOEP-grafted PET, (c) collagen-immobilized PET, and (d) HAp-deposited PET.

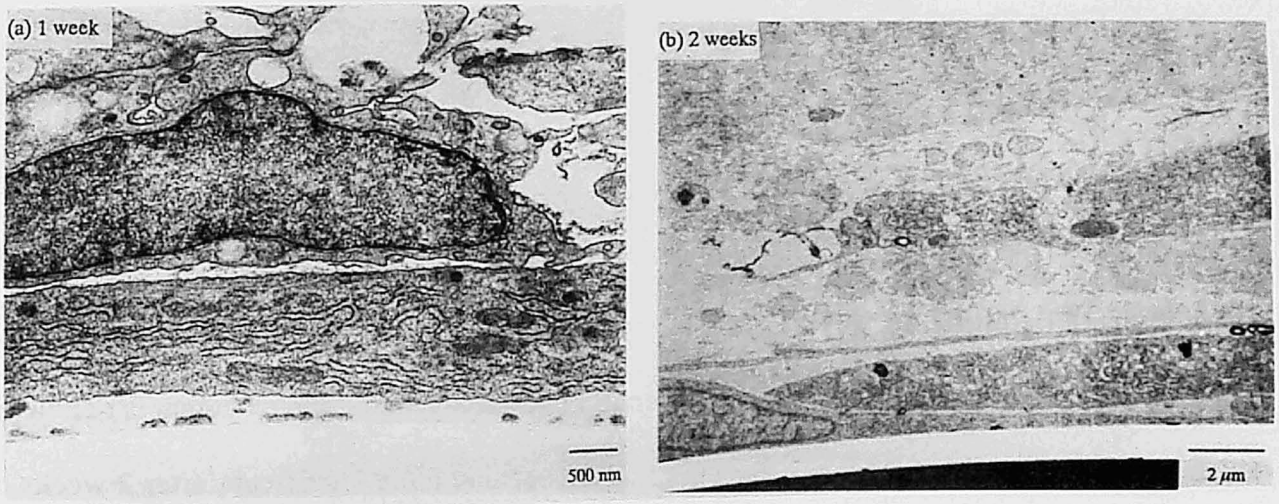

Figure 3. TEM photographs of the cross-section of osteoblasts cultured on the untreated PET surface for (a) 1 and (b) 2 weeks.

Differentiation of rat bone marrow cell

In the optical microscopic observation after 2 weeks of subculture, colonization of RBM cells was noticed under formation of bone nodules on all the substrates used in this study (data not shown). In situ staining specific for membrane alkaline-phosphatase showed expression of the enzyme at a periphery of the nodules, strongly suggesting differentiation of the RBM cells into osteoblasts (data not shown) [17].

Untreated film surface/cell interface

Figure 3 shows TEM photographs of the osteoblasts cultured on the unmodified hydrophobic PET surface. Numerous endoplasmic reticula in spread cells are noticed in Figure 3a, suggesting a high synthetic activity of matrix proteins. This is in good agreement with the photograph in Figure 3b, where type I collagen fibrils with bundles are clearly seen in the extracellular space between layered cells, but no matrix protein is observed between the cultured cells and the substrate. No intact cross-section of the interface could be prepared, as seen in Figure 3b, although the ultrathin sectioning was carefully performed.

PMOEP-grafted surface/cell interface

Figures 4a–4c represent TEM photographs of the interface between cultured osteoblasts and the PET film with grafted MOEP polymer chains. The material/cell interface was well reserved after ultrathin sectioning. As is seen in Figure 4a, endoplasmic reticulum is rich in the intracellular space of spread cells. This feature became more significant after 2 weeks of culture, as seen in Figure 4b, where many spread cells containing numerous lipid inclusions and actively elaborating matrix proteins to fill the extracellular space are observed. This matrix is

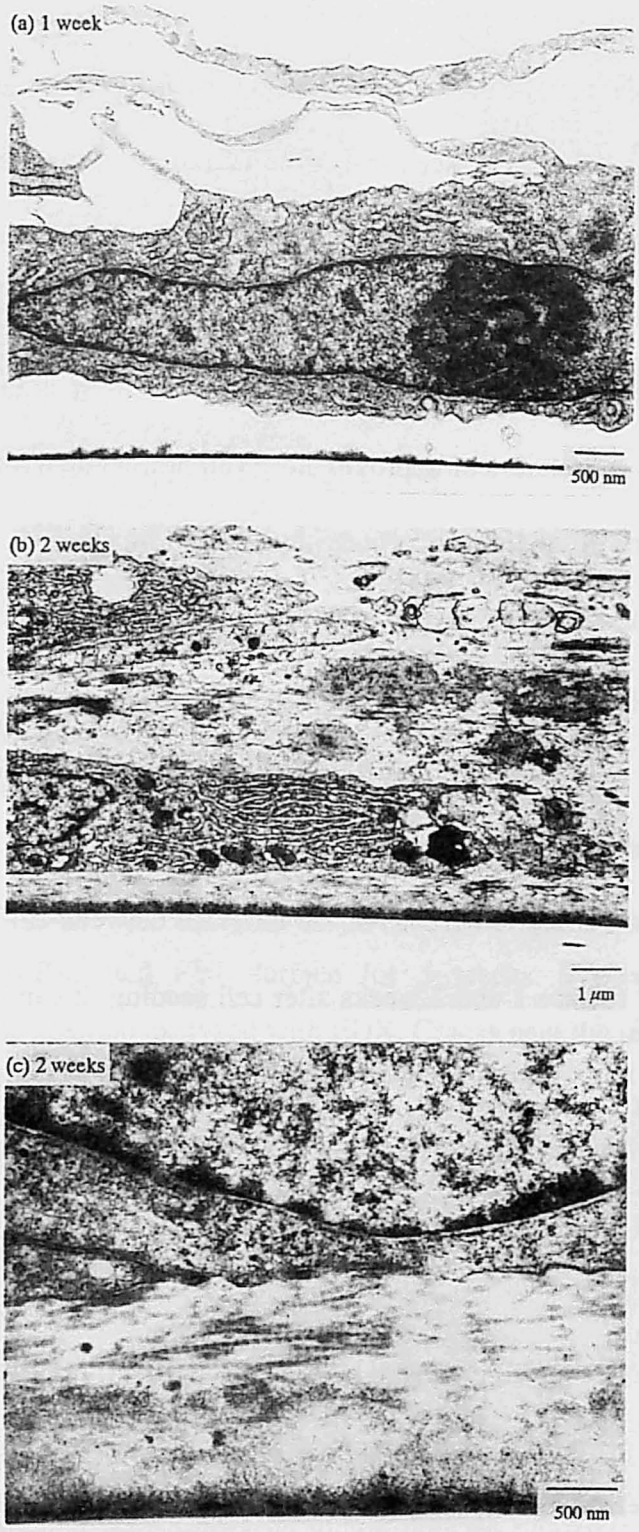

Figure 4. TEM photographs of the cross-section of osteoblasts cultured on the PMOEP-grafted PET surface for (a) 1 and (b, c) 2 weeks.

mostly composed of collagen fibrils with a diameter of approximately 100 nm and clear bundles, lining the surface of the grafted substrate in the parallel direction.

The most remarkable result seen in Figure 4a and 4b is that an electron-dense layer is uniformly deposited directly onto the substrate surface with a thickness of 180 nm, prior to collagen fiber production. The TEM photograph under a higher magnification is shown in Figure 4c. Obviously, an afibrillar, highly electron-positive layer is in direct contact with the substrate surface with a thickness of approximately 180 nm, while a more light zone is noticed at the outermost surface of the layer incorporating collagen fibrils.

EDX microanalysis after 3 weeks of culture revealed that this electron-dense layer was composed of calcium phosphate, as shown in Figure 5.

Collagen-immobilized surface/cell interface

Figure 6 shows TEM photographs of the interface between cultured osteoblasts and the collagen-immobilized surface 1 and 2 weeks after cell seeding. It can be seen that the cells are rich in endoplasmic reticulum and cell processes and, in addition, contain numerous lipid inclusions. Active collagen production was noted 2 weeks after cell seeding, as shown in Figure 6b. No calcification is observed in the extracellular space at this stage. A dark but not electron-dense layer with a thickness of 500 nm covering the substrate observed in Figure 6a may be attributed to the afibrilar collagen covalently immobilized onto the PET surface. This collagen layer still remained uncalcified 1 week after cell seeding. After 2 weeks of culture, the bottom layer adjacent to the substrate became highly electron-dense, which was associated with an early deposition of afibrillar substances to the outermost surface of the immobilized collagen layer.

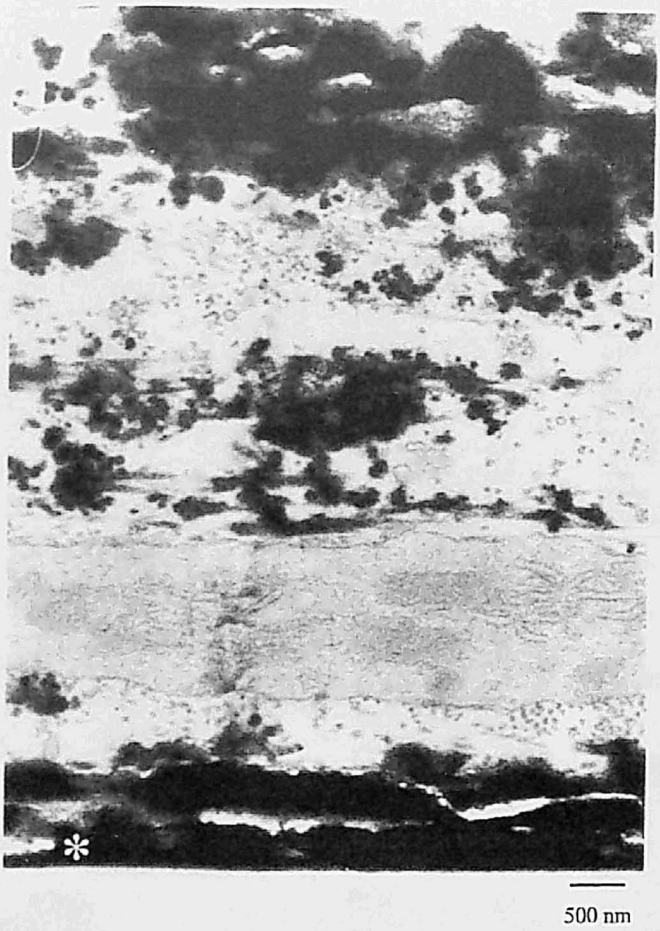

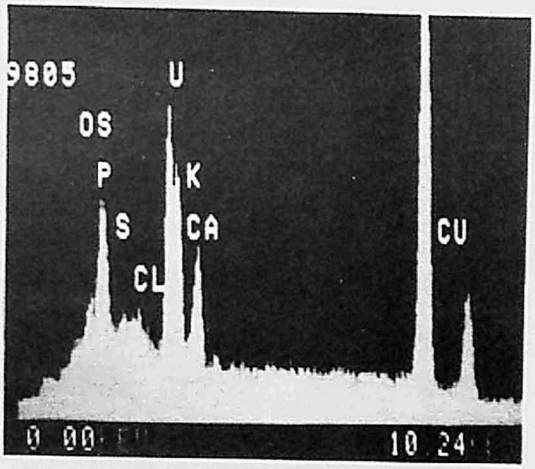

Figure 5. TEM photograph and EDX microanalysis of the cross-section of osteoblasts cultured on the PMOEP-grafted PET surface for 3 weeks. The asterisk in the TEM photograph indicates the position analyzed with EDX. Cracks near the interface are artifacts.

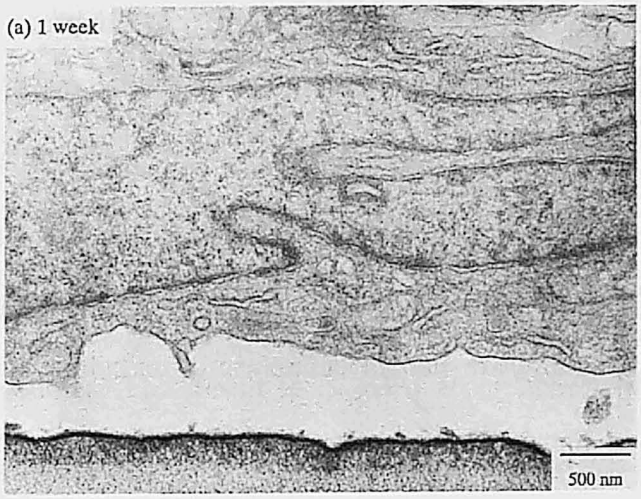

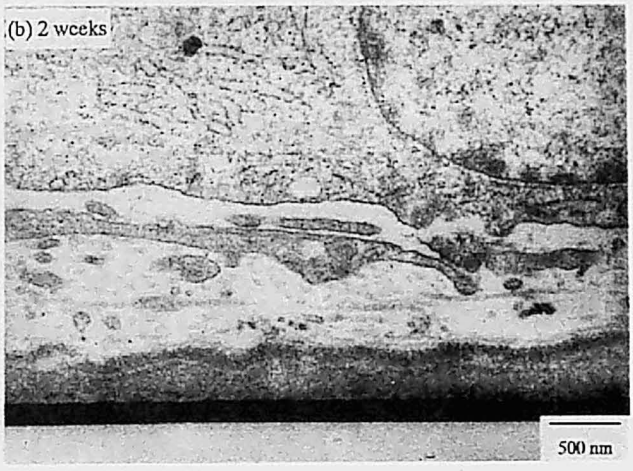

Figure 6. TEM photographs of the cross-section of osteoblasts cultured on the collagen-immobilized PET surface for (a) 1 and (b) 2 weeks.

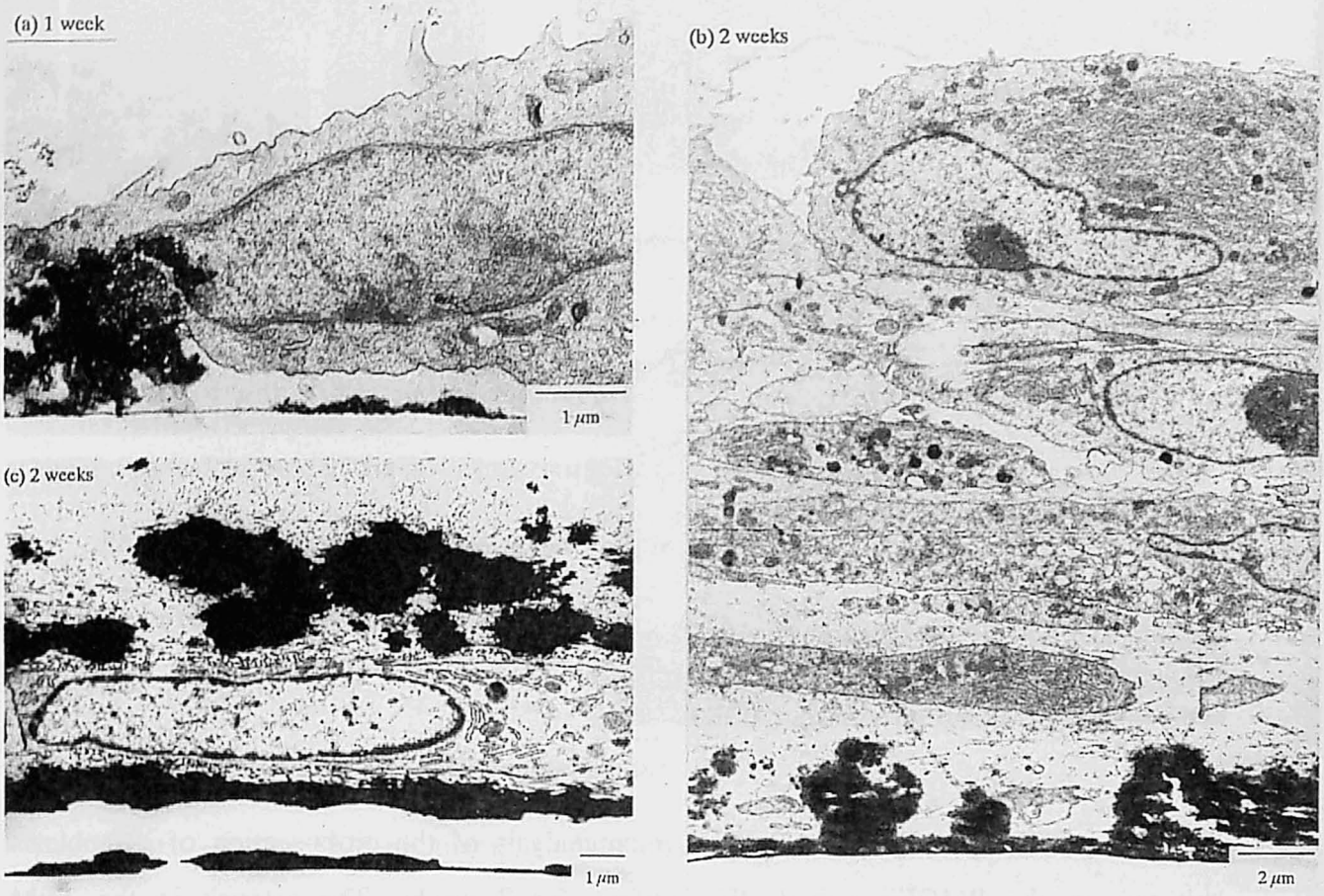

Figure 7. TEM photographs of the cross-section of osteoblasts cultured on the HAp-deposited PET surface for (a) 1 and (b, c) 2 weeks. Cracks and an electron-lucent zone near the interface in the photographs (b, c) are artifacts generated during ultrathin cross-sectioning.

HAp-deposited surface/cell interface

Figure 7 shows the osteoblasts cultured on the HAp-deposited surface for 1 and 2 weeks. Osteoblasts observed after 1 week of culture are rich in endoplasmic reticulum and contain numerous lipid inclusions, as seen in Figure 7a. It is also apparent that large pre-deposited HAp crystals are present beneath osteoblasts. After 2 weeks of culture, multilayered osteoblasts are observed, as seen in Figure 7b. These cells are very rich in endoplasmic

reticulum and have numerous intracellular lipid inclusions, and, in addition, secrete many collagen fibers and deposit many electron-dense substances, probably HAp, to the extracellular matrix. It was occasionally observed that the cuboidal cells with less endoplasmic reticulum, very similar to the phenotype of osteocyte, were surrounded by the deposited substances, as is seen in Figure 7c.

DISCUSSION

To study the ultrastructural morphology of the interfaces between bone forming cells and synthetic substrates, four kinds of surfaces were prepared through surface graft polymerization onto the same PET substrate. The untreated and the PMOEP-grafted PET films provide artificial surfaces, but have different chemical natures each other, especially in their hydrophilicity, surface charge, and bone-bonding property. The surfaces with immobilized collagen and deposited HAp mimic organic and inorganic components of the bone tissue, respectively. On all the surfaces employed in this chapter, RBM cells could differentiate into osteoblasts. This was confirmed by assessing the alkaline-phosphatase expression localized on the cell membrane after 1 week of subculture in the presence of dexamethasone and ascorbic acid. RBM cells proliferated and maintained their phenotype, occasionally forming bone nodules. This result is in good accordance with the observation reported by other research groups[9-12].

A remarkable finding related to surfaces having phosphate-containing polymer chains, type I collagen, and HAp microcrystallites is firm attachment of osteoblasts to these surfaces, in

contrast to the untreated PET surface. Cell adhesion to the untreated PET surface was so weak that no intact cross-section of the interface could be prepared, while the modified surfaces exhibited high resistance to the mechanical stress applied during cross-sectioning.

An interesting morphology observed at the interface between the PMOEP-grafted PET film and osteoblasts is formation of a thin calcium phosphate layer without including fibrillar collagen (Figure 4b). Davies et al. reported a similar interfacial structure in an in vitro RBM cell culture system[10-12]. Such a layer seems to be generated at material/osteoblast interfaces in a cell-dependent manner through the same mechanism by which a cement line is formed at a natural bone remodeling site. On the other hand, the PMOEP-grafted surface induced in situ HAp deposition under the physiologic condition in a cell-independent manner[18]. This is in agreement with the result shown in Figure 2b, where a very thin deposited layer was noticed. Formation of this calcium phosphate layer suggests that this surface has an ability to initiate bone formation, similar to a remodeling site in the living bone.

As demonstrated in Figure 6, the collagen layer immobilized onto the PET substrate remained unchanged after 2 weeks of subculture without appreciable degradation and resorption, but underwent deposition of a dense calcium phosphate layer just on the substrate surface. An early deposition of an afibrillar, extracellular matrix was also noticed on the outermost surface of collagen layer at this stage (Figure 6b). A similar morphology has been reported by many research groups as an indication of active bone formation[1,2,5-7,10-12,19,20].

Such an early deposition of both calcium phosphate and an extracellular matrix was hardly detected at the interface between osteoblasts and the HAp-deposited surface (Figure 7a). This is probably due to overshadowing by the presence and growth of HAp microcrystals predeposited onto the PET film. The rate of HAp deposition onto the HAp predeposited

substrate was found to be approximately ten times as high as that onto the PMOEP-grafted surface in the physiologic environment[16]. It is likely that the predeposited HAp has accelerated the differentiation of osteoblasts into osteocyte-like cells with a cuboidal shape and less endoplasmic reticulum, similar to the mature bone tissue. This interfacial development of bone-like structure with cuboidal, osteocyte-like cells is different from the three other surfaces studied here.

In conclusion, the surface modifications of a hydrophobic polymer substrate by grafting of phosphate polymer chains, immobilization of collagen, and deposition of a thin HAp layer all effectively improved cell adhesion. The RBM cells differentiated into osteoblasts maintaining their phenotype on these modified surfaces, similar to those involved in natural bone formation at the surface of a remodeling site. Osteoblasts cultured on the surface of HAp-deposited substrate exhibited the highest activity of interfacial bone formation.

References

1. D. Bakker, C. A. van Blitterswijk, S. C. Hesseling, W. Th. Daems, and J. J. Grote, Tissue/biomaterial interface characteristics of four elastomers. A transmission electron microscopical study, *J. Biomed. Mater. Res.*, **24**, 277-293 (1990).

2. *The Bone-Biomaterial Interface*, J. E. Davies ed. , University of Toronto Press, Toronto, 1991.

3. L. Linder, Ultrastructure of the bone-cement and the bone-metal interface, *Clin. Orthop. Rel. Res.*, **276**, 127-156 (1992).

4. M. Neo, T. Nakamura, C. Ohtsuki, T. Kokubo, and T. Yamamuro, Apatite formation on three kinds of bioactive material at an early stage in vivo: a comparative study by transmission electron microscopy, *J. Biomed. Mater. Res.*, **27**, 999-1006 (1993).

5. D. E. Steflik, G. R. Parr, A. L. Sisk, F. T. Lake, P. J. Hanes, D. J. Berkery, and P. Brewer, Osteoblast activity at the dental implant-bone interface: transmission electron microscopic and high voltage electron microscopic observations, *J. Periodontol*, **65**, 404-413 (1994).

6. J. D. de Bruijn, C. A. van Blitterswijk, and J. E. Davies, Initial bone matrix formation at the hydroxyapatite interface in vivo, *J. Biomed. Mater. Res.*, **29**, 89-99 (1995).

7. C. M. Müller-Mai, S. I. Stupp, C. Voigt, and U. Gross, Nanoapatite and organoapatite implants in bone: histology and ultrastructure of the interface, *J. Biomed. Mater. Res.*, **29**, 9-18 (1995).

8. J. N. Beresford, S. E. Graves, and C. A. Smoothy, Formation of mineralized nodules by bone derived cells *in vitro*: a model of bone formation?, *Am. J. Med. Genet.*, **45**, 163-178 (1993).

9. G. Maniatopoulos, J. Sodek, and A. H. Melcher, Bone formation in vitro by stromal cells obtained from bone marrow of young adult rats, *Cell Tissue Res.*, **254**, 317-330 (1988).

10. J. E. Davies, R. Chernecky, B. Lowenberg, and A. Shiga, Deposition and resorption of calcified matrix in vitro by rat marrow cells, *Cells & Mater.*, **1**, 3-15 (1991).

11. B. Lowenberg, R. Chernecky, A. Shiga, and J. E. Davies, Mineralized matrix production by osteoblasts on solid titanium in vitro, *Cells & Mater.*, **1**, 177-187 (1991).

12. J. D. de Bruijn, J. E. Davies, J.. S. Flach, K. de Groot, Ultrastructure of the mineralized tissue/calcium phosphate interface in vitro, in *Mater. Res. Symp. Proc.* Vol. 252, L. G. Cima and E. S. Ron eds., Materials Research Society, Pittsburgh, 1992, pp. 63-70.

13. B. W. Callen, R. N. S. Sodhi, R. M. Shelton, and J. E. Davies, Behavior of primary bone cells on characterized polystyrene surfaces, *J. Biomed. Mater. Res.*, **27**, 851-859 (1993).

14. E. Uchida, Y. Uyama, and Y. Ikada, Surface graft polymerization of ionic monomers onto poly(ethylene terephthalate) by UV irradiation without degassing, *J. Appl. Polym. Sci.*, **47**, 417-424 (1993).

15. T. Okada and Y. Ikada, Surface modification of silicone for percutaneous implantation, *J. Biomater. Sci. Polymer Edn.*, **7**, 171-180 (1995).

16. K. Kato, Y. Eika, and Y. Ikada, Deposition of a hydroxyapatite thin layer onto a polymer surface carrying grafted phosphate polymer chains, *J. Biomed. Mater. Res.*, **32**, 687-691 (1996).

17. C. G. Bellows, J. E. Aubin, J. N. M. Heersche, and M. E. Antosz, Mineralized bone nodules formed *in vitro* from enzymatically released rat calvaria cell populations, *Calcif. Tissue Int.*, **38**, 143-154 (1986).

18. O. N. Tretinnikov, K. Kato, and Y. Ikada, In vitro hydroxyapatite deposition onto a film surface-grafted with organophosphate polymer, *J. Biomed. Mater. Res.*, **28**, 1365-1373 (1994).

19. B. T. Garvey and R. Bizios, A transmission electron microscopy examination of the interface between osteoblasts and metal biomaterials, *J. Biomed. Mater. Res.*, **29**, 987-992 (1995).

20. X. Shen, E. Roberts, S. A. F. Peel, and J. E. Davies, Organic extracellular matrix components at the bone cell/substratum interface, *Cells & Mater.*, **3**, 257-272 (1993).

Chapter 6

Structure of bone tissue ectopically regenerated by biodegradable hydrogel matrices incorporating BMP-2

INTRODUCTION

Bone regeneration has attracted much attention in the field of tissue engineering because of its high clinical needs. To regenerate patient's own bone tissue in osseous defects a number of methods have been proposed including space making with a membrane especially in the maxillofacial surgery for guided bone regeneration (GBR) and scaffolding for bone ingrowth in orthopedic, plastic, and skull-base surgeries. The scaffolds employed in bone regeneration basically function as the substrate for bone cell attachment and are, therefore, made of porous biodegradable materials such as glycolide-lactide copolymer non-woven fabrics[1-5], collagen-sponges[1-3,5-7], and porous calcium phosphate blocks[1-3,8-10]. On the other hand, biodegradable matrices incorporating cell growth factors such as BMP[1-3,11-26], TGF-β[27-30], and FGF[31,32] have been placed in bone defects or implanted at an ectopic site. In this case the matrices serve as the carrier or depot of the growth factors, and occasionally

function also as the substrate for bone cell attachment. Fibrin glue[12,13], PLGA[14-22], and calcium phosphates[23,24] have been used as the matrix of bone-related growth factors.

The purpose of this chapter is to study the effect of the shape of carriers on bone regeneration. For this purpose BMP-2 is used as the bone growth factor and two different biodegradable materials as the carrier of BMP-2. One of the materials is a non-woven fabric made from polyglycolide (PGA) fiber and the other a gelatin hydrogel[33,34]. The PGA non-woven fabric is a highly porous material, allowing diffusion of nutrients and infiltration of cells into the device following implantation. On the other hand, the proposed hydrogel mimics the mechanism in which BMP is stored in the extracellular matrix, resulting in preventing BMP from the rapid denaturation in the body. The degradation period of hydrogels can be controlled depending on their crosslinking extent. The carriers incorporating BMP-2 are implanted in the thigh muscle of rat to induce ectopic bone formation.

EXPERIMENTAL

Materials

BMP-2 with an IEP of 8.5 was supplied by Yamanouchi Pharmaceutical Co., Tokyo, Japan. Gelatin was isolated from bovine bone by an alkaline process and had an IEP of 5.0 and an average molecular weight of 99,000 (Nitta Gelatin Co., Osaka, Japan). A PGA non-woven fabric made from PGA fibers with 20 μm diameter without use of any binders was

supplied from Gunze Co., Kyoto, Japan. The non-woven fabric was made with the scratching method using polyfilament yarns[33]. The volume percentage of PGA fibers in the fabric was estimated to be approximately 25 vol% when the density of PGA was assumed to be 1 g/ cm^3. Figure 1 shows scanning electron microscopic photographs of the lyophilized gelatin hydrogel and the PGA non-woven fabric. Other chemicals were obtained from Wako Pure Chemical Industries, Osaka, Japan and used without further purification.

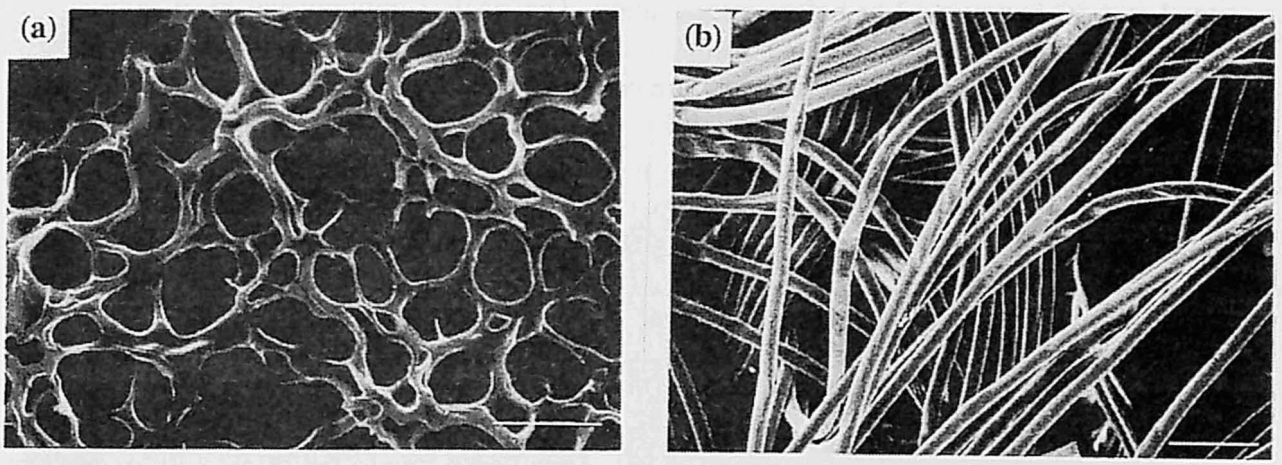

Figure 1. Scanning electron micrographs of the lyophilized gelatin hydrogel (a) and the PGA non-woven fabric (b). Bars correspond to 20 μm (a) and 100 μm (b).

Preparation of hydrogel matrices

Gelatin hydrogel was prepared by crosslinking of gelatin in aqueous solution with glutaraldehyde. Briefly, 10 wt% aqueous solution of gelatin containing 0.1 wt% glutaraldehyde was poured into a mold having a disk shape of 1 mm thickness and 5 mm diameter (ϕ). Following the crosslinking reaction at 4 °C for 12 hr, the resulting hydrogel was immersed in 50 mM glycine at 37 °C for 1.5 hr, followed by washing with DDW. The water

content of the gelatin hydrogel disk swollen with water at 37 °C was approximately 95 %. The gelatin hydrogel and the PGA non-woven fabric of 1 mm x 5 ϕ were put in 70 % ethanol for sterilization at room temperature for 1.5 hr, washed with DDW to remove ethanol, and then lyophilized. 10 μL of 1 mg / mL BMP-2 was added to matrices to amount to 10 μg per each carrier. According to Smith et al[21], the dose of BMP-2, 50 μg per 0.1 mL implant, is enough to induce bone formation. The BMP-2-impregnated gelatin hydrogels were allowed to stand at 4 °C for over 12 hr before implantation. The BMP-2-impregnated PGA non-woven fabrics were lyophilized at room temperature before implantation.

Implantation of hydrogel matrices incorporating BMP-2

Each of the carriers with impregnated BMP-2 was implanted aseptically into the left thigh muscle of three 7-week-old male Wistar rats. The matrix without BMP-2 was implanted as a control in the right side of the same animal. After 1 and 2 weeks of implantation, the legs were examined by soft x-rays generated from Hitex HX-100, Hitachi, Japan, at a generator tension of 46 KVP and current of 2.5 mA for 15 sec. The tissue from the implant site was explanted for histological observation. The explanted specimens were fixed with 10 % neutral formalin, replaced with ethanol, and embedded in paraffin. The fixed specimens were sectioned to 10 μm thickness with a microtome and stained with H-E solution. In addition, alizarin red S - light green staining was applied for identifying calcium deposition. The cross-sections were photographed with an optical microscope. An ultrathin cross-section was cut

from the formed bone tissue with an ultramicrotome, stained with lead citrate and uranyl acetate, and then observed with a TEM (JEM-1200EX II, JEOL, Tokyo, Japan).

RESULTS

Soft x-ray observation

Both of the PGA non-woven fabric and the gelatin hydrogel containing BMP-2 showed no ectopic bone formation when observed by soft x-ray after 1 week of implantation.

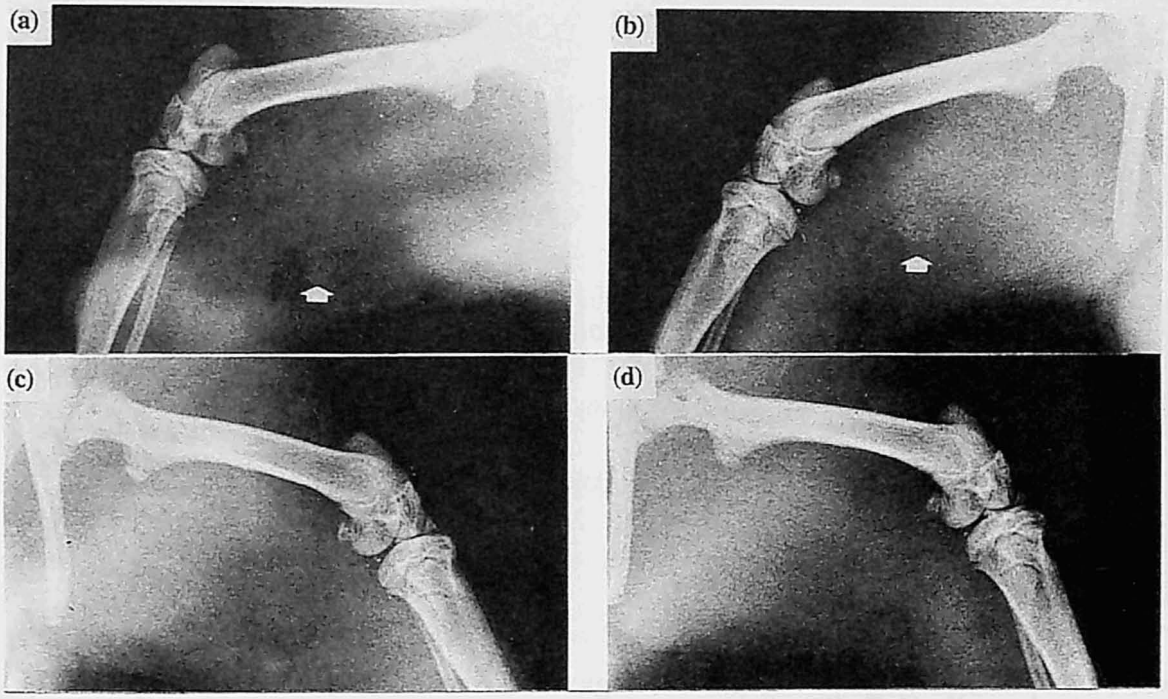

Figure 2. Soft x-ray photographs of the ectopic bone induced by the BMP-2-impregnated gelatin hydrogel (a) and the BMP-2-impregrated PGA non-woven fabric (b) after 2 weeks of implantation. (a and b) Arrows indicate the ectopic bone. (c and d) Soft x-ray photographs show the body sites, respectively, where the gelatin hydrogel and the PGA non-woven fabric without BMP-2 were implanted.

However, after 2 weeks of implantation, a radiopaque area (arrow) due to BMP-2-induced bone formation could be seen in both the matrices, as is shown in Figure 2. No ectopic bone formation was observed when the carriers did not contain BMP-2.

Histological observation

Figure 3 shows histological observation of the tissue including the BMP-impregnated

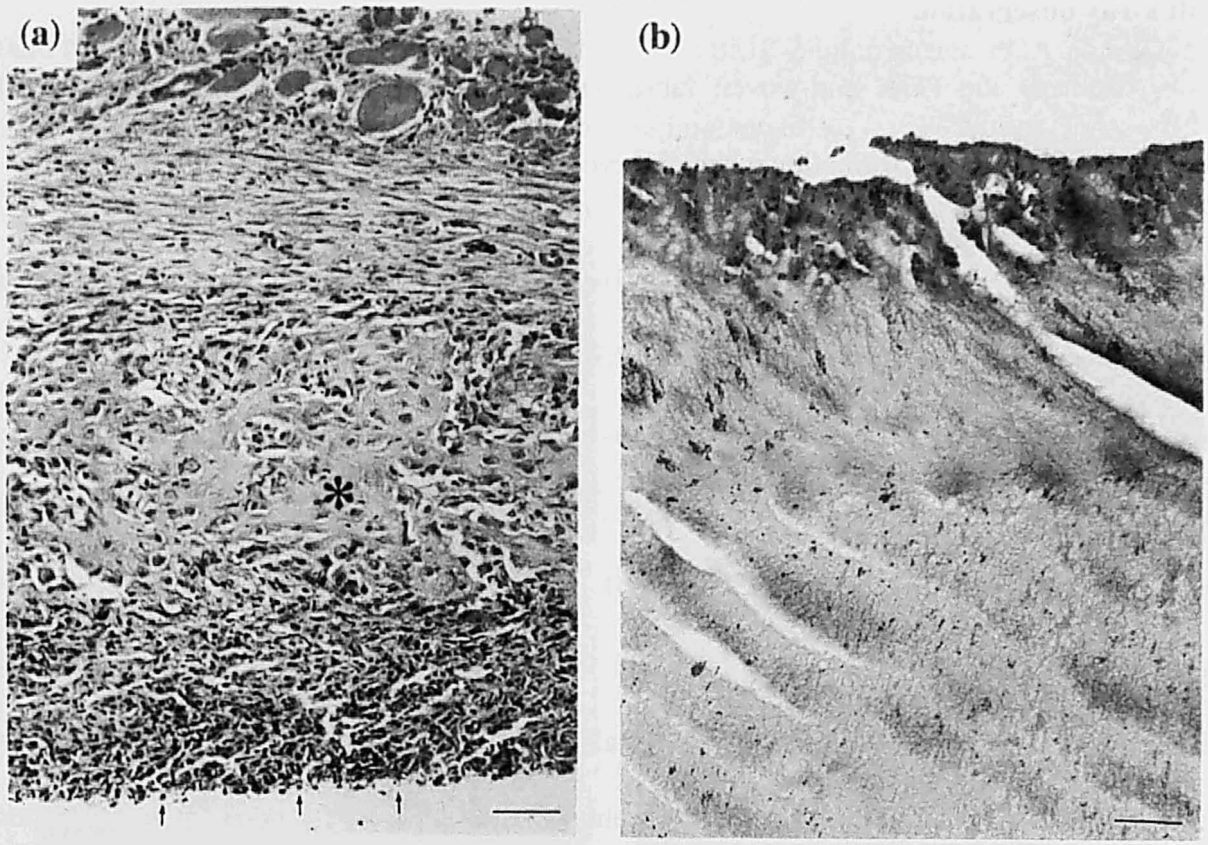

Figure 3. Optical photographs of the histologic cross-section of the surrounding tissue (a), the gelatin hydrogel (b), and the surrounding tissue (c) after 1 week of implantation. Cross-sections were stained with H-E (a and b) and alizarin red S. (a) Woven bone (asterisk) was formed in the center of the tissue. Inflammatory response (arrows) was noticed around the gelatin hydrogel. Bars correspond to 50 μm (a and b) and 100 μm (c).

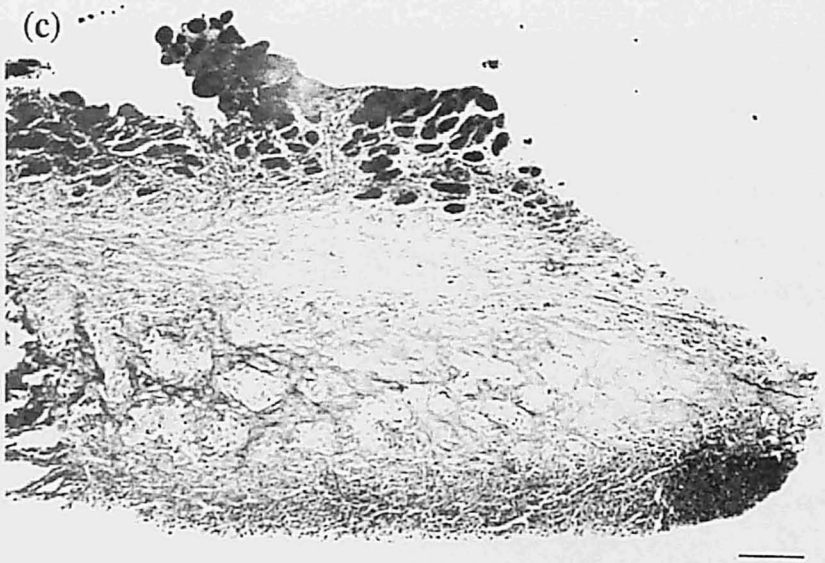

Figure 3. (Continued).

gelatin hydrogel after 1 week of implantation. Woven bone is formed in the center of the tissue in Figure 3a and the gelatin hydrogel still remains, as is shown in Figure 3b. Inflammatory cells are seen at the periphery of the gelatin hydrogel, but infiltration of any cells into the gelatin hydrogel cannot be noticed in Figure 3a and 3b. Figure 3c shows histological observation of the cross-section stained with alizarin red S - light green. No calcium deposition is observed. The cross-section of the tissue after 2 weeks of implantation is shown in Figure 4. Ectopic bone formation is noticed in the tissue surrounding the gelatin hydrogel. As shown in Figure 4b, alizarin red S - light green staining clearly reveals a newly formed bone with calcium deposition. However, even after 2 weeks of implantation, the gelatin hydrogel has not been completely degraded yet and no bone formation is observed

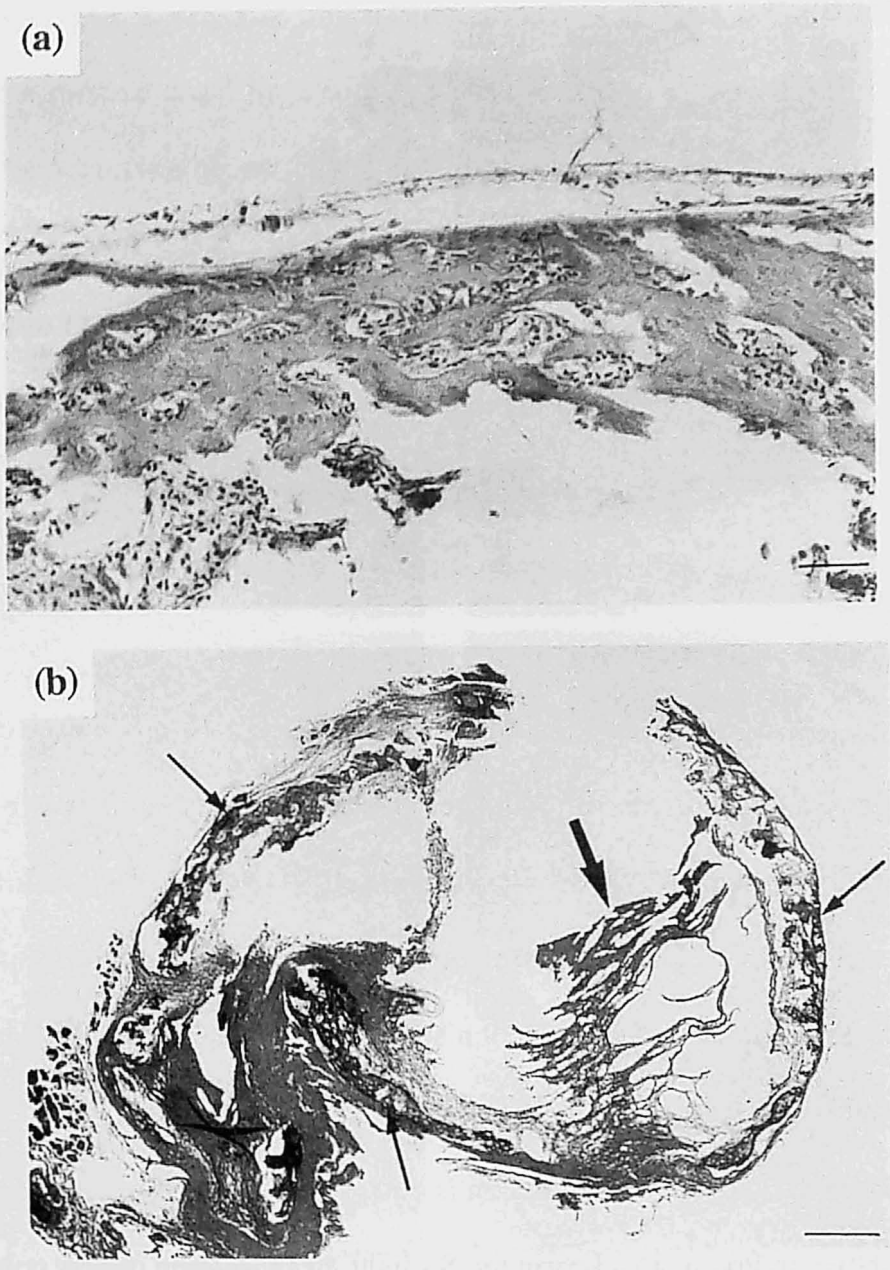

Figure 4. Optical photographs of the histologic cross-section of the ectopic bone induced by the BMP-2-impregnated gelatin hydrogel after 2 weeks of implantation. Cross-sections were stained with H-E (a) and alizarin red S (b). (b) Newly formed bone with calcium deposition (arrows) and the residual gelatin hydrogel (heavy arrow) were noticed. Bars correspond to 50 μm (a) and 250 μm (b).

inside the gelatin hydrogel. Figure 5 shows TEM observation of the ectopic bone. It is seen that osteoblasts have actively produced an extracellular matrix containing collagen fibers,

Figure 5. TEM photographs of the cross-section of the ectopic bone induced by the BMP-2-impregnated gelatin hydrogel after 2 weeks of implantation. The ultrathin cross-section was stained with lead citrate and uranyl acetate. (a) Osteoblasts (O) and unmineralized (star) and mineralized (asterisk) matrices are evident. (b) At a higher magnification, heavily mineralized collagen fibers (arrow) are evident. Bars correspond to 1 μm (a) and 200 nm (b).

Figure 5. (Continued).

which have been partially calcified. This result well agrees with histological observation of the cross-sections stained with alizarin red S. The cross-section of the control carriers exhibited the same responses and gelatin hydrogel degradation without bone formation at the same period as that with BMP (data not shown).

Histological observation of the tissue after 1 week of implantation of the PGA non-woven fabric is shown in Figure 6. No bone formation is noticed, in good agreement with the soft x-ray observation (Figure 6b). However, many cells involving inflammatory response

have infiltered into the non-woven matrix, in contrast to the gelatin hydrogel (Figure 6a). Figure 7 shows the tissue after 2 weeks of implantation. Obviously, bone is formed inside the PGA non-woven fabric. This can be clearly identified by alizarin red S - light green staining of the cross-section of the explant. It is also apparent in Figure 6 that some of PGA fibers are still present, maintaining the round shape after 2 weeks of implantation. Similar responses and cell infiltration into carrier, but no bone formation was observed for the control carriers (data not shown).

Figure 6. Optical photographs of the histologic cross-section of the BMP-2-impregnated PGA non-woven fabric after 1 week of implantation. Cross-sections were stained with H-E (a) and alizarin red S (b). Many cells infiltered into the pores of PGA non-woven fabric. (b) No calcium deposition was evident. Arrow indicates the PGA fibers still remaining. Bars correspond to 100 μm (a) and 250 μm (b).

Figure 6. (Continued).

DISCUSSION

As carriers of BMP, two kinds of biodegradable polymeric materials of different forms and chemical natures were employed in this chapter. Histological staining of the explanted carriers with alizarin red S, which can bind to calcium in a tissue, has clearly demonstrated that both the gelatin gel and the PGA non-woven fabric with impregnated BMP-2 have stimulated cells to new bone formation in an intramuscular site at 2nd week postimplantation.

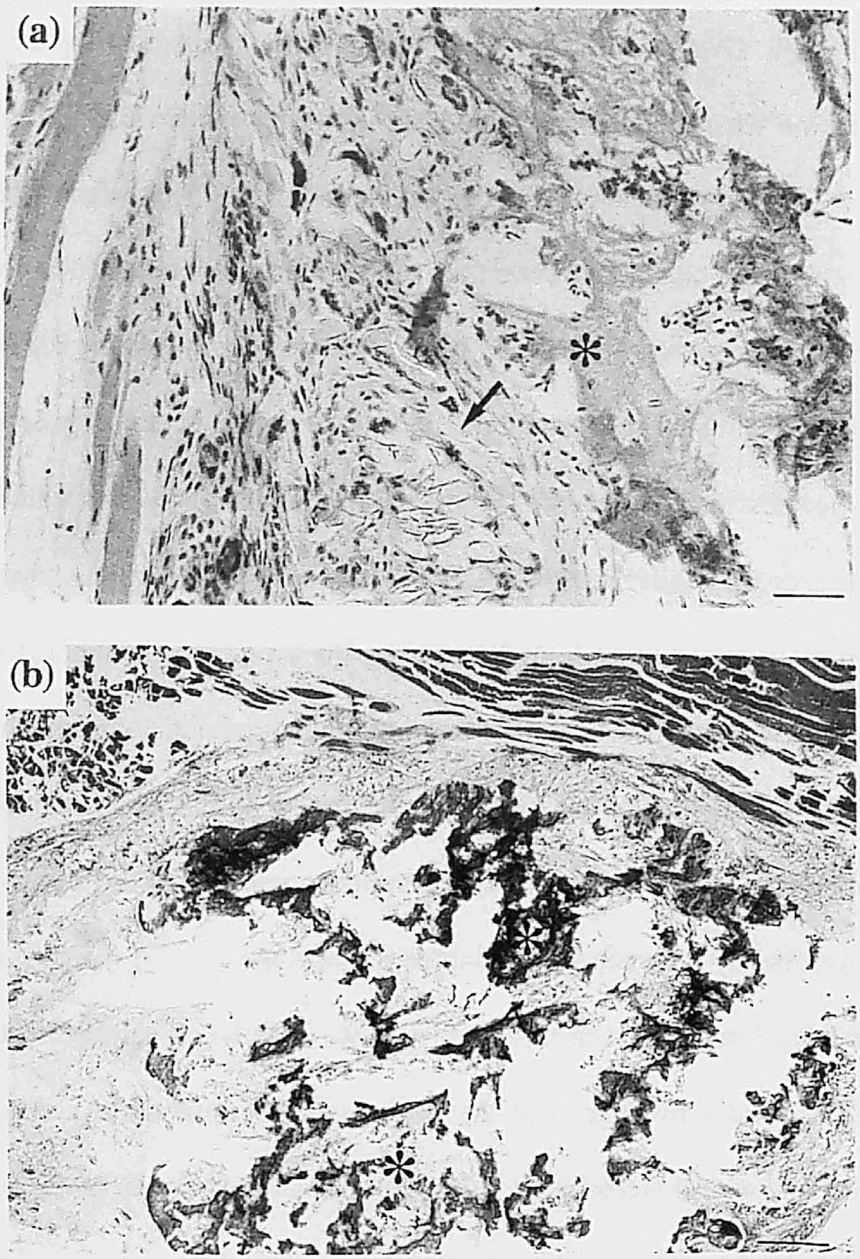

Figure 7. Optical photographs of the histologic cross-section of the BMP-2-impregnated PGA non-woven fabric after 2 week of implantation. Cross-sections were stained with H-E (a) and alizarin red S (b). Arrow and asterisks indicate that the PGA non-woven fibers still remaining and newly formed bone with calcium deposition, respectively. Bars correspond to 50 μm (a) and 250 μm (b).

Effect of the structure of BMP-2 carrier

It is well known that BMP alone may quickly diffuse out into the surrounding tissue with very weak bone formation when injected in a solution form at an ectopic site. Only the use of a carrier may allow BMP to remain at a high concentration around the implanted site and come into contact with cells responsible for bone formation long enough to initiate bone induction. The above results strongly suggest that both of the two carriers can retain BMP-2 without a significant loss of activation and release it into the body, inducing ectopic bone formation.

BMP molecules may be trapped in the PGA non-woven fabric matrix simply by physical adsorption on the biodegradable fiber surface, whereas the trapping mode of BMP in the gelatin hydrogel is not as simple as that in the PGA non-woven fabric because BMP molecules can diffuse into the hydrogel. It is very important to elucidate the mechanism of the trapping mode and release profile of BMP, but the extent of inactivation of BMP caused during its incorporation into the carriers has not yet been studied. Both in vitro and in vivo BMP-2 release has already been shown in Chapters 1 and 2.

An interesting result found in this chapter is the morphological difference in formed bones between the gelatin hydrogel and the PGA non-woven fabric. As demonstrated in Figure 7, ectopic bone was induced in the inside of the PGA non-woven fabric, whereas bone was formed at the periphery of the gelatin hydrogel, as seen in Figure 4. This difference may be primarily due to the porosity of the carriers. As obvious from Figure 1, the PGA non-woven fabric is highly porous with approximately 25 vol% of PGA fibers in the fabric. Therefore, the osteoprogenitor cells surrounding the PGA non-woven fabric will be able to infiltrate into the pores and receive stimulation from the released BMP-2 to differentiate into

osteoblasts. On the contrary, as seen in Figure 1, the homogeneous gelatin hydrogel with the water content of 95 % is not porous and hence does not allow the cells to infiltrate into the hydrogel unless remarkably degraded. As a result, formation of ectopic bone may be limited only at the periphery of the gelatin hydrogel, since only the osteoprogenitor cells surrounding the outside of the gelatin hydrogel will be stimulated to differentiate into osteoblasts by BMP-2 molecules released from the hydrogel matrix into the outside. The gelatin hydrogel used in this chapter was almost completely resorbed after 3 weeks of implantation.

These results indicate that some improvements are required on the hydrogel matrix if it is used for tissue engineering in such a case as here. The biodegradable non-woven fabric has also a problem that the release of growth factors from the fabric is not controllable.

It has been pointed out that a porous structure is needed for the scaffold of tissue regeneration to facilitate cell seeding and proliferation as well as tissue ingrowth[4-10] as shown in Chapter 4. Since a non-woven fabric is useful as a scaffold of osteoblasts, as Crane et al. also reported[5], combination of the PGA non-woven fabric and the gelatin hydrogel seems to be a good means to compromise their disadvantage. A promising improvement is to use microcapsules of gelatin hydrogel as a polypeptide drug carrier and to combine them with the PGA non-woven fabric as a scaffold of both the drug carrier and cells. Such composite carriers have been already reported for bone tissue regeneration[20,21,25,26].

References

1. C. J. Damien and J. R. Parsons, Bone graft and bone graft substitutes: a review of current technology and applications, *J. Appl. Biomater.*, **2**, 187-208 (1991).

2. T. S. Lindholm and T. J. Gao, Functional carriers for bone morphogenetic proteins, *Ann. Chir. Gynaecol.*, **82**, 3-12 (1993).

3. J. Yaszemski, R. G. Payne, W. C. Hayes, R. Langer, and A. G. Mikos, Evolution of bone transplantation: molecular, cellular and tissue strategies to engineer human bone, *Biomaterials*, **17**, 175-185 (1996).

4. R. C. Thomson, M. J. Yaszemski, J. M. Powers, and A. G. Mikos, Fabrication of biodegradable polymer scaffolds to engineer trabecular bone, *J. Biomater. Sci. Polymer Edn.*, **7**, 23-38 (1995).

5. G. M. Crane, S. L. Ishaug, and A. G. Mikos, Bone tissue engineering, *Nature Medicine*, **1**, 1322-1324 (1995).

6. S. -T. Li, D. Yuen, P. C. Li, W. G. Rodkey, and K. R. Stone, Collagen as a biomaterial: an application in knee meniscal fibrocartilage regeneration, *Mat. Res. Soc. Symp. Proc.* Vol. **331**, 25-32 (1994).

7. T.Fujisato, T. Sajiki, Q. Liu, and Y. Ikada, Effect of basic fibroblast growth factor on cartilage regeneration in chondrocyte-seeded collagen sponge scaffold, *Biomaterials*, **17**, 155-162 (1996).

8. H. A. Hoogendoorn, W. Renooij, L. M. A. Akkermans, W. Visser, and P. Wittebol, Long-term study of large ceramic implants (porous hydroxyapatite) in dog femora, *Clin. Orthop. Rel. Res.*, **187**, 281-288 (1984).

9. H. Ohgushi, Y. Dohi, S. Tamao, and S. Tabata, Osteogenic differentiation of marrow stromal stem cells in porous hydroxyapatite ceramics, *J. Biomed. Mater. Res.*, **27**, 1401-1407 (1993).

10. E. C. Shors and R. E. Holmes, Porous hydroxyapatite, in "*An introduction to bioceramics, Advanced series in ceramics Vol. 1*", L. L. Hench and J. Wilson eds., World Scientific, Singapore, 1993, pp. 181-198.

11. J. M. Wozney, V. Rosen, A. J. Celeste, L. M. Mitsock, M. J. Whitters, R. W. Kriz, R. M. Hewick, and E. A. Wang, Novel regulators of bone formation: molecular clones and activities, *Science*, **242**, 1528-1534 (1988).

12. M. Kawamura and M. R. Urist, Human fibrin is a physiologic delivery system for bone morphogenetic protein, *Clin. Orthop. Rel. Res.*, **235**, 302-310 (1987).

13. N. Schwarz, H. Redl, L. Zeng, G. Schlag, H. P. Dinges, and J. Eschberger, Early osteoinduction in rats is not altered by fibrin sealant, *Clin. Orthop. Rel. Res.*, **293**, 353-359 (1993).

14. S. Miyamoto and K. Takaoka, Bone induction and bone repair by composites of bone morphogenetic protein and biodegradable synthetic polymers, *Ann. Chir. Gynaecol.*, **82**, 69-76 (1993).

15. M. C. Meikle, S. Papaioannou, T. J. Ratledge, P. M. Speight, S. R. Watt-Smith, P. A. Hill, and J. J. Reynolds, Effect of poly DL-lactide-co-glycolide implants and xenogeneic bone matrix-derived growth factors on calvarial bone repair in the rabbit, *Biomaterials.*, **15**, 513-21 (1994).

16. S. Miyamoto, K. Takaoka, T. Okada, H. Yoshikawa, J. Hashimoto, S. Suzuki, and K. Ono, Polylactic acid-polyethylene glycol block copolymer, *Clin. Orthop. Rel. Res.*, **294**, 333-343 (1993).

17. S. C. Lee, M. Shea, M. A. Battle, K. Kozitza, E. Ron, T. Turek, R. G. Schaub, and W. C. Hayes, Healing of large segmental defects in rat femurs is aided by rhBMP-2 in PLGA matrix, *J. Biomed. Mater. Res.*, **28**, 1149-1156 (1994).

18. T. J. Sigurdsson, M. B. Lee, K. Kubota, T. J. Turek, J. M. Wozney, and U. M. E. Wikesjö, Periodontal repair in dogs: recombinant human bone morphogenetic protein-2 significantly enhances periodontal regeneration, *J. Periodontol.*, **66**, 131-138 (1995).

19. Y. Yamazaki, S. Oida, K. Ishihara, and N. Nakabayashi, Ectopic induction of cartilage and bone by bovine bone morphogenetic protein using a biodegradable polymer reservoir, *J. Biomed. Mater. Res.*, **30**, 1-4 (1996).

20. R. Kenley, L. Marden, T. Turek, L. Jin, E. Ron, and J. O. Hollinger, Osseous regeneration in the rat calvarium using novel delivery systems for recombinant human bone morphogenetic protein-2(rhBMP-2), *J. Biomed. Mater. Res.*, **28**, 1139-1147 (1994).

21. J. L. Smith, L. Jin, T. Parsons, T. Turek, E. Ron, C. M. Philbrook, R. A. Kenley, L. Marden, J. Hollinger, M. P. G. Bostrom, E. Tomin, and J. M. Lane, Osseous regeneration in preclinical models using bioabsorbable delivery technology for recombinant human bone morphogenetic protein 2 (rhBMP-2), *J. Controll. Release*, **36**, 183-195 (1995).

22. J. O. Hollinger and K. Leong, Poly(α-hydroxy acids): carriers for bone morphogenetic proteins, *Biomaterials*, **17**, 187-194 (1996).

23. M. R. Urist, A. Lietze, and E. Dawson, β-tricalcium phosphate delivery system for bone morphogenetic protein, *Clin. Orthop. Rel. Res.*, **187**, 277-280 (1984).

24. Y. Horisaka, Y. Okamoto, N. Matsumoto, Y. Yoshimura, J. Kawada, K. Yamashita, and T. Takagi, Subperiosteal implantation of bone morphogenetic protein adsorbed to hydroxyapatite, *Clin. Orthop. Rel. Res.*, **268**, 303-312 (1991).

25. T. Sato, M. Kawamura, K. Sato, H. Iwata, and T. Miura, Bone morphogenesis of rabbit bone morphogenetic protein-bound hydroxyapatite-fibrin composite, *Clin. Orthop. Rel. Res.*, **263**, 254-262 (1988).

26. I. Ono, T. Ohura, M. Murata, H. Yamaguchi, Y. Ohnuma, and Y. Kuboki, A study on bone induction in hydroxyapatite combined with bone morphogenetic protein, *Plast. Reconstr. Surg.*, **90**, 870-879 (1991).

27. W. R. Gombotz, S. C. Pankey, L. S. Bouchard, J. Ranchalis and P. Puolakkainen, Controlled release of TGF-β from a biodegradable matrix for bone regeneration, *J. Biomater. Sci. Polymer Edn.*, **5**, 49-63 (1993).

28. L. S. Beck, E. P. Amento, Y. Xu, L. Deguzman, W. P. Lee, T. Nguyen, and N. A. Gillett, TGF-ß$_1$ induces bone closure of skull defects: temporal dynamics of bone formation in defects exposed to rhTGF-β1, *J. Bone Mineral Res.*, **8**, 753-761 (1993).

29. W. R. Gombotz, S. C. Pankey, L. S. Bouchard, D. H. Phan, and P. Puolakkainen, Stimulation of bone healing by transforming growth factor-beta1 released from polymeric or ceramic implants, *J. Appl. Biomater.*, **5**, 141-150 (1994).

30. D. R. Sumner, T. M. Turner, A. F. Purchio, W. R. Gombotz, and J. O. Galante, Enhancement of bone ingrowth by transforming growth factor-β, *J. Bone Joint Surg.*, **77-A**, 1135-1147 (1995).

31. H. Kawaguchi, T. Kurokawa, K. Hanada, Y. Hiyama, M. Tamura, E. Ogata, and T. Matsumoto, Stimulation of fracture repair by recombinant human basic fibroblast growth factor in normal and streptozotocin-diabetic rats, *Endocrinology*, **135**, 774-781 (1994).

32. T. Nakamura, K. Hanada, M. Tamura, T. Shibanushi, H. Nigi, M. Tagawa, S. Fukumoto, and T. Matsumoto, Stimulation of endosteal bone formation by systemic injections of recombinant basic fibroblast growth factor in rats, *Endocrinology*, **136**, 1276-1284 (1995).

33. Nakamura, T., Shimizu, Y., Watanabe, S., Shiraki, K., Hyon, S. -H., Suzuki, M., Shimamoto, T., and Ikada, Y. Bioabsorbable non-woven fabric for surgery, in "*Medical textiles for implantation*" H. Plank, M. Dauner, and M. Renardy eds., Berlin: Springer-Verlag, 1990, pp. 329-332.

34. Y. Tabata, S. Hijikata, and Y. Ikada, Enhanced vascularization and tissue granulation by basic fibroblast growth factor impregnated in gelatin hydrogel, *J. Controll. Release*, **31**, 189-199 (1994).

Chapter 7

Ultrastructure of bone tissue ectopically regenerated by biodegradable hydrogel matrices incorporating BMP-2

INTRODUCTION

Biological tissues have excellent mechanical properties compared with artificial materials. A typical example is bone. However, currently available biomaterials for bone substitute have poor mechanical property compared with that of the natural bone[1]. As the alternative treatment of the bone reconstruction to solve such a mechanical incompatibility, bone regeneration has attracted much attention in the field of tissue engineering. A promising way to induce regeneration of autogeneous osseous tissues in bone defect is to make use of bone-related growth factors, as described in Chapters 2 to 4.

High toughness of the bone is due to the exquisite composite structure of organic and inorganic materials, that is, collagen and hydroxyapatite, respectively. Ultrastructure of mineralized tissues, such as tendon, bone and dentin, has been studied by use of various methods including small angle x-ray scattering[2-4], Fourier transform infrared spectroscopy and microspectroscopy[5,6], conventional and high voltage electron microscopies[7-22], tomography (3D) at the electron microscopic level[23-28], immunocytochemistry[29,30], and atomic force microscopy[10,28]. Most of these studies use a mineralized turkey leg tendon for evaluation of

the ultrastructure as a model of mineralized tissues, because of the tendon's high degree of collagen fibril alignment, thereby permitting the ease of sequential analyses of the mineralization process and constancy of fibril orientation.

In this chapter, the ultrastructure of the bone ectopically formed with the gelatin hydrogel incorporating BMP-2 was investigated, referring to the collagen-mineral interaction described in the mineralized turkey leg tendon. An anhydrous method with ethylene glycol and unstained cross-sections were employed for transmission electron microscopic analyses of formed bones in order to reduce the artifacts induced in hydroxyapatite crystals by aqueous solutions[21]. The mineralized collagen will be noticed in the electron microscopic observation due to the electron dense feature of hydroxyapatite. A crystallographic analysis combined with dark field electron imaging was performed to demonstrate the mineral-collagen structure in the ectopic bone.

EXPERIMENTAL

Materials

BMP-2 was supplied by Yamanouchi Pharmaceutical Co., Tokyo, Japan. Gelatin was isolated from bovine bone with an alkaline process with an IEP of 5.0 and an average molecular weight of 99,000 (Nitta Gelatin Co., Osaka, Japan). Other chemicals were obtained from Wako Pure Chemical Industries, Osaka, Japan and used without further purification.

Preparation of hydrogel matrices

Glutaraldehyde was added to 30 mL of 5 wt% aqueous solution of gelatin to give the final concentration of 0.05 wt%. The mixed solution was cast into a polypropylene mold (138 x 138 mm^2), followed by leaving at 4 °C for 12 hr to allow crosslinking reaction of gelatin to proceed. The crosslinked hydrogel sheets were punched out to obtain gelatin hydrogel discs (5 mm diameter and 2 mm thickness). Then, the hydrogel discs were placed in 100 mM glycine aqueous solution at 37 °C for 1 hr to block residual aldehyde groups of glutaraldehyde and washed 3 times at 37 °C with DDW. Finally, they were freeze-dried and sterilized with ethylene oxide gas. The weight percentage of water in the wet hydrogel was determined from the hydrogel weight measured before and after drying at 70 °C under vacuum for 6 hr. The water content of the acidic and basic gelatin hydrogels used in this chapter was approximately 95 wt%.

Implantation of hydrogel matrices incorporating BMP-2

20 μL of 0.5 mg / mL BMP-2 was added to matrices to amount to 10 μg per each matrix. The BMP-2-incorporating gelatin hydrogels were allowed to stand at 4 °C for 12 hr before implantation. Each of the hydrogels incorporating BMP-2 was implanted aseptically into the left thigh muscle of three 7-week-old male Wistar rats. After 2 weeks of implantation, the legs were examined by soft x-rays generated from Hitex HX-100, Hitachi, Japan, at a generator tension of 46 KVP and a current of 2.5 mA for 15 sec.

TEM observation

The tissue from the implant site was explanted for transmission electron microscopic

evaluation. The explanted specimens were divided into two groups for the following treatment: group 1 was fixed with 2.5 wt% glutaraldehyde in 0.1 M phosphate buffer (pH 7.4) at 4 °C for 1 hr and postfixed with 1 wt% osmium tetroxide in 0.1 M phosphate buffer (pH 7.4) containing 0.1 M sucrose at 4 °C for 2 hr (aqueous preparation). Group 2 was treated with 100 % ethylene glycol at 4 °C for 24 hr under vacuum state (anhydrous preparation)[21]. The fixed specimens in group 1 were dehydrated in an ascending series of ethanol and placed in propylene oxide and subsequently in propylene oxide and an Epon resin mixture at room temperature. Then, the specimens in group 1 were soaked in the Epon resin under vacuum and embedded in the Epon resin. On the other hand, the treated specimens in group 2 were immersed in 2-ethoxyethanol at 4 °C for 24 hr under vacuum and placed in propylene oxide and the Epon resin mixture. Finally, the specimens in group 2 were embedded in the Epon resin. An ultrathin cross-section of 70 nm thickness was cut with an ultramicrotome from the formed bone tissue in both groups 1 and 2. The cross-sections were stained with both lead citrate and uranyl acetate or unstained with any chemicals.

Bright field electron imaging was performed for both stained and unstained sections with a TEM (JEM 1200EX II, JEOL, Tokyo, Japan) operating at 80 kV. Furthermore, the unstained specimen treated with the anhydrous preparation was investigated by selected area diffraction (SAD) combined with selected area dark field electron imaging under the same TEM condition as the bright field electron imaging.

RESULTS

Bright field electron imaging of stained and unstained cross-sections

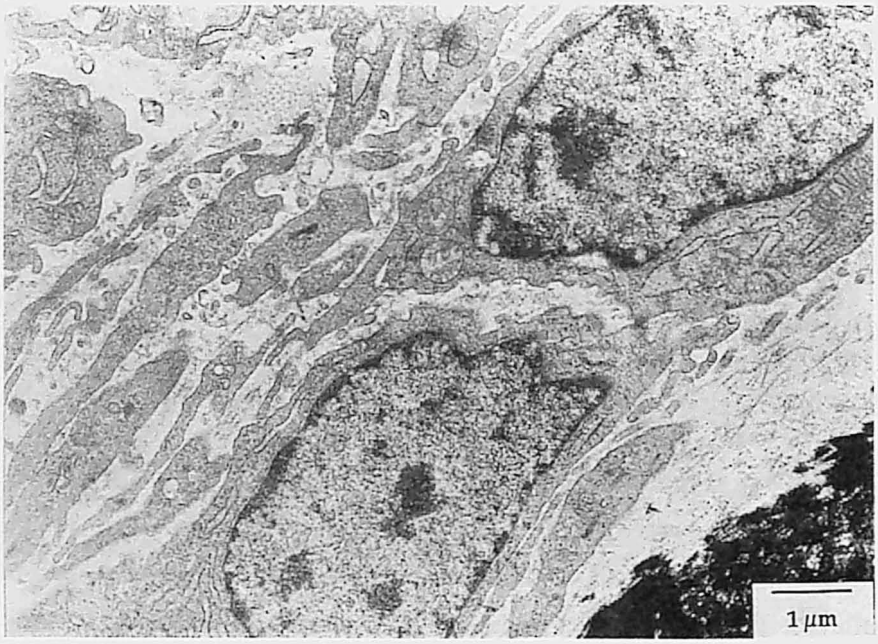

Figure 1. Bright field electron imaging of the stained cross-section of the ectopic bone prepared with the aqueous method.

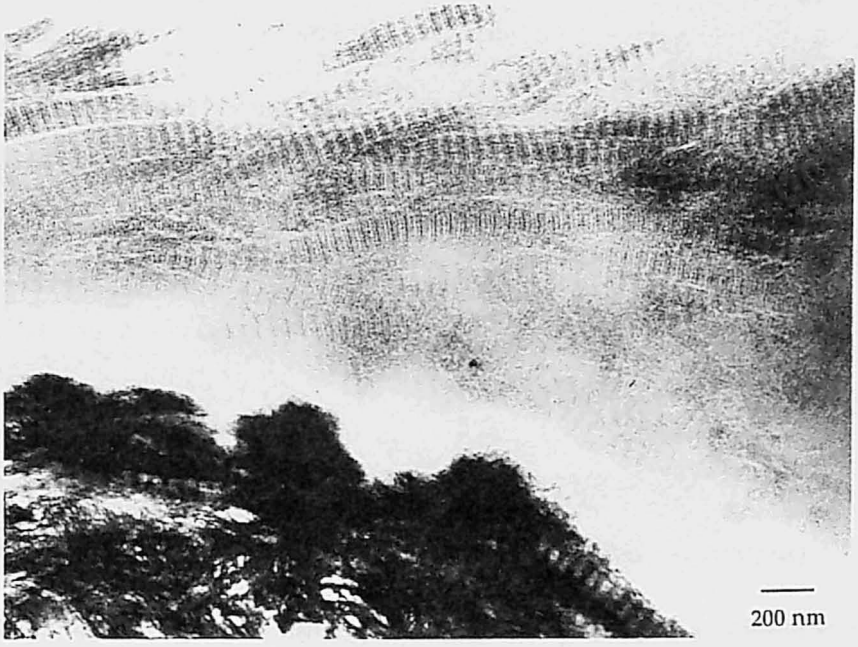

Figure 2. Bright field electron imaging of the stained cross-section of the ectopic bone prepared with the anhydrous method.

From soft x-ray observation, a radiopaque area could be seen at the leg receiving BMP-2 incorporating gelatin hydrogels after 2 weeks of implantation as shown in Chapter 2. Figures 1 and 2 show bright field electron imaging of stained cross-sections for the ectopic bone treated with both the aqueous and anhydrous preparations. As seen in Figure 1, osteoblasts have actively produced an extracellular matrix containing collagen fibers, which have been partially mineralized. Collagen fibers with a fine structural periodic banding of 64 nm and partial mineralization are seen in Figure 2[31-33].

Figure 3 shows bright field electron imaging of the unstained cross-sections for the ectopic bone treated with the anhydrous preparation. A 64 nm well-banded feature of mineralized collagen fibril was observed even in the unstained cross-sections, due to the electron opacity of calcium phosphate. As seen in Figure 3, mineral deposits were identified in two regions, the periphery of the collagen fibrils (extrafibrillar crystallites) and the gap zone of collagen fibrils with a fine structural periodic width of 37 nm (intrafibrillar crystallites)[31-33]. Extrafibrillar crystallites appeared needle-shaped and were inclined at various angles to the long axis of the collagen fibril. On the other hand, intrafibrillar crystallites were readily apparent in the gap zones of the collagen fibrils without such a fine structural feature as that seen in the extracellular crystallites although a less extent of the crystallites is seen in the overlap zones of the collagen fibrils.

Selected area diffractograms and dark field electron imaging of unstained cross-sections

Figure 4 shows a bright field electron microphotograph of the unstained cross-sections together with the SAD of extrafibrillar crystallites. Two distinct electron diffraction

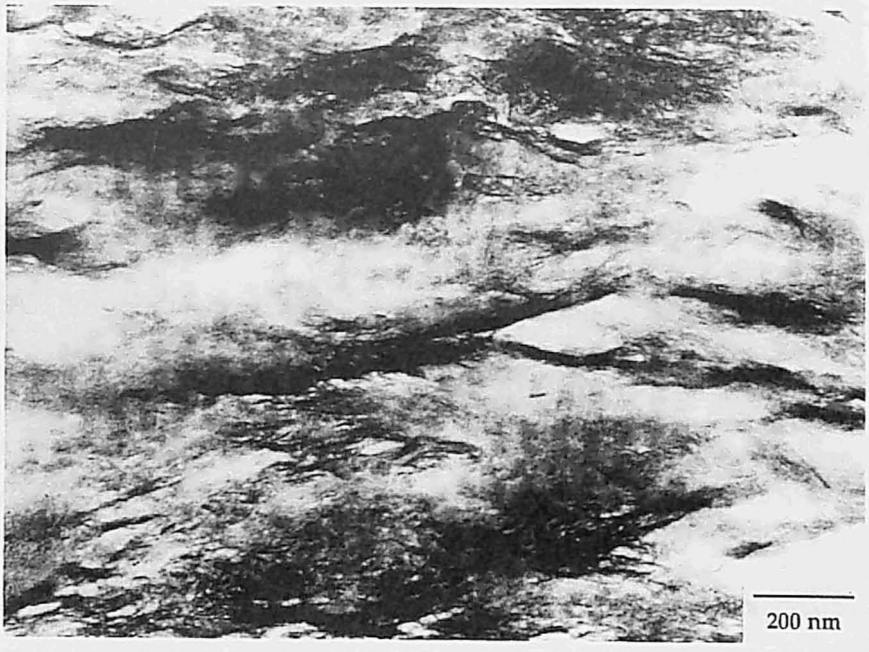

Figure 3. Bright field electron imaging of the unstained cross-section of the ectopic bone prepared with the anhydrous method.

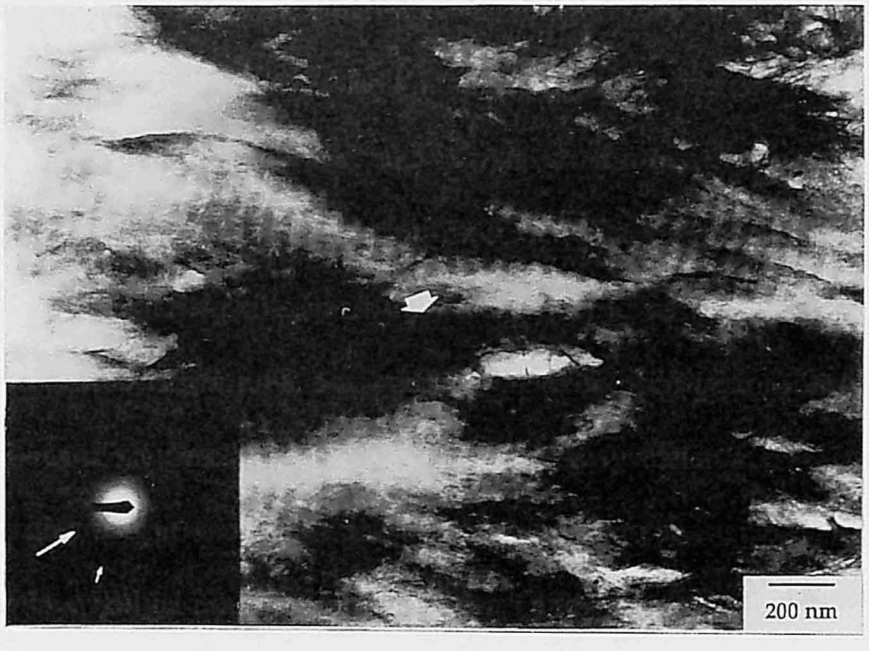

Figure 4. Bright field electron imaging and SAD imaging of the unstained cross-section of the ectopic bone prepared with the anhydrous method. Heavy arrow indicates the area of extrafibrillar crystallites used for SAD imaging. The large and small arrows in SAD imaging correspond to (002) and (211) lattice planes, respectively.

patterns seen in Figure 4 corresponded to the (002) and (211) lattice planes of hydroxyapatite (HAp) crystal and appeared ring-shaped. On the contrary, Figure 5 shows a different SAD pattern observed for the intrafibrillar crystallites, especially in the gap zones of the mineralized collagen fibril, when viewed at a higher magnification. The diffraction pattern assigned to (002) lattice plane indicated the c-axis preferential orientation of HAp crystal to the long axis of collagen fibril.

Figure 6 shows dark field electron imaging of the c-axis of HAp crystals corresponding to the bright field electron imaging shown in Figure 5. The dark field electron imaging enabled direct visualization of the HAp crystals and determination of their c-axial orientation. The dark field electron imaging appeared in reverse contrast to the conventional bright field electron imaging with the HAp crystals appearing as white highlights. The white highlights corresponding to the c-axial diffraction of HAp crystals lay in the direction oriented to the long axis of collagen fibril, as seen in Figure 6.

DISCUSSION

In this chapter, the ultrastructure of the bone induced by growth factor was investigated at an electron microscopic level, similar to the mineralized turkey leg tendon[5,6,10,11,15,17,18,23-25,27,28]. The mineralized tendon has been widely studied as a model for collagen-based mineralized tissues such as bone and dentin. In order to reduce the artifacts induced in hydroxyapatite crystals by aqueous solutions, the anhydrous method[21] was used in this chapter for specimen preparation of the formed bone and the cross-sections were not

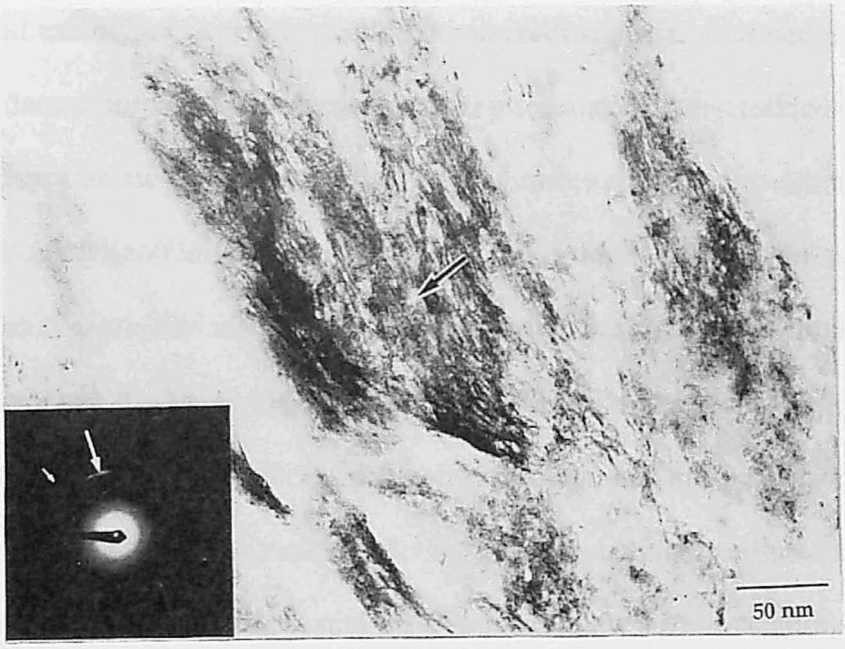

Figure 5. Bright field electron imaging and SAD imaging of the unstained cross-section of the ectopic bone prepared with the anhydrous method. A black arrow indicates the area of intrafibrillar crystallites used for SAD imaging. Large and small arrows in SAD imaging correspond to (002) and (211) lattice planes, respectively.

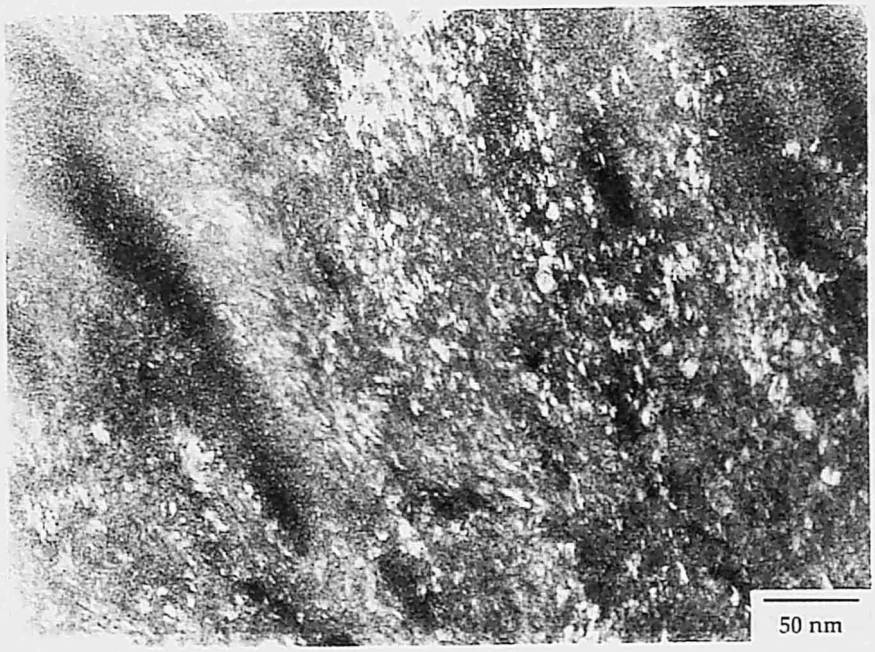

Figure 6. Dark field electron imaging of the c-axis of HAp crystals corresponding to the bright field electron imaging shown in Figure 5.

stained with any chemicals. The electron microscopically observed mineralized collagen fibril together with osteoblasts in the active form indicates that the radiopaque area of the soft x-ray photographs and the calcium deposition histologically observed at the surrounding tissue of the hydrogel was not simple calcification of the hydrogel but the bone induced by BMP-2-incoporating gelatin hydrogel. The morphological change of the mineralized collagen due to the anhydrous method was not identified as shown in Figure 2. It is possible that the morphological evidence of the mineralized collagen in the formed bone shown in this chapter may imply its intact ultrastructure.

Various models have been proposed to explain the mineralized tissue structure. For intrafibrillar crystallites, two issues, their orientation and their location in collagen fibrils, have been discussed. Intrafibrillar crystallites are oriented to each other within the gap zones along the whole length of the collagen fibril and to the longitudinal collagen fibril axis at an acute angle. Most of the intrafibrillar crystallites are found in the gap zones, but with increased mineralization, the crystallites in the gap zones extend into the overlap zones with or without changing the structure of the collagen fibrils. Intrafibrillar crystallites observed for the ectopic bone localized in the gap zone of the collagen fibrils, because their clear periodic width of 37 nm was in accord with that observed in the non-mineralized collagen (Figure 3). However, the origin of the crystallites in the overlap zones is still unclear. SAD imaging and subsequent dark field electron imaging suggest that intrafibrillar crystallites may be oriented to each other and to the longitudinal axis of the collagen fibrils (Figures 5 and 6).

On the other hand, extrafibrillar crystallites do not have such a spatial orientation as intrafibrillar crystallites. Bright field electron imaging and subsequent SAD imaging clearly indicate that extrafibrillar crystallites observed in the ectopic bone are not oriented to the

collagen fibril axis as seen in the intrafibrillar crystallites (Figure 4). This feature is consistent with that observed for the mineralized turkey leg tendon. However, detailed information of needle-shaped, extrafibrillar crystallites of the ectopic bone could not be obtained from Figure 4. Extrafibrillar crystallites of mineralized tissue have been discussed in terms of their shape and their exact location of crystal nucleation. With regard to the former issue, needle-like appearing has been discussed elsewhere whether it may be their intact shape or the shape viewing on the edge of the platelet crystallites, but the precise structural events are unknown.

Not only collagen-mineral interaction but also orientation of mineralized collagen fibrils has been demonstrated to explain the mechanically efficient composite structure of mineralized tissues[3,19,20,25,28,34]. In addition, a fracture-healing model has been studied on the basis of external periosteal callus of repaired femoral fracture in both children and adults to understand the mechanism of bone repair and regeneration[12,13]. When compared with the spatial orientation of collagen fibrils observed in fracture callus, well-ordered collagen fibrils, approximately parallel to each other and to columns of the mineral hydroxyapatite, appeared in the lamellar bone. From this viewpoint, collagen fibril orientation also seems to be important with respect to the mechanical compatibility of the ectopic bone. However, as shown in this chapter, preferred orientation of the collagen fibrils is still unclear. Combination of the information obtained from x-ray diffraction and scanning electron microscopy with the results shown in this chapter will be helpful for understanding the ultrastructure of the regenerated bone.

References

1. *An introduction to bioceramics*, L. L. Hench and J. Wilson eds., World Scientific, Singapore (1993)
2. P. Fratzl, N. Fratzl-Zelman, K. Klaushofer, G. Vogl, and K. Koller, Nucleation and growth of mineral crystals in bone studied by small-angle x-ray scattering, *Calcif. Tissue Int.*, **48**, 407-413 (1991).
3. P. Fratzl, O. Paris, K. Klaushofer, and W. J. Landis, Bone mineralization in an osteogenesis imperfecta mouse model studied by small-angle x-ray scattering, *J. Clin. Invest.*, **97**, 396-402 (1996).
4. P. Fratzl, S. Schreiber, and K. Klaushofer, Bone mineralization as studied by small-angle x-ray scattering, *Connect. Tissue Res.*, **34**, 247-254 (1996).
5. S. J. Gadaleta, N. P. Camacho, R. Mendelsohn, and A. L. Boskey, Fourier transform infrared microscopy of calcified turkey leg tendon, *Calcif. Tissue Int.*, **58**, 17-23 (1996).
6. S. J. Gadaleta, W. J. Landis, A. L. Boskey, and R. Mendelsohn, Polarized FT-IR microscopy of calcified turkey leg tendon, *Connect. Tissue Int.*, **34**. 203-211 (1996).
7. U. Plate, S. Arnold, L. Reimer, H. Höhling, and A. Boyde, Investigation of the early mineralisation on collagen in dentine of rat incisors by quantitative electron spectroscopic diffraction (ESD), *Cell Tissue Res.*, **278**, 543-547 (1994).
8. E. Bonucci, Ultrastructural organic-inorganic relationships in calcified tissues: cartilage and bone vs. enamel, *Connect. Tissue Res.*, **33**, 157-162 (1995).
9. H. J. Höhling, S. Arnold, R. H. Barckhaus, U. Plate, and H. P. Wiesmann, Structural

relationship between the primary crystal formations and the matrix macromolecules in different hard tissues. Discussion of a general principle, *Connect. Tissue Res.*, **33**, 171-178 (1995).

10. S. Lee, K. S. Prostak, V. K. Ingle, and K. Kjoller, The loci of mineral in turkey leg tendon as seen by atomic force microscope and electron microscopy, *Calcif. Tissue Int.*, **55**, 180-189 (1994).

11. K. S. Prostak and S. Lee, Visualization of crystal-matrix structure. In situ demineralization of mineralized turkey leg tendon and bone, *Calcif. Tissue Int.*, **59**, 474-479 (1996).

12. H. B. Wen, F. Z. Cui, Q. L. Feng, H. D. Li, and X. D. Zhu, Microstructural investigation of the early external callus after diaphyseal fractures of human long bone, *J. Struct. Biol.*, **114**, 115-122 (1995).

13. F. Z. Cui, H. B. Wen, X. W. Su, and X. D. Zhu, Microstructures of external periosteal callus of repaired femoral fracture in children, *J. Struct. Biol.*, **117**, 204-208 (1996).

14. A. L. Arsenault and E. B. Hunziker, Electron microscopic analysis of mineral deposits in the calcifying epiphyseal growth plate, *Calcif. Tissue Int.*, **42**, 119-126 (1988).

15. A. L. Arsenault, Crystal-collagen relationships in calcified turkey leg tendons visualized selected-area dark field electron microscopy, *Calcif. Tissue Int.*, **43**, 202-212 (1988).

16. A. L. Arsenault and M. D. Grynpas, Crystals in calcified epiphyseal cartilage and cortical bone of the rat, *Calcif. Tissue Int.*, **43**, 219-225 (1988).

17. A. L. Arsenault, Image analysis of collagen-associated mineral distribution in

cryogenically prepared turkey leg tendon, *Calcif. Tissue Int.*, **48**, 56-62 (1991).

18. A. L. Arsenault, B. W. Frankland, and F. P. Ottensmeyer, Vectorial sequence of mineralization in the turkey leg tendon determined by electron microscopic imaging, *Calcif. Tissue Int.*, **48**, 46-55 (1991).

19. M. M. Giraud-Guille, Twisted plywood architecture of collagen fibrils in human compact bone osteons, *Calcif. Tissue Int.*, **42**, 167-180 (1988).

20. D. H. Isaac and M. Green, The origin of preferred orientation in bone, *Clin. Mater.*, **15**, 79-87 (1994).

21. W. J. Landis, M. C. Paine, and M. J. Glimcher, Electron microscopic observations of bone tissue prepared anhydrously in organic solvents, *J. Ultrastruct. Res.*, **59**, 1-30 (1977).

22. V. Ziv, I. Sabanay, T. Arad, W. Traub, and S. Weiner, Transitional structures in lamellar bone, *Microscop. Res. Tech.*, **33**, 203-213 (1996).

23. D. M. Kohler, M. A. Crenshaw, and A. L. Arsenault, Three-dimensional analysis of mineralizing turkey leg tendon:matrix vesicle-collagen relationship, *Matrix Biol.*, **14**, 543-552 (1994).

24. W. J. Landis, M. J. Song, A. Leith, L. McEwen, and B. F. McEwen, Mineral and organic matrix interaction in normally calcifying tendon visualized in three dimensions by high-voltage electron microscopic tomography and graphic image reconstruction, *J. Struct. Biol.*, **110**, 39-54 (1993).

25. W. J. Landis, The strength of a calcified tissue depends in part on the molecular structure and organization of its constituent mineral crystals in their organic matrix, *Bone*, **16**, 553-544 (1995).

26. W. J. Landis, K. J. Hodgens, J. Arena, M. J. Song, and B. F. McEwen, Structural relations between collagen and mineral in bone as determined by high voltage electron microscopic tomography, *Microscop. Res. Tech.*, **33**, 192-202 (1996).

27. W. J. Landis, K. J. Hodgens, M. J. Song, J. Arena, S. Kiyonaga, M. Marko, C. Owen, and B. F. McEwen, Mineralization of collagen may occur on fibril surfaces: evidence from conventional and high-voltage electron microscopy and three-dimensional imaging, *J. Struct. Biol.*, **117**, 24-35 (1996).

28. W. J. Landis, Mineral characterization in calcifying tissues: atomic, molecular, and macromolecular perspectives, *Connect. Tissue Res.*, **34**, 239-246 (1996).

29. M. Riminucci, G. Silvestrini, E. Bonucci, L. W. Fisher, P. G. Robey, and P. Bianco, The anatomy of bone sialoprotein immunoreactive sites in bone as revealed by combined ultrastructural histochemistry and immunohistochemistry, *Calcif. Tissue Int.*, **57**, 277-284 (1995).

30. M. D. McKee and A. Nanci, Osteopontin at mineralized tissue interface in bone, teeth, and osseointegrated implants: ultrastructural distribution and implications for mineralized tissue formation, turnover, and repair, *Microscop. Res. Tech.*, **33**, 141-164 (1996).

31. J. A. Chapman, The staining patterns of collagen fibrils I. An analysis of electron micrographs, *Connect. Tissue Res.*, **2**, 137-150 (1974).

32. J. A. Chapman and R. A. Hardcastle, The staining pattern of collagen fibril II. A comparison with patterns computergenerated from the amino acid sequence, *Connect Tissue Res.*, **2**, 151-159 (1974).

33. K. M. Meek, J. A. Chapman and R. A. Hardcastle, The staining pattern of collagen

fibrils. Improved correlation with sequence data, *J. Biol. Chem.*, **254**, 10710-10714 (1979).

34. W. J. Landis, J. J. Librizzi, M. G. Dunn, and F. H. Silver, A study of the relationship between mineral content and mechanical properties of turkey gastrocnemius tendon, *J. Bone Miner. Res.*, **10**, 859-867 (1995).

SUMMARY

Chapter 1. One of the key technologies for regeneration of damaged and lost tissues is the sustained release of biologically active growth factors. This chapter was undertaken to investigate sorption and desorption of various growth factors from the hydrogels prepared through glutaraldehyde crosslinking of gelatin with IEPs of 5.0 and 9.0, which are named "acidic" and "basic" gelatins, respectively, because of their electrical feature. Basic bFGF and TGF-β1 were well sorbed with time to the acidic gelatin hydrogel, while less sorption was observed for the basic gelatin hydrogel. This could be explained in terms of the electrostatic interaction between the basic growth factors and the acidic gelatin. However, VEGF and BMP-2, though their IEPs are higher than 7.0, were sorbed to the acidic gelatin hydrogel to a less extent than the other two growth factors. An in vivo experiment revealed that the hydrogels were degraded with time. The growth factors were retained in the body for a longer time period, as their in vitro sorption to the acidic gelatin hydrogel increased. These findings indicate that the growth factors polyionically complexed to the gelatin hydrogel were released in the body as a result of hydrogel degradation.

Chapter 2. Biodegradable hydrogels were prepared from gelatin by glutaraldehyde crosslinking for release matrix of BMP-2. BMP-2 solution was impregnated into the dried hydrogels to prepare BMP-2-incorporating gelatin hydrogels. In the in vitro study, enhanced retention of BMP-2 was observed from the BMP-2-incorporating gelatin hydrogels after an initial burst of BMP-2 incorporated initially in

the hydrogel. Following subcutaneous implantation of ^{125}I-labeled BMP-2-incorporating gelatin hydrogels in the back of mice, the radioactivity remaining in the hydrogels was measured to estimate the in vivo release profile of BMP-2. It was found that BMP-2 was retained in the hydrogels for longer than 30 days, whereas 99 % of BMP-2 injected in the solution form was cleared from the injected site within one day, completely disappearing within 3 days. Ectopic bone formation studies demonstrated that the BMP-2-incorporating gelatin hydrogels exhibited a more potent ability for bone induction than solution injection of BMP-2. This finding indicates that enhanced retention of BMP-2 promotes its ability to induce ectopic bone formation.

Chapter 3. This chapter described the sustained release of TGF-β1 from a biodegradable hydrogel based on polyion complexation and the significant enhancement of its bone regeneration activity. Basic TGF-β1 could be sorbed into the biodegradable hydrogel of acidic gelatin with an IEP of 5.0 because of their electrostatic interaction, but not into that of basic gelatin. When acidic gelatin hydrogels incorporating ^{125}I-labeled TGF-β1 were implanted into the back subcutis of mice, the remaining radioactivity decreased with time and the in vivo retention of TGF-β1 prolonged with a decrease in the water content of hydrogels. The higher the water content of hydrogels, the faster their biodegradation. The in vivo retention of TGF-β1 well correlated with that of gelatin hydrogels, indicating that TGF-β1 was released from the gelatin hydrogel as a result of hydrogel biodegradation. The ability of TGF-β1-incorporating acidic gelatin hydrogels to induce bone regeneration was evaluated by use of a rabbit model with a skull defect. Eight weeks after treatment, the gelatin hydrogels with water

contents of 90 and 95 wt% induced significantly high bone regeneration at the skull defect compared with those with lower and higher water contents and free TGF-β1. This indicates that the sustained release of TGF-β1 from the hydrogel with suitable in vivo degradability is necessary to effectively enhance its osteoinductive function. Rapid hydrogel degradation will result in the in vivo short retention of TGF-β1 which is not enough to induce bone regeneration. It is likely that the slow degradation let the hydrogel physically block TGF-β1-induced bone regeneration at the skull defect. It was concluded that the gelatin hydrogel functioned not only as a matrix of TGF-β1 release but also as a space provider to prevent the ingrowth of soft tissues to the defect.

Chapter 4. Fibrovascular tissue ingrowth into PVA sponges of different pore sizes was investigated by incorporating bFGF into the sponges. The average pore size of PVA sponges used in this chapter was 30, 60, 110, 250, 350, and 700 μm and gelatin microspheres were employed as release carrier of bFGF. The sponges were subcutaneously implanted into the back of mice after incorporating free bFGF or gelatin microspheres containing bFGF into the sponges. Fibrovascular tissue infiltrated with time into the sponge pores and the extent of fibrous tissue ingrowth showed a maximum at a pore size around 250 μm 1 and 6 weeks after implantation. Significant promotion of fibrous tissue growth by bFGF was observed only at 3 weeks post-implantation. New capillaries were formed in the tissue any time, as far as bFGF was given to the sponges. The extent of vascularization was a little high when bFGF was entrapped in gelatin microspheres in comparison with free bFGF. Both empty gelatin microspheres and phosphate buffered solution neither promoted tissue ingrowth nor induced capillary

formation in the sponges. It was concluded that bFGF was essential to induce the fibrovascular tissue ingrowth into the pores of PVA sponge.

Chapter 5. Osteoblasts derived from RBM cells were cultured on surface-modified PET films in the presence of ascorbic acid, β-glycerophosphate, and dexamethasone. The surfaces employed for cell culture included the untreated hydrophobic surface and three modified surfaces possessing immobilized phosphate polymer chains, collagen molecules, and a thin HAp-deposited layer. They were all produced by photo-induced graft polymerization and subsequent surface-modifications of the graft chains. The ultrastructural morphology of the substrate/cell interfaces formed in in vitro osteoblast culture on these substrates was studied by TEM. The osteoblasts cultured for 1 week on the modified surfaces showed rough endoplasmic reticula rich in the intracellular space and early matrix production in the extracellular space, irrespective of the surface chemistry. After 2 weeks of culture, osteoblasts exhibited active elaboration of extracellular matrix proteins, mostly composed of collagen, on all the surfaces. A remarkable result observed at this stage was direct deposition of an electron-dense, afibrillar layer of 180 nm thickness onto the surface having phosphate polymer chains. This layer became much more electron-dense after 3 weeks of culture. EDX microanalysis revealed the presence of calcium phosphate in this layer. It was further found that the pre-deposited HAp layer on the phosphate polymer grafted surface promoted mineral deposition in the extracellular matrix which surrounded cuboid, osteocyte-like cells.

Chapter 6. To study the effect of the shape of carriers on bone regeneration, two

biodegradable polymeric materials, a PGA non-woven fabric and a gelatin hydrogel, were used as carriers of recombinant BMP-2. The PGA non-woven fabric was made from PGA fibers of 20 μm diameter without using any binders while the gelatin hydrogel was prepared by crosslinking of gelatin in aqueous solution with glutaraldehyde to a water content of 95 % when swollen with water. Following impregnation of BMP-2, the carriers of disk type were implanted into the Wistar rat thigh muscle. The induction of ectopic bone formation from the BMP-2-impregnated carriers was evaluated by soft x-ray and histological observation after staining the explanted tissue with alizarin red S to identify calcium deposition. Both the biodegradable polymeric carriers containing 10 μg of BMP-2 induced ectopic bone formation after 2 weeks of implantation but not at 1st week postimplantation. A remarkable finding was a difference in the macroscopic morphology between the ectopic bones induced by the PGA non-woven fabric and the gelatin hydrogel. The PGA non-woven fabric containing BMP-2 induced ectopic bone formation inside of the carrier, whereas the gelatin hydrogel formed bone at the periphery of the carrier.

Chapter 7. To study the ultrastructure of the ectopically formed bone induced by a BMP-2-incorporating gelatin hydrogel, TEM microanalyses including bright field electron imaging, SAD imaging, and dark field electron imaging were employed. After 2 weeks of implantation, ectopic bone induction was apparent at Wistar rat thigh muscles receiving BMP-2-incorporating gelatin hydrogels through soft x-ray observation. The specimens for TEM study were prepared with an anhydrous method using ethylene glycol to maintain the structure of HAp crystals. TEM observation of the unstained cross-sections of ectopic bone showed that electron dense substances were

deposited on the gap zone of collagen fibers (intrafibrillar crystallites), while needle-like electron dense substances were observed in the intermolecular space of collagen fiber (extrafibrillar crystallites). SAD patterns suggested that these electron dense substances were HAp crystals. Furthermore, from the SAD pattern and dark field electron image of intrafibrillar crystallites, it was presumed that the crystallographic c-axis of apatite crystals oriented to the direction of collagen fibril.

LIST OF PUBLICATIONS

Chapter 1. Yasuhiko TABATA, Masaya YAMAMOTO, and Yoshito IKADA, "Comparison of release profiles of various growth factors from biodegradable carriers", in *Mat. Res. Soc. Symp. Proc.*, Vol. 530, R. C. Thomson, D. J. Mooney, K. E. Healy, Y. Ikada, and A. G. Mikos eds., Materials Research Society, Pennsylvania, 1998, pp. 13-18.

Chapter 2. Masaya YAMAMOTO, Yasuhiko TABATA, and Yoshito IKADA, "Ectopic bone formation induced by biodegradable hydrogels incorporating bone morphogenetic protein", *J. Biomater. Sci. Polym. Edn.*, **9**, 439-458 (1998).

Chapter 3. Masaya YAMAMOTO, Yasuhiko TABATA, Liu HONG, Susumu MIYAMOTO, Nobuo HASHIMOTO, and Yoshito IKADA, "Bone regeneration by transforming growth factor β1 released from a biodegradable hydrogel", *J. Controll. Release*, in press.

Chapter 4. Masaya YAMAMTO, Yasuhiko TABATA, Hideo KAWASAKI, and Yoshito IKADA, "Promotion of fibrovascular tissue ingrowth into porous sponges by basic fibroblast growth factor", *J. Mater. Sci. Materials in Medicine*, submitted.

Chapter 5. Masaya YAMAMOTO, Koichi KATO, and Yoshito IKADA, "Ultrastructure of the interface between cultured osteoblasts and surface-modified polymer substrates", *J. Biomed. Mater. Res.*, **37**, 29-36 (1997).

Chapter 6. Masaya YAMAMOTO, Koichi KATO, and Yoshito IKADA, "Effect of the structure of bone morphogenetic protein carriers on ectopic bone

regeneration", *Tissue Engineering*, **2**, 315-326 (1996).

Chapter 7. In preparation

ACKNOWLEDGEMENTS

The present research was carried out under the continuous guidance of Dr. Yoshito Ikada, Professor of Institute for Frontier Medical Sciences, Kyoto University. The author is deeply indebted to Professor Ikada for his constant guidance, encouragement, valuable discussion, and detailed criticism on the manuscript throughout the present work. The completion of the present research has been an exciting project and one which would not have been possible without his guidance.

The author wishes to express his thanks to Dr. Hiroo Iwata and Dr. Yasuhiko Tabata, Associate Professors of Institute for Frontier Medical Sciences, Kyoto University, and Dr. Koichi Kato, Research Associate of the Department of Chemical Science and Engineering, Kobe University, for their constant guidance, encouragement, valuable discussion, intimate advice, and detailed criticism on whole experiments as well as the manuscript throughout the present work.

The author is also grateful to Dr. Nobuo Hashimoto, Professor of the Department of Neurosurgery, Kyoto University, Dr. Susumu Miyamoto, Lecturer of the Department of Neurosurgery, Kyoto University, Dr. Keisuke Yamada of Tsukaguchi Hospital, and Mr. Hong Liu of the Department of the Neurosurgery, Kyoto University, for their significant advice and helps on the rabbit experiments.

The author wishes to express his sincere appreciation to Dr. Shigeko Takaichi of the Department of Medical Virology, Stellenbosch University, South Africa, and Mr. Makio Fujioka of the Faculty of Medicine, Kyoto University, for the technical instruction of TEM and EDX, respectively. The author also expresses his great thanks to Dr. Emiko Uchida, Professor of the Kacho Junior College, for her appreciable advice on surface graft

polymerization, and to Dr. Toshiya Fujisato of National Cardiovascular Center Research Institute, Japan, and Dr. Noriyuki Morikawa, Gunze Co. Ltd., for their instruction of cell culture technique and animal experiments.

General acknowledgement is due to Dr. Toshio Hayashi, Professor of the Research Institute for Advanced Science and Technology, Osaka Prefecture University, Dr. Naohide Tomita, Associate Professor of Institute for Frontier Medical Sciences, Kyoto University, Mr. Sakae Ogata, Dr. Yoshikimi Uyama, Dr. Won-Ill Cha of Institute for Frontier Medical Sciences, Kyoto University, and Dr. Ryusuke Nakaoka of National Institute for Health and Sciences, Japan, for their helpful suggestion and intimate advice.

The author is much indebted to the following students of Professor Ikada's Laboratory for their contribution to the present studies: Mr. Yoshiyuki Murakami, Yamanouchi Pharmaceutical Co. Ltd., Mr. Atsuhiro Nagano, Teijin Co. Ltd., Mr. Yasuhiro Matsui, Sumitomo Pharmaceutical Co. Ltd., and Mr. Hideo Kawasaki.

The author likes to take an opportunity to extend his heartily thanks to Ms. Yoshiko Suzuki and other members of Professor Ikada's Laboratory and of Institute for Frontier Medical Sciences for their kind help.

December, 1998

Kyoto

Masaya Yamamoto